AD-A182 380 FURTHER RESULTS IN BEND-BUCKLING ANALYSIS OF RING STIFFENED CYLINDRICAL SHELLS(U) NAVAL SURFACE WEAPONS CENTER SILVER SPRING MD M MOUSSOUROS AUG 86 1/1

UNCLASSIFIED NSWC/TR-86-326 F/G 20/11 NL

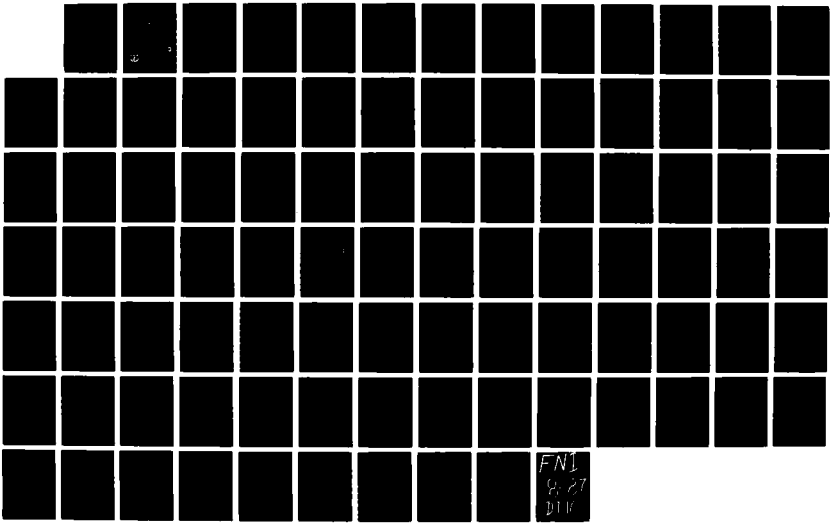

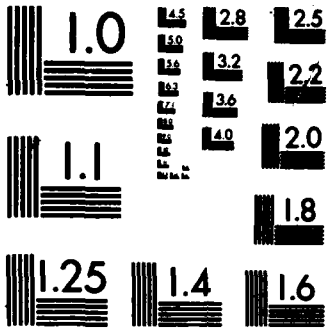

MICROCOPY RESOLUTION TEST CHART
NATIONAL BUREAU OF STANDARDS-1963-A

(12)

NSWC TR 86-326

DTIC FILE COPY

FURTHER RESULTS IN BEND-BUCKLING ANALYSIS OF RING STIFFENED CYLINDRICAL SHELLS

AD-A182 380

BY MINOS MOUSSOUROS

RESEARCH AND TECHNOLOGY DEPARTMENT

AUGUST 1986

Approved for public release; distribution is unlimited.

DTIC
ELECTE
JUL 1 6 1987
S D
E

NAVAL SURFACE WEAPONS CENTER

Dahlgren, Virginia 22448-5000 • Silver Spring, Maryland 20903-5000

87

UNCLASSIFIED
SECURITY CLASSIFICATION OF THIS PAGE

A182380

REPORT DOCUMENTATION PAGE

1a REPORT SECURITY CLASSIFICATION UNCLASSIFIED	1b RESTRICTIVE MARKINGS
2a SECURITY CLASSIFICATION AUTHORITY	3 DISTRIBUTION/AVAILABILITY OF REPORT Approved for public release; distribution is unlimited.
2b DECLASSIFICATION/DOWNGRADING SCHEDULE	
4 PERFORMING ORGANIZATION REPORT NUMBER(S) NSWC TR 86-326	5 MONITORING ORGANIZATION REPORT NUMBER(S)
6a NAME OF PERFORMING ORGANIZATION Naval Surface Weapons Center 6b OFFICE SYMBOL (If applicable) Code R14	7a NAME OF MONITORING ORGANIZATION
6c ADDRESS (City, State, and ZIP Code) 10901 New Hampshire Avenue Silver Spring, MD 20903-5000	7b ADDRESS (City, State, and ZIP Code)
8a NAME OF FUNDING/SPONSORING ORGANIZATION 8b OFFICE SYMBOL (If applicable)	9 PROCUREMENT INSTRUMENT IDENTIFICATION NUMBER
8c ADDRESS (City, State, and ZIP Code)	10 SOURCE OF FUNDING NUMBERS PROGRAM ELEMENT NO. 62633N; PROJECT NO. F33327; TASK NO SF33327; WORK UNIT ACCESSION NO R19BA

11 TITLE (Include Security Classification)

Further Results in Bend-Buckling Analysis of Ring Stiffened Cylindrical Shells

12 PERSONAL AUTHOR(S)
Moussouros, Minos

13a TYPE OF REPORT	13b TIME COVERED FROM 1984 TO 1986	14 DATE OF REPORT (Year, Month, Day) 1986, August	15 PAGE COUNT 92

16 SUPPLEMENTARY NOTATION

17 COSATI CODES			18 SUBJECT TERMS (Continue on reverse if necessary and identify by block number)
FIELD	GROUP	SUB-GROUP	bend, buckling, finite element, cylindrical shells,
13	13		

19 ABSTRACT (Continue on reverse if necessary and identify by block number)

This report presents finite element bend-buckling analysis results, including short wavelength (local) buckling, and an analysis of the surface of a nearly circular cylinder through a double Fourier series.

(Keywords:

20 DISTRIBUTION/AVAILABILITY OF ABSTRACT ☐ UNCLASSIFIED/UNLIMITED ☒ SAME AS RPT ☐ DTIC USERS	21 ABSTRACT SECURITY CLASSIFICATION UNCLASSIFIED
22a NAME OF RESPONSIBLE INDIVIDUAL Minos Moussouros	22b TELEPHONE (Include Area Code) (202) 394-1681 22c OFFICE SYMBOL Code R14

DD FORM 1473, 84 MAR 83 APR edition may be used until exhausted. All other editions are obsolete.

SECURITY CLASSIFICATION OF THIS PAGE

U.S. Government Printing Office 1986: 607-044

UNCLASSIFIED

FOREWORD

This report presents finite element bend-buckling analysis results, including short wavelength (local) buckling and an analysis of the surface of a "nearly circular cylinder" through a double Fourier series.

This study used the nonlinear finite element program ABAQUS. It was performed under an ongoing program aimed at realistic modeling of shell structures and capturing all the developing phenomena during static buckling of circular cylindrical shells subject to either bending moments or axial compression.

This work was supported by the Office of Naval Technology through the Naval Surface Weapons Center Block Program, "Undersea Weapons, Warheads and Fuzes" (D.E. Phillips).

Approved by:

KURT F. MUELLER, Head
Energetic Materials Division

CONTENTS

	Page
INTRODUCTION	1
METHOD	2
FINITE ELEMENT MODELING	2
BOUNDARY CONDITIONS AND APPLIED LOADING	3
APPLICATIONS AND RESULTS	3
SUMMARY	7
REFERENCES	59
NOMENCLATURE	61
APPENDIX A -- ANALYSIS OF A NEARLY EXACT CYLINDRICAL SURFACE	A-1
APPENDIX B -- SUBROUTINE TO RUN ABAQUS BEND BUCKLING ANALYSIS	B-1

Accession For
NTIS GRA&I ☒
DTIC TAB ☐
Unannounced ☐
Justification

By
Distribution/
Availability Codes
Dist | Avail and/or Special
A-1

QUALITY INSPECTED 4

ILLUSTRATIONS

Figure		Page
1	STRAIGHT CYLINDRICAL SHELL OF HALF LENGTH $L/_2$, MEAN RADIUS R, THICKNESS h, AND ASSOCIATED GLOBAL CARTESIAN COORDINATE SYSTEM (x, y, z)	8
2	(A) CYLINDRICAL SHELL (SHOWN AS A BEAM) OF LENGTH L SUBJECT TO SHEARING LOADS F, PRODUCING A BENDING MOMENT M = Fa	
	(B) CYLINDRICAL SHELL OF A REDUCED LENGTH L_R SUBJECT TO AN EXTERNAL BENDING MOMENT M = Fa	9
3	COMPARISON OF BENDING MOMENT VERSUS MEAN CURVATURE FOR MODELS 10A AND 10AN	10
4	COMPARISON OF BENDING MOMENT VERSUS MEAN CURVATURE FOR MODELS 16A AND 16AN	11
5	COMPARISON OF BENDING MOMENT VERSUS MEAN CURVATURE FOR MODELS 20A AND 20AN	12
6	MOMENT VERSUS ROTATION FOR MODEL 10AN	13
7	AXIAL AND HOOP STRESS DISTRIBUTIONS AT MIDLENGTH FOR MODEL 10AN	14

ILLUSTRATIONS (Cont.)

Figure		Page
8	AXIAL AND HOOP STRESS DISTRIBUTIONS AT MIDLENGTH FOR MODEL 10AN	16
9	MOMENT VERSUS ANGLE OF ROTATION FOR MODEL 16AN	17
10	MOMENT VERSUS ANGLE OF ROTATION FOR MODEL 20AN	18
11	AXIAL AND HOOP STRESS DISTRIBUTIONS AT MIDLENGTH FOR MODEL 20AN AT THE FIRST LOAD STEP	19
12	MAGNITUDE OF AXIAL HARMONICS (OF COSINE-COSINE TERMS) FOR MODEL 20A WITH IMPERFECTIONS	20
13	MAGNITUDE PERIPHERAL HARMONICS (OF COSINE-COSINE TERMS) FOR MODEL 20A WITH IMPERFECTIONS	21
14	DEFORMED AND UNDEFORMED PROFILES FOR MODEL IC1 AT STEP 3, INCREMENT 30	22
15	(A) DISTRIBUTION OF AXIAL STRESS AT MIDLENGTH FOR MODEL IC1	
	(B) DISTRIBUTION OF HOOP STRESS AT MIDLENGTH FOR MODEL IC1	23
16	ENERGIES AND BENDING MOMENTS VERSUS ANGLE OF ROTATION FOR MODEL IC1	24
17	BENDING MOMENT COMPUTATION THROUGH CONSISTENT FORCES AT MIDDLE FOR MODEL IC1 (FOR HALF ONLY)	25

ILLUSTRATIONS (Cont.)

Figure		Page
18	PARAMETERS FOR MODEL IC1	29
19	CROSS-SECTION FLATTENING PARAMETER w/h VERSUS MEAN CURVATURE FOR MODEL IC1	31
20	$M/M_{ULTIMATE}$ VERSUS WORK DONE FOR MODEL IC1	32
21	$M/M_{CRITICAL}$ VERSUS CROSS-SECTION FLATTENING PARAMETER w/h FOR MODEL IC1	33
22	(A) AXIAL STRESS VERSUS PERIPHERAL LOCATION AT MIDLENGTH FOR MODEL IC1 (STEP 3, INCREMENT 30)	
	(B) HOOP STRESS VERSUS PERIPHERAL LOCATION AT MIDLENGTH FOR MODEL IC1 (STEP 3, INCREMENT 30)	34
23	(A) CRITICAL PARAMETER w/h FOR SHORT AXIAL WAVE LENGTH BUCKLING FOR MODEL IC1	
	(B) BENDING MOMENT VERSUS ANGLE OF ROTATION FOR MODEL IC1	
	(C) $M/M_{ULTIMATE}$ VERSUS $K/K_{CRITICAL}$ FOR MODEL IC1	35
24	DEFORMED AND UNDEFORMED PROFILES FOR MODEL IC1 (WITH ADDITIONAL CONSTRAINT W = 0 AT END PLATE) FOR STEP 3, INCREMENT 20	36

ILLUSTRATIONS (Cont.)

Figure		Page
25	CRITICAL PARAMETER w/h FOR SHORT AXIAL WAVE LENGTH BUCKLING FOR MODEL IC1 (WITH ADDITIONAL CONSTRAINT W = 0 AT LEFT END, WITH END PLATE) AT LOAD STEP 3, INCREMENT 4	37
26	(A) DISTRIBUTION OF AXIAL STRESS AT MIDLENGTH FOR MODEL IC1	
	(B) DISTRIBUTION OF HOOP STRESS AT MIDLENGTH FOR MODEL IC1	38
27	DEFORMED AND UNDEFORMED PROFILES FOR MODEL IC3 AT STEP 2, INCREMENT 50	39
28	BENDING MOMENT VERSUS ROTATION FOR MODEL IC3	40
29	$M/M_{ULTIMATE}$ VERSUS $K/K_{CRITICAL}$ FOR MODEL IC3	41
30	CRITICAL PARAMETER w/h PARAMETER FOR SHORT AXIAL WAVE LENGTH FOR MODEL IC3	42
31	(A) DISTRIBUTION OF AXIAL STRESS AT MIDLENGTH FOR MODEL IC3	
	(B) DISTRIBUTION OF HOOP STRESS AT MIDLENGTH FOR MODEL IC3	43

ILLUSTRATIONS (Cont.)

Figure		Page
32	(A) DISTRIBUTION OF AXIAL STRESS AT MIDLENGTH FOR MODEL IC3	
	(B) DISTRIBUTION OF HOOP STRESS AT MIDLENGTH FOR MODEL IC3	44
33	ENERGIES AND BENDING MOMENTS VERSUS ANGLE OF ROTATION FOR MODEL IC3	45
34	BENDING MOMENT COMPUTATION THROUGH CONSISTENT FORCES AT MIDDLE FOR MODEL IC3 (FOR HALF ONLY)	46
35	PARAMETERS FOR MODEL IC3	50
A-1	FORM OF DOUBLE FOURIER COEFFICIENTS IS DISPLAYED SCHEMATICALLY	A-12

TABLES

Table		Page
1	GEOMETRICAL AND MATERIAL PROPERTIES OF MODELS	51
2	CHARACTERISTIC PARAMETERS OF MODELS	52
3	IMPERFECTION ORDINATES FOR MODEL 20A	53
4	FOURIER COEFFICIENTS OF MODEL 20A WITH IMPERFECTIONS	55
5	GEOMETRICAL AND MATERIAL PROPERTIES USED FOR MODELS	57
6	CHARACTERISTICS OF MODELS OF TABLE 5	58

INTRODUCTION

The ability to analyze cylindrical shells subjected to bending loads was the topic of an earlier study.[1] In that report, three unstiffened long circular cylindrical shells were analyzed by the nonlinear finite element program ABAQUS. The computational results were then compared with experimental data. The agreement was good. This report presents:

1. Further analysis results of circularly perfect models subject to end-bending moments. This is a follow-up of References 1 and 2, including short wavelength buckling for ring-stiffened cylinders.

2. An analysis of the surface of a "nearly" circular cylinder, given its Fourier components; or inversely, construction of the Fourier coefficients from given data representing the surface.[23,24] We intend to be able to generate imperfect geometries from a perfect model and easily generate the topological model employed in the ABAQUS general nonlinear finite element computer program.[25]

Furthermore, this report extends the list of references in References 1 and 2. References 3 through 13 represent additional works on bend-buckling analysis of cylindrical shells. References 14 through 22 are additional general works on analysis of shells. Reference 23 deals with the fast Fourier transform algorithm which was not used here.

The methods applied here in connection with the surface representation[23,24] of a "nearly" cylindrical shell are described in Reference 24. Appendix A contains the mathematical details of the method employed in this report.

Appendix B contains the actual FORTRAN listing of the subroutine to be used with ABAQUS in these computations.

METHOD

FINITE ELEMENT MODELING

The analysis of a circular or near-circular cylindrical shell subject to end bending moments will be addressed here numerically. For this purpose the nonlinear finite element program ABAQUS[25] is used.

In this work, we establish first our global Cartesian frame of reference (x,y,z, Figure 1). The shell axial direction is along z. The vertical direction is indicated by x, while the transverse y is along an axis pointing out of the paper towards the reader. Again only 180° of the structure peripherally and L/2 axially are discretized with finite elements. If the cylinder is not exactly circular, then Fourier analysis of the kind indicated in Appendix A will produce the various dominant harmonics axially and peripherally. In such cases, it may be necessary to analyze 360° of the shell peripherally and even its entire length. Here it is assumed that both cylinder and loads are symmetrical for this simplification to be correct.

We discretize the cylindrical surface by ABAQUS S8R shell elements with 3 integration points across the thickness. This means that both outside, inside, and midsurfaces of the shell are considered, when stresses are computed later. The element consists of 8 nodes, 4 corner and 4 midside ones, and employs reduced integration to calculate the stiffness matrix. The program allows for geometric and material nonlinearities. Furthermore, the constitutive equations consist of a von Mises yield surface with the associated flow rule. The hardening rule considered here is isotropic.

Peripherally, the discretization allows 25 nodes (including midside ones) over 180°. Axially, depending on the length analyzed, we have a variety of total nodes.

BOUNDARY CONDITIONS AND APPLIED LOADING

The boundary conditions are given in the global system. (See Figure 1.*) They are:

1. Symmetry about the x-z plane.

   At $\theta = 0$ and $\theta = \pi$ we must have:

   $v = \varphi_x = \varphi_z = 0$

2. Symmetry about the x-y plane at midlength ($x = L/2$).

   $w = \varphi_x = \varphi_y = 0$

3. We must also remove the vertical rigid body motion (x axis) and apply our external loading in the form of a rotation about the global transverse axis y. These two aspects have been explained in length in References 1, 2, and 25, and are omitted here.

APPLICATIONS AND RESULTS

This report contains results on two types of cylindrical shells, unstiffened and ring-stiffened. The unstiffened shells represent variations of the Jisra models reported in.[1,2] The ring-stiffened models represent results of shells already tested in purely axial compression[26] and can only be used for further study, since no other ring-stiffened data suitable for marine applications are available.

In this report we analyzed again models 10A, 16A, and 20A of Jisra[1,2] and they will be referred to as models 10AN, 16AN, and 20AN, respectively. They differ from models 10A, 16A, and 20A because, in this case, the analyzed span L_R is shorter, as indicated in Figure 2. Tables 1 and 2 give the model characteristics.

Figure 3 is a comparison of the analysis of models 10A and 10AN.[1,2] Furthermore, the included tabular form can facilitate the comparison. Figures 4 and 5 report results for models 16AN and 20AN compared with previous computations. The disagreement is more pronounced for model 20AN than the first two. Looking at Figures 4 and 5 we also notice that the slopes are not exactly the same. However, if more initial points were saved at the beginning of the computations, then the slopes would have agreed. This is known from model 10AN, for which the initial analyses were stored for this purpose. Our first conclusion, therefore, is that the thicker and shorter the cylinder is, the more important the length becomes (reduction in computed bending moment was about 9%).

---

* v = Translation along global y axis (laterally)
w = Translation along global z axis (longitudinally)
φ_x = Rotation about global x axis
φ_y = Rotation about global y axis
φ_z = Rotation about global z axis

Figures 6, 7, and 8 pertain to model 10AN. In Figure 6 the moment-rotation relation is given. The table in Figure 6 gives the corresponding total energies as deformation progresses. Figure 7 shows how the bending moment is independently computed for various angles of rotation (indicated as steps*). Axial and hoop stresses are also given for the first stored step of the analysis. Figure 8 gives the stresses for the last stored step.

Figure 9 pertains to model 16AN and is similar to Figure 6. It is the moment-rotation relation that is displayed. Figure 10 contains the same information as in Figures 6 and 9, but it applies to model 20AN. Figure 11 is a tabular form of the axial and hoop stresses at midlength for the very first increment, i.e. for an angle of 0.948961 degs. The previous given figures (6-11) only add to a better understanding of the type of results to expect with the method so far.

Table 3 gives the ordinates of the imperfect model 20A and Table 4, the corresponding double Fourier coefficients. We observe that the imperfections of this model are over 360°. Figures 12 and 13 display some of the harmonics. For example, Figure 12 gives the magnitude of the fundamental, first, and second axial harmonics of the cosine-cosine coefficients. Similarly, Figure 13 displays the magnitude of the fundamental, first, and second peripheral harmonics of the cosine-cosine coefficients. The purpose of this analysis is to establish the software for quickly producing the dominant harmonics of imperfect cylindrical shells. It is known that preexisting mode patterns will affect the final pattern whether there will be a change of mode or not. In fact, there will be an amplification along the "preferred imperfection." Such behavior will induce buckling and lead to faster collapse. The application is certainly obvious, not only for bend-buckling but for other forms of structural instabilities, static or dynamic. As a result, a FORTRAN computer program was written for VAX 11/785, implementing Appendix A in such a way that the user can either obtain the Fourier coefficients of given imperfection data or, given the imperfection Fourier coefficients, obtain the configuration. Here we observe again that some of the boundary conditions will have to change to correctly account for 360° models, and bend-buckling results with imperfections will be presented elsewhere.

Tables 5 and 6 display some of the geometric characteristics of the ring-stiffened shells which form the second topic of this report. The models are referred to by names IC1 and IC3.[26,27] They were chosen because, at least, axial compression tests had already been carried out and reported elsewhere.[26] Figure 14 represents the deformed profile of model IC1 at step 3, increment 30, i.e. for an angle of rotation of 0.231937 degs, as can be deduced from Figure 16. Figure 15 displays the longitudinal and hoop stresses for the very first stored step (step 1, increment 5). We observe that the hoop

*In these analyses, the rotation is increased gradually. During such a process or "step" or "increment," various quantities are computed and stored. For example, in Figure 6, what the ABAQUS computer program refers to as "step 1, increment 15" was the third "stored increment" or "step."

The step size is not constant but usually changes during the computation. It increases linearly and in the present context it represents change of angle of rotation. The reported values represent the stored values and not the actual number of steps carried out by ABAQUS.

stress distribution at midlength (because this is the location for which it has been plotted together with the longitudinal stresses at the midsurface) differs markedly from the stress distribution of unstiffened cylinders in bending (see Figure 7 for example).

Figure 16 relates to energies, bending moments, angles of rotation, while Figure 17 gives results of bending moments from consistent loads. Figure 18 is additional information for model IC1.

Figure 19 plots cross-section flattening* versus mean curvature. Figure 20 displays external work versus nondimensional bending moment M/M_{ULT}.

Figure 21 displays cross-section flattening versus M/M_{CR}. Figure 22 gives the distribution of axial and hoop stresses at the last step (step 3, increment 30) graphically and numerically. Finally, Figure 23 contains 3 plots. The last two are moment curvature plots, while the first represents the plot of the difference of radial displacements** from the left end (0%) of the cylinder, where the moment (rotation actually) is applied up to midlength (50%). This is for the compression side at midthickness. Observe that at the left end (0%) this difference is nonzero, because the radial displacement w is not restricted there. Essentially, similar results (Figure 24) are obtained when the displacement w is restricted (w = o) at the left end cross-section, where the bending moment is being applied. This is the case in this situation because of end plates. Notice that in this case, Figure 25 compares with the top plot of Figure 23, except that at the left end (0%) the nondimensional difference of radial displacements is zero.

By Figure 16 or 18, when the *bending moment* is about 21,574 K-in (at center and end sections of cylindrical shell) the finite element program (ABAQUS) predicts short wavelength (local) buckling. Table 6 indicates that the critical theoretical bifurcation bending moment of the end panel there reaches 21,495.3 K-in with a theoretical end panel critical stress of 69.5 ksi. The approximate compressive buckling stress by ABAQUS was about 49.18 ksi. (See Figure 26.) In all of these finite element calculations, the bending moment has been obtained in two different ways, i.e. either as:

(1) A direct output from ABAQUS (See bottom of Figure 16, where bending moments are given in terms of angle of rotation.) In the case of model IC1, the critical bending moment was calculated this way as 21,574 K-in.

---

*Cross-section flattening ($\Delta w/h$) is defined as:
$\Delta w/h = [\ w(L/2,0) + w(L/2,\pi)\ ]/h$

**More specifically, consider the radial displacement w at a load level (in the present instant rotation level) at which instability is assumed to occur (reference state). Then following Almroth's suggestion, we construct the nondimensional difference of radial displacement distributions $\delta w/h$ at the compression side for load levels higher than the reference one. These are plotted axially and are referred to as "critical parameter for short axial wavelength buckling." Figures 19, 20, 21, and 23 indicate discontinuities at the point of buckling.

(2) Indirectly, based on the consistent reaction forces and their respective arms from the position of neutral axis. (See the last four pages of Figure 17.) In the case of model IC1, such an analysis gave 2 X 10,783.8 = 21.567 K-in. (Refer also to Figure 18 for such a summary.)

Reference 26 (Table 5) gives a much lower "failure stress" (25.6 ksi) for the center panel, for the case of pure compression. Figure 26, used in conjunction with Figure 16, gives the axial and hoop stress distributions for model IC1 at step 2, increment 20, i.e. around the onset of buckling.

Figure 27 displays the deformed and undeformed profile of model IC3. Figures 28 and 29 are plots of bending moment versus angle of rotation and a nondimensional curvature, while Figure 30 gives the critical parameter for short wavelength (local) buckling.

Figures 31 and 32 present the axial and hoop stress distributions for model IC3 for two different loading states. Figure 31 corresponds to step 2, increment 25, while Figure 32 to step 2, increment 50. This means that Figure 31 corresponds to the onset of buckling (giving an approximate maximum compressive stress of 51.72 ksi) while Figure 32, to the last recorded load step with a maximum compressive stress of 52.2 ksi. Therefore, for model IC3 ABAQUS directly predicted a peak bending moment of 8,689.45 K-in (Figure 33) or by indirect computation (as explained for model IC1) 8,690.34 K-in (Figure 34). This can be seen from Figure 33 which relates energies, moments, angle of rotation, step, and increment for model IC3. Here some further background is necessary to bridge these results with the few experimental data that are available. In 1961 (see Reference 59 of Reference 1), Seide and Weingarten performed a bifurcation analysis for a circular cylindrical shell subject to end bending moments and concluded that "the critical stress attained was very close to the one of a circular cylinder subject to axial loading." (In Table 2, the critical stress and moment are identified as σ_{CR}, M_{CR}.) Consequently, although the experimental results for models IC1 and IC3 pertain to axial compression and "failure loads," an assessment is in order to evaluate our own modeling strategy in this light with the objective of further validation of the employed modeling. Very specifically, the experimental failure stresses should be less than the ones predicted by ABAQUS. How much smaller they should be depends on the exact position reached (axial compressive strain at failure) at the end of the test. Furthermore, the stresses and bending moments obtained by the finite element procedure should not exceed the values by bifurcation theory for purely elastic cases (within round off errors). In the case of plasticity, the bending moment obtained by simple beam theory offers such a guide. A final point in this discussion concerns the fact that the experimentally obtained stresses represent "failure stresses" and not stresses at the exact point of instability, hence the drop in the load that could be carried there.

Finally, we observe from Table 5 that the experimental end panel failure stress for IC3 for pure compression is 36.404 ksi. Table 6 gives the theoretical buckling stress for model IC3 as 115.928 ksi. At this point, observe that the differences between both experimental failure stress (25.671 ksi and 36.404 ksi for models IC1 and IC3) and the computational results (49.18 ksi and 51.72 ksi, respectively) are due to the highly unstable postbuckling behavior of the structure.

There are small differences between some of the constants of Table 6 and their values on Figure 18 (model IC1) and Figure 35 (model IC3). This is because Table 6 was manually generated.

In conclusion, in spite of the differences in stress levels, which might be attributed to the fact that some of the material constants were inconsistent (see Ref. 26), it has been demonstrated that plots of the critical parameter for short axial wavelength (local) buckling do indeed capture the mechanism as it grows with load increase. The hoop stress distribution changes shape radically (compare Figure 15 with Figure 22). Furthermore, the cross-section flattening parameter plot shows a discontinuity at the point of short wavelength buckling initiation.

SUMMARY

The present strategy is easy to grasp and it can be used in conjunction with a general nonlinear finite element computer program to predict the mode of failure of a cylindrical shell subject to end-bending moments. However, a number of problems exist that must be addressed, such as verification of the moment-curvature relations for ring-stiffened shells.

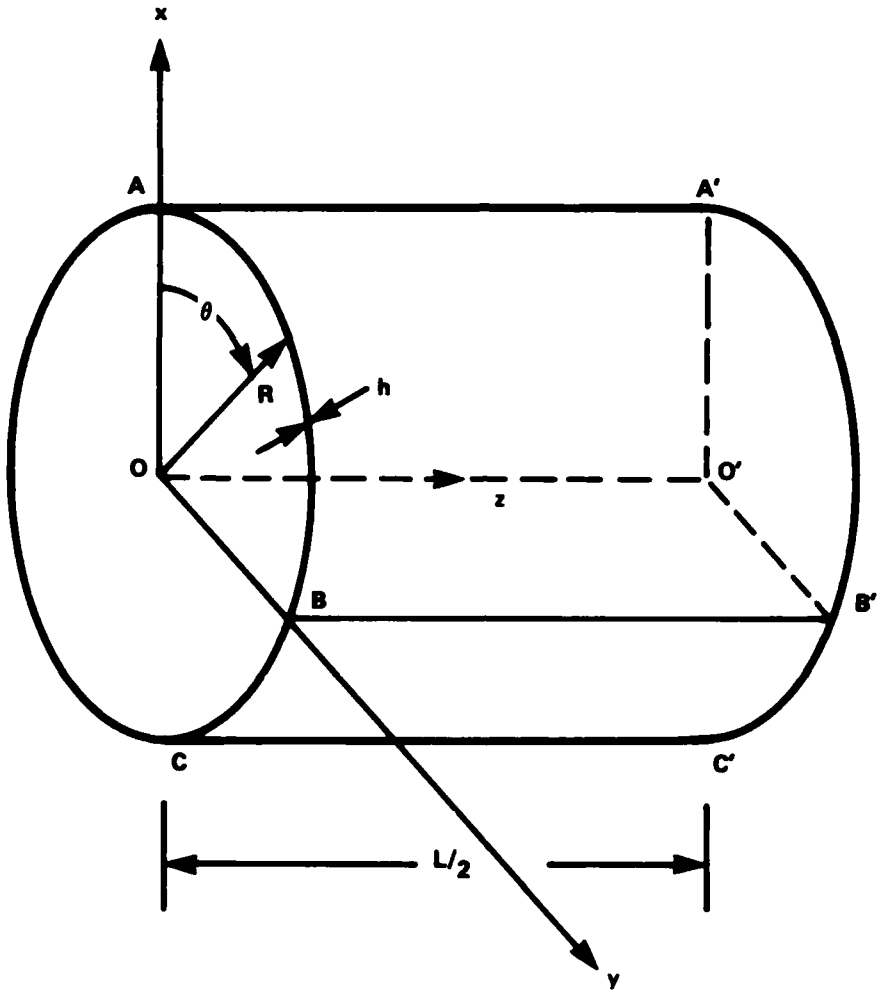

FIGURE 1. STRAIGHT CYLINDRICAL SHELL OF HALF LENGTH $L/_2$, MEAN RADIUS R, THICKNESS h, AND ASSOCIATED GLOBAL CARTESIAN COORDINATE SYSTEM (x, y, z)

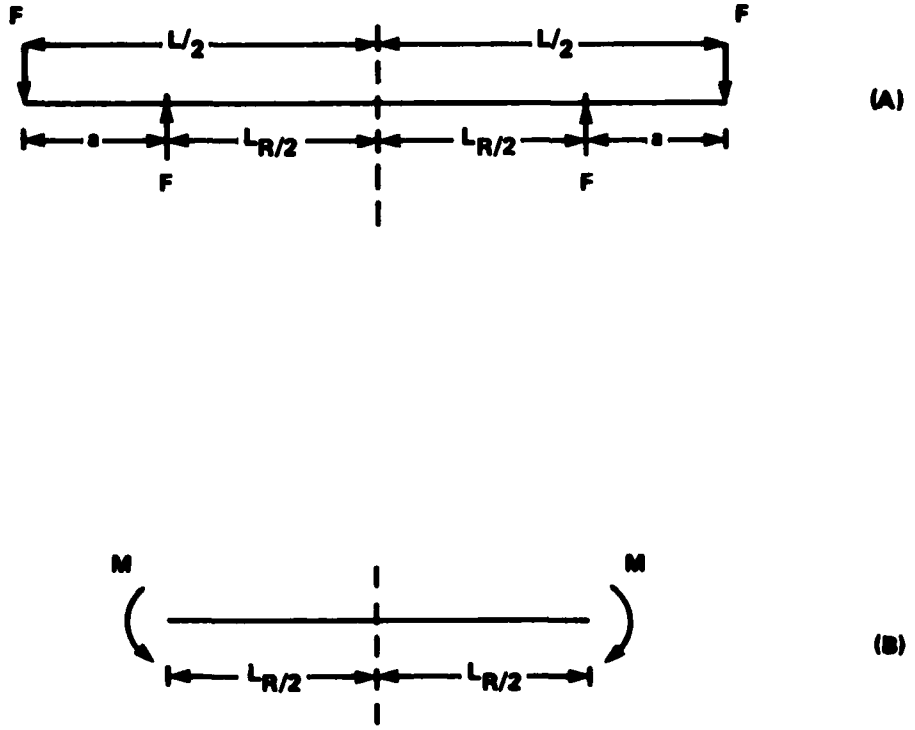

FIGURE 2. (A) CYLINDRICAL SHELL (SHOWN AS A BEAM) OF LENGTH L SUBJECT TO SHEARING LOADS F, PRODUCING A BENDING MOMENT M = Fa (THIS CONFIGURATION APPLIES TO MODELS 10A, 16A, 20A.)
(B) CYLINDRICAL SHELL OF A REDUCED LENGTH L_R SUBJECT TO AN EXTERNAL BENDING MOMENT M = Fa (THIS APPLIES TO MODELS 10AN, 16AN AND 20AN, RESPECTIVELY.)

MODELS 10A AND 10AN

MEAN CURVATURE (1/FT)	BENDING MOMENT (KIP-FT)	
0.00000000E+00	0.00000000E+00	
0.27777806E-02	0.59377747E+02	
0.56555041E-02	0.10160806E+03	
0.66667171E-02	0.10742601E+03	
0.73611043E-02	0.10972126E+03	
0.80556478E-02	0.11122174E+03	
0.87501332E-02	0.11254790E+03	
0.94446018E-02	0.11338049E+03	
0.10139077E-01	0.11408494E+03	
0.10833550E-01	0.11476392E+03	
0.11528044E-01	0.11538371E+03	MODEL 10A
0.12222553E-01	0.11592906E+03	
0.12917073E-01	0.11643250E+03	
0.13611565E-01	0.11684409E+03	
0.14306070E-01	0.11721547E+03	
0.15000574E-01	0.11757902E+03	
0.17028568E-01	0.11859760E+03	
0.18752335E-01	0.11944928E+03	
0.19764664E-01	0.11992509E+03	
0.20224798E-01	0.12011456E+03	
0.20684898E-01	0.12030072E+03	
0.21144971E-01	0.12049264E+03	
0.00000000E+00	0.00000000E+00	
0.33333303E-02	0.71204742E+02	
0.66667181E-02	0.10739919E+03	
0.70833978E-02	0.10890540E+03	
0.91668135E-02	0.11303976E+03	MODEL 10AN
0.11250257E-01	0.11510048E+03	
0.13333785E-01	0.11660181E+03	
0.15417339E-01	0.11766798E+03	
0.17500974E-01	0.11862437E+03	

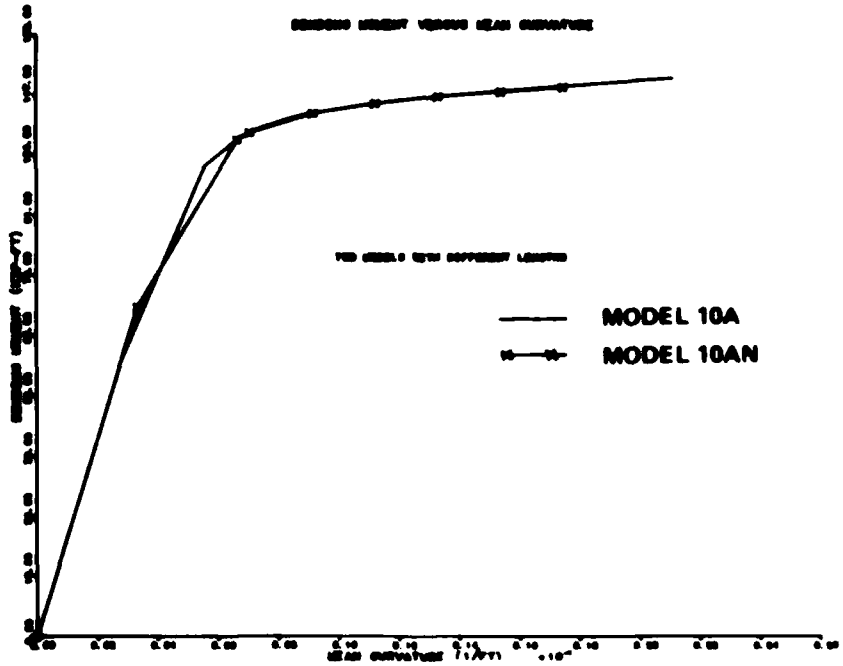

FIGURE 3. COMPARISON OF BENDING MOMENT VERSUS MEAN CURVATURE FOR MODELS 10A AND 10AN

MODELS 16A AND 16AN

MEAN CURVATURE (1/FT)	BENDING MOMENT (KIP-FT)	
0.00000000E+00	0.00000000E+00	MODEL 16A
0.33796293E-03	0.20035555E+02	
0.16504445E-02	0.13672000E+03	
0.30667229E-02	0.22251400E+03	
0.34192301E-02	0.23593643E+03	
0.39707906E-02	0.24120400E+03	
0.43223710E-02	0.24516673E+03	
0.46739401E-02	0.24707016E+03	
0.50255167E-02	0.25024496E+03	
0.51055022E-02	0.25100702E+03	
0.53456426E-02	0.25174000E+03	
0.55057057E-02	0.25227562E+03	
0.56657679E-02	0.25279304E+03	
0.58258316E-02	0.25330969E+03	
0.59858942E-02	0.25382596E+03	
0.61459580E-02	0.25434104E+03	
0.63060224E-02	0.25485419E+03	
0.64660879E-02	0.25535779E+03	
0.66261524E-02	0.25580310E+03	
0.67862179E-02	0.25621359E+03	
0.69462800E-02	0.25661322E+03	
0.70967493E-02	0.25697522E+03	
0.72472114E-02	0.25733237E+03	
0.73976777E-02	0.25765933E+03	
0.75481444E-02	0.25791724E+03	
0.76986030E-02	0.25813006E+03	
0.78490591E-02	0.25834747E+03	
0.79995161E-02	0.25853864E+03	
0.81499666E-02	0.25871335E+03	
0.83004134E-02	0.25889285E+03	
0.83831567E-02	0.25899762E+03	
0.84207663E-02	0.25904730E+03	
0.00000000E+00	0.00000000E+00	MODEL 16AN
0.22222255E-02	0.15088214E+03	
0.36111205E-02	0.22463954E+03	
0.38889109E-02	0.23067369E+03	
0.41666939E-02	0.23567586E+03	
0.52778362E-02	0.24721289E+03	
0.66667804E-02	0.25350754E+03	
0.80557400E-02	0.25707211E+03	

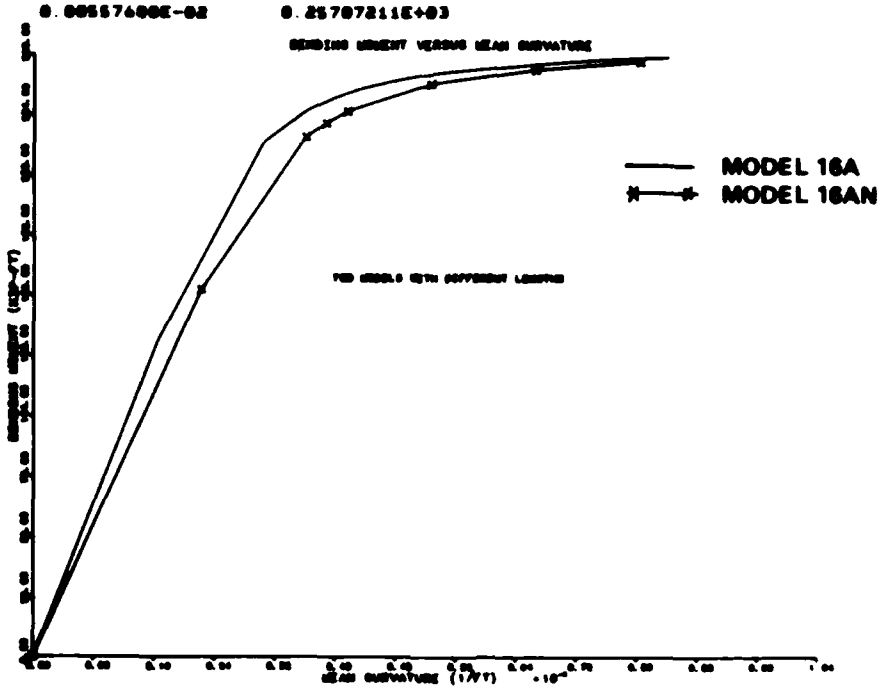

FIGURE 4. COMPARISON OF BENDING MOMENT VERSUS MEAN CURVATURE FOR MODELS 16A AND 16AN

MODELS 20A AND 20AN

MEAN CURVATURE (1/FT)	BENDING MOMENT (KIP-FT)	
0.00000000E+00	0.00000000E+00	
0.33796293E-03	0.52361568E+02	
0.12754640E-02	0.19720113E+03	
0.22129680E-02	0.33730643E+03	
0.31504813E-02	0.39875580E+03	
0.39473758E-02	0.42090363E+03	
0.41817576E-02	0.42434280E+03	
0.44161407E-02	0.42765866E+03	
0.46505262E-02	0.43050354E+03	
0.48849112E-02	0.43245026E+03	MODEL 20A
0.51192953E-02	0.43406573E+03	
0.53536799E-02	0.43553680E+03	
0.55880644E-02	0.43698962E+03	
0.58224513E-02	0.43836884E+03	
0.60568429E-02	0.43963071E+03	
0.62912297E-02	0.44069992E+03	
0.65256148E-02	0.44175455E+03	
0.67600049E-02	0.44282471E+03	
0.69943932E-02	0.44368170E+03	
0.72287684E-02	0.44451007E+03	
0.73576709E-02	0.44500220E+03	
0.00000000E+00	0.00000000E+00	
0.22222276E-02	0.30878256E+03	
0.36111395E-02	0.37701691E+03	
0.36805850E-02	0.37863193E+03	
0.40278197E-02	0.38478830E+03	
0.43750522E-02	0.38916733E+03	
0.47222944E-02	0.39271204E+03	
0.92442269E-02	0.40399887E+03	MODEL 20AN
0.95767342E-02	0.40403351E+03	
0.99092554E-02	0.40399268E+03	
0.10042273E-01	0.40395041E+03	
0.10121251E-01	0.40391843E+03	
0.10200233E-01	0.40388010E+03	
0.10279216E-01	0.40383749E+03	
0.10358199E-01	0.40378708E+03	

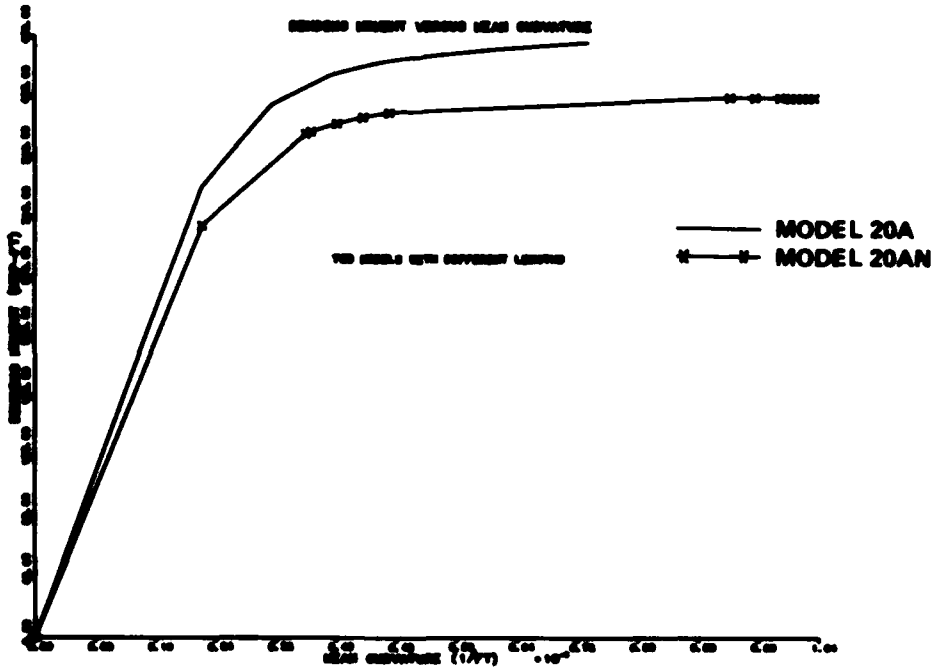

FIGURE 5. COMPARISON OF BENDING MOMENT VERSUS MEAN CURVATURE FOR MODELS 20A AND 20AN

INCREMENT NO	STRAIN ENERGY	EXTERNAL WORK DONE	PLASTIC DISSIPATION	ABAQUS STEP	ABAQUS INCREMENT
1	0.103621E+05	0.203182E+05	0.668660E+04	1	5
2	0.115080E+05	0.287017E+05	0.139008E+05	1	10
3	0.122100E+05	0.372748E+05	0.217550E+05	1	15
4	0.128000E+05	0.459785E+05	0.298566E+05	1	20
5	0.132372E+05	0.547727E+05	0.382039E+05	1	25
6	0.136610E+05	0.636412E+05	0.466388E+05	1	30

THIS TABLE IS DIRECTLY COMPUTED BY ABAQUS

STEP NO	TOTAL BENDING MOMENT AT AUXILIARY NODE (LB-IN)	ROTATION ABOUT GLOBAL Y-AXIS (DEGREES)
1	0.130686E+07	0.121754E+01
2	0.135648E+07	0.157563E+01
3	0.138121E+07	0.193373E+01
4	0.139922E+07	0.229183E+01
5	0.141202E+07	0.264993E+01
6	0.142349E+07	0.300803E+01

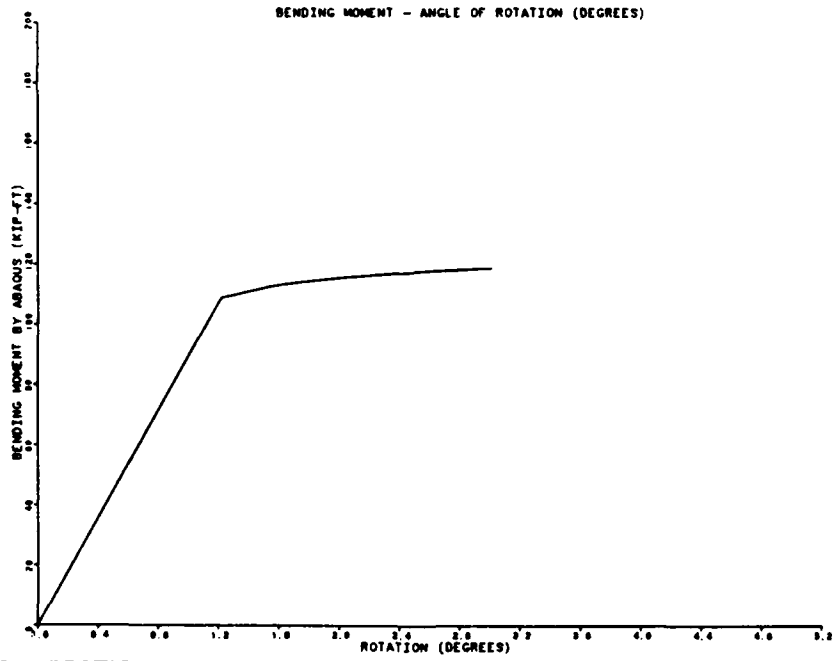

NOTE: MODEL 10AN WITH IMPERFECTIONS

FIGURE 6. MOMENT VERSUS ROTATION FOR MODEL 10AN

TOTAL MOMENTS ARE FOR 180° OF CYLINDER

BENDING MOMENTS AT CUT NO 2

NODE NO	STEP 1 FORCE ZZ	STEP 1 ARM XX	STEP 2 FORCE ZZ	STEP 2 ARM XX	STEP 3 FORCE ZZ	STEP 3 ARM XX
301	0.295076E+04	0.561824E+01	0.297070E+04	0.572101E+01	0.299015E+04	0.582279E+01
302	0.118120E+05	0.557386E+01	0.118917E+05	0.567692E+01	0.119696E+05	0.577900E+01
303	0.590555E+04	0.544165E+01	0.594461E+04	0.554551E+01	0.598351E+04	0.564850E+01
304	0.117901E+05	0.522339E+01	0.118696E+05	0.532848E+01	0.119456E+05	0.543285E+01
305	0.589048E+04	0.492276E+01	0.593407E+04	0.502937E+01	0.597122E+04	0.513542E+01
306	0.115516E+05	0.454341E+01	0.118262E+05	0.465164E+01	0.118932E+05	0.475948E+01
307	0.569194E+04	0.409396E+01	0.591234E+04	0.420374E+01	0.592028E+04	0.431328E+01
308	0.108397E+05	0.358011E+01	0.115208E+05	0.369122E+01	0.117765E+05	0.380223E+01
309	0.496124E+04	0.301064E+01	0.577251E+04	0.312280E+01	0.592445E+04	0.323495E+01
310	0.723926E+04	0.239547E+01	0.923241E+04	0.250834E+01	0.103604E+05	0.262125E+01
311	0.247760E+04	0.174561E+01	0.323185E+04	0.185891E+01	0.414004E+04	0.197225E+01
312	0.245366E+04	0.107116E+01	0.315793E+04	0.118466E+01	0.386874E+04	0.129820E+01
313	-0.247159E+02	0.385290E+00	-0.410146E+02	0.498845E+00	-0.541710E+02	0.612437E+00
314	-0.254678E+04	-0.300755E+00	-0.331268E+04	-0.187217E+00	-0.407170E+04	-0.736398E-01
315	-0.252116E+04	-0.975737E+00	-0.331093E+04	-0.862189E+00	-0.424340E+04	-0.748601E+00
316	-0.736040E+04	-0.162644E+01	-0.931519E+04	-0.151278E+01	-0.104597E+05	-0.139908E+01
317	-0.498287E+04	-0.224272E+01	-0.577450E+04	-0.212877E+01	-0.591846E+04	-0.201479E+01
318	-0.108425E+05	-0.281351E+01	-0.115111E+05	-0.269905E+01	-0.117532E+05	-0.258449E+01
319	-0.567959E+04	-0.332884E+01	-0.589420E+04	-0.321360E+01	-0.589582E+04	-0.309820E+01
320	-0.115163E+05	-0.377980E+01	-0.117714E+05	-0.366358E+01	-0.118261E+05	-0.354707E+01
321	-0.586702E+04	-0.416058E+01	-0.589915E+04	-0.404327E+01	-0.592839E+04	-0.392554E+01
322	-0.117306E+05	-0.446244E+01	-0.117896E+05	-0.434408E+01	-0.118477E+05	-0.422513E+01
323	-0.587018E+04	-0.468166E+01	-0.589969E+04	-0.456240E+01	-0.592863E+04	-0.444244E+01
324	-0.117397E+05	-0.481448E+01	-0.117985E+05	-0.469462E+01	-0.118557E+05	-0.457399E+01
325	-0.293211E+04	-0.485906E+01	-0.294669E+04	-0.473900E+01	-0.296080E+04	-0.461813E+01
TOTAL OUT OF BALANCE FORCE ZZ	-0.324707E-01		0.129395E-01		0.214844E-01	
TOTAL MOMENT	0.653390E+06		0.678197E+06		0.690534E+06	
FORCE ZZ ON TOP QUARTER	0.836139E+05		0.892646E+05		0.927438E+05	
FORCE ZZ ON BOTTOM QUARTER	-0.836140E+05		-0.892646E+05		-0.927438E+05	
POINT OF ZERO FORCE	0.532552E+00		0.658711E+00		0.778992E+00	
PERCENTAGE OUT OF BALANCE FORCE ZZ	0.00		0.00		0.00	

NOTE: MODEL 10AN WITH IMPERFECTIONS COMPUTES BENDING MOMENTS FOR HALF MODEL

FIGURE 7. AXIAL AND HOOP STRESS DISTRIBUTIONS AT MIDLENGTH FOR MODEL 10AN

TOTAL MOMENTS ARE FOR 180° OF CYLINDER

NODE NO	STEP 4 FORCE ZZ	STEP 4 ARM XX	STEP 5 FORCE ZZ	STEP 5 ARM XX	STEP 6 FORCE ZZ	STEP 6 ARM XX
301	0.301479E+04	0.592331E+01	0.304174E+04	0.602250E+01	0.306793E+04	0.612048E+01
302	0.120650E+05	0.587988E+01	0.121733E+05	0.597946E+01	0.122788E+05	0.607786E+01
303	0.602911E+04	0.575037E+01	0.608350E+04	0.585105E+01	0.613642E+04	0.595065E+01
304	0.120259E+05	0.553624E+01	0.121307E+05	0.563861E+01	0.122353E+05	0.574004E+01
305	0.600720E+04	0.524067E+01	0.605581E+04	0.534508E+01	0.610830E+04	0.544874E+01
306	0.119596E+05	0.486671E+01	0.120334E+05	0.497330E+01	0.121228E+05	0.507932E+01
307	0.594796E+04	0.442240E+01	0.597627E+04	0.453105E+01	0.600905E+04	0.463932E+01
308	0.118314E+05	0.391296E+01	0.118743E+05	0.402338E+01	0.119157E+05	0.413357E+01
309	0.593475E+04	0.334692E+01	0.593568E+04	0.345870E+01	0.592712E+04	0.357035E+01
310	0.111729E+05	0.273405E+01	0.114054E+05	0.284673E+01	0.115142E+05	0.295935E+01
311	0.490622E+04	0.208552E+01	0.538661E+04	0.219870E+01	0.580640E+04	0.231185E+01
312	0.455724E+04	0.141168E+01	0.525773E+04	0.152508E+01	0.594174E+04	0.163845E+01
313	-0.783798E+02	0.725966E+00	-0.962802E+02	0.839412E+00	-0.125566E+03	0.952836E+00
314	-0.485238E+04	0.398707E-01	-0.561892E+04	0.153300E+00	-0.634439E+04	0.266707E+00
315	-0.500499E+04	-0.635085E+00	-0.549745E+04	-0.521645E+00	-0.591537E+04	-0.408228E+00
316	-0.112339E+05	-0.128544E+01	-0.114537E+05	-0.117188E+01	-0.115742E+05	-0.105830E+01
317	-0.593465E+04	-0.190080E+01	-0.593223E+04	-0.178684E+01	-0.592279E+04	-0.167279E+01
318	-0.118020E+05	-0.246984E+01	-0.118405E+05	-0.235509E+01	-0.118780E+05	-0.224016E+01
319	-0.591970E+04	-0.298253E+01	-0.594356E+04	-0.286663E+01	-0.597292E+04	-0.275040E+01
320	-0.118806E+05	-0.343012E+01	-0.119429E+05	-0.331276E+01	-0.120210E+05	-0.319488E+01
321	-0.595653E+04	-0.380715E+01	-0.599837E+04	-0.368818E+01	-0.604302E+04	-0.356849E+01
322	-0.119111E+05	-0.410535E+01	-0.119989E+05	-0.398481E+01	-0.120858E+05	-0.386336E+01
323	-0.596519E+04	-0.432149E+01	-0.600948E+04	-0.419963E+01	-0.605251E+04	-0.407671E+01
324	-0.119321E+05	-0.445227E+01	-0.120200E+05	-0.432953E+01	-0.121051E+05	-0.420563E+01
325	-0.298056E+04	-0.449613E+01	-0.300220E+04	-0.437308E+01	-0.302308E+04	-0.424883E+01
TOTAL OUT OF BALANCE FORCE ZZ	0.153809E-01		0.610352E-02		0.371094E-01	
TOTAL MOMENT	0.699495E+06		0.705810E+06		0.711425E+06	
FORCE ZZ ON TOP QUARTER	0.954521E+05		0.973544E+05		0.990638E+05	
FORCE ZZ ON BOTTOM QUARTER	-0.954521E+05		-0.973544E+05		-0.990638E+05	
POINT OF ZERO FORCE	0.900390E+00		0.101820E+01		0.113577E+01	
PERCENTAGE OUT OF BALANCE FORCE ZZ	0.00		0.00		0.00	

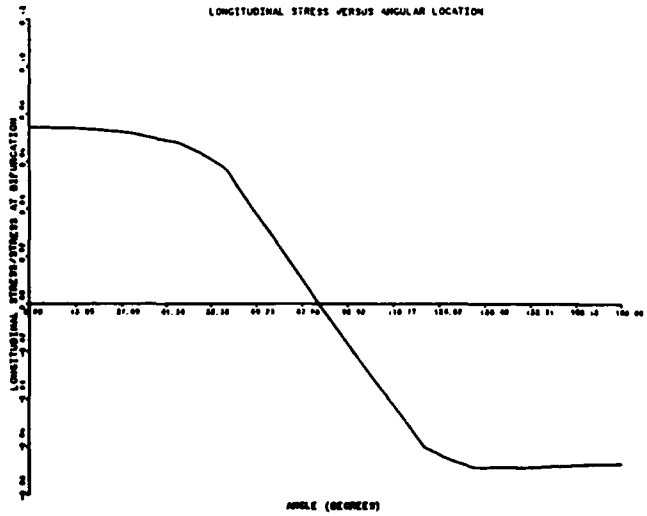

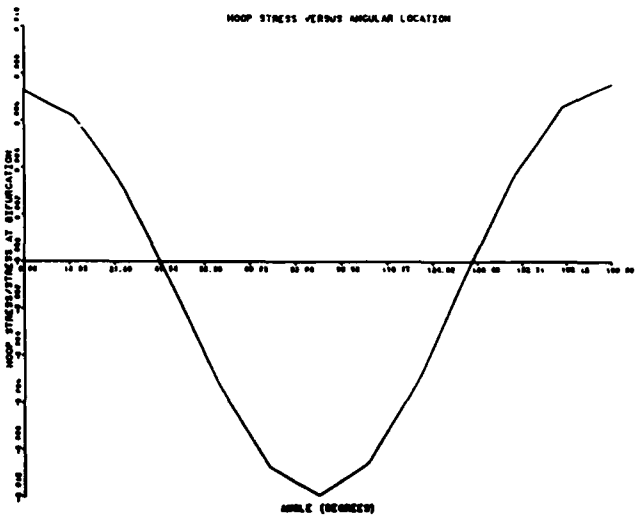

NOTE: MODEL 10AN WITH IMPERFECTIONS

STEP 1, INCREMENT 5, WITH PLASTIC DISSIPATION = 6686.6 lb-in, ANGLE OF ROTATION = 1.217 deg
TOTAL BENDING MOMENT = 1.30686×10^6 lb-in

FIGURE 7. (CONTINUED)

STEP NO 6 FOR STRESSES

ANGLE (DEGREES)	LONGITUDINAL MEMBRANE STRESS (PSI)	NONDIMENSIONAL MEMBRANE LONGITUDINAL STRESS	HOOP STRESS (PSI)	NONDIMENSIONAL HOOP STRESS
0.000	0.627772E+05	0.808620E-01	0.133165E+05	0.171527E-01
7.576	0.623431E+05	0.803028E-01	0.122682E+05	0.158025E-01
15.151	0.619201E+05	0.797579E-01	0.111956E+05	0.144209E-01
22.704	0.605740E+05	0.780241E-01	0.825298E+04	0.106305E-01
30.241	0.592030E+05	0.762582E-01	0.526428E+04	0.678081E-02
37.761	0.568482E+05	0.732250E-01	0.104852E+04	0.135058E-02
45.246	0.544551E+05	0.701424E-01	-.319071E+04	-.410989E-02
52.707	0.514739E+05	0.663024E-01	-.765981E+04	-.986644E-02
60.159	0.485925E+05	0.625910E-01	-.121387E+05	-.156356E-01
67.587	0.452500E+05	0.582855E-01	-.155863E+05	-.200763E-01
75.000	0.453430E+05	0.584053E-01	-.192195E+05	-.247563E-01
82.414	0.207462E+05	0.267227E-01	-.210021E+05	-.270524E-01
89.817	-.754981E+04	-.972475E-02	-.223950E+05	-.288465E-01
97.222	-.354746E+05	-.456941E-01	-.212457E+05	-.273661E-01
104.642	-.616167E+05	-.793672E-01	-.201164E+05	-.259115E-01
112.067	-.606059E+05	-.780652E-01	-.162286E+05	-.209038E-01
119.514	-.608407E+05	-.784192E-01	-.123108E+05	-.158573E-01
126.990	-.591007E+05	-.761367E-01	-.765263E+04	-.985719E-02
134.482	-.575799E+05	-.741674E-01	-.302055E+04	-.389457E-02
142.003	-.557753E+05	-.718429E-01	0.118424E+04	0.152539E-02
149.564	-.539557E+05	-.694992E-01	0.537192E+04	0.691946E-02
157.146	-.524104E+05	-.675190E-01	0.825548E+04	0.106337E-01
164.747	-.508948E+05	-.655566E-01	0.111154E+05	0.143175E-01
172.373	-.502908E+05	-.647785E-01	0.121446E+05	0.156432E-01
180.000	-.497258E+05	-.640508E-01	0.131365E+05	0.169209E-01

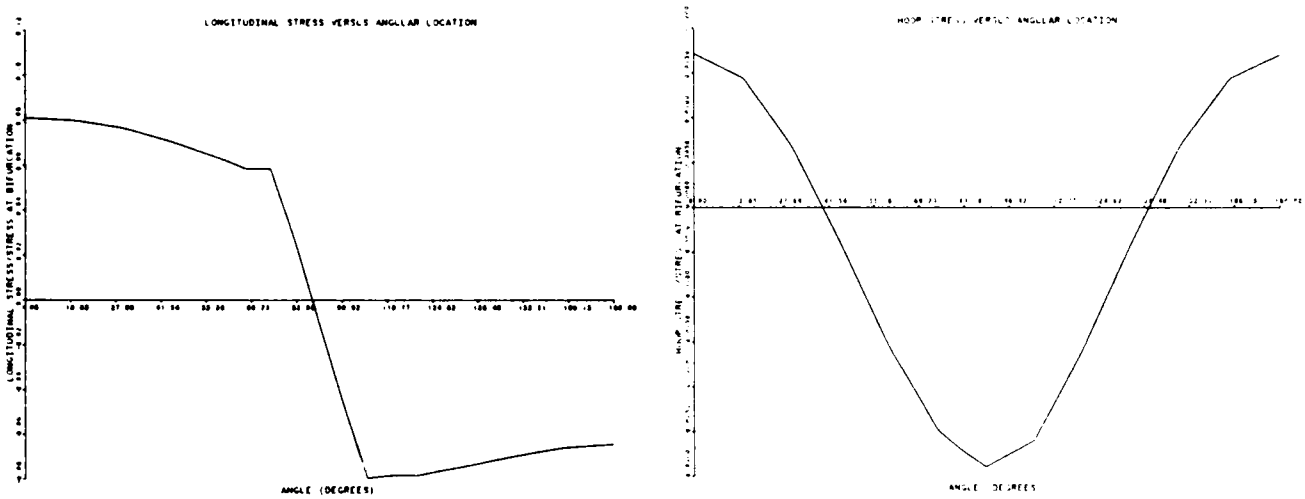

MODEL 10AN

STEP 1, INCREMENT 30, PLASTIC DISSIPATION = 46638.8 lb-in, ANGLE OF ROTATION = 3.008 deg
TOTAL BENDING MOMENT = 1.42349x10^6 lb-in

FIGURE 8. AXIAL AND HOOP STRESS DISTRIBUTIONS AT MIDLENGTH FOR MODEL 10AN

INCREMENT NO	STRAIN ENERGY	EXTERNAL WORK DONE	PLASTIC DISSIPATION	ABAQUS STEP	ABAQUS INCREMENT
1	0.205964E+05	0.341737E+05	0.695294E+04	1	5
2	0.244616E+05	0.523336E+05	0.211079E+05	1	10
3	0.265357E+05	0.711984E+05	0.378447E+05	1	15
4	0.281037E+05	0.903815E+05	0.554258E+05	1	20

THIS TABLE IS DIRECTLY COMPUTED BY ABAQUS

STEP NO	TOTAL BENDING MOMENT AT AUXILIARY NODE (LB-IN)	ROTATION ABOUT GLOBAL Y-AXIS (DEGREES)
1	0.276808E+07	0.100268E+01
2	0.296655E+07	0.136077E+01
3	0.304209E+07	0.171887E+01
4	0.308487E+07	0.207697E+01

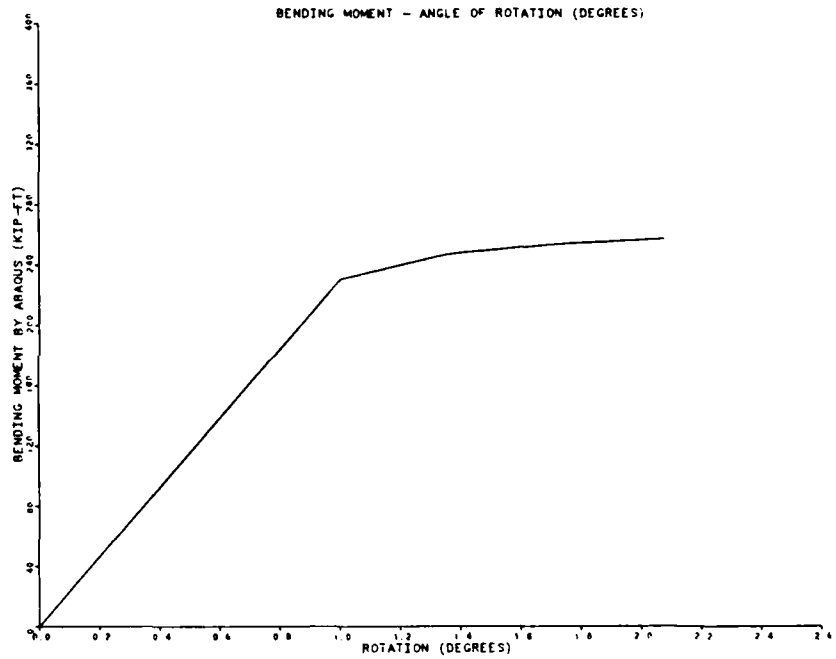

NOTE: MODEL 16AN

FIGURE 9. MOMENT VERSUS ANGLE OF ROTATION FOR MODEL 16AN

INCREMENT NO.	STRAIN ENERGY	EXTERNAL WORK DONE	PLASTIC DISSIPATION	ABAQUS STEP	ABAQUS INCREMENT
1	0.289405E+05	0.572052E+05	0.170639E+05	1	5
2	0.302689E+05	0.643799E+05	0.228967E+05	1	10
3	0.313454E+05	0.716441E+05	0.290754E+05	1	15
4	0.323225E+05	0.789833E+05	0.354289E+05	1	20
5	0.391977E+05	0.177143E+06	0.126261E+06	2	5
6	0.395849E+05	0.184396E+06	0.133108E+06	2	10
7	0.399546E+05	0.191650E+06	0.139970E+06	2	15
8	0.400947E+05	0.194551E+06	0.142721E+06	2	20
9	0.401752E+05	0.196273E+06	0.144356E+06	3	5
10	0.402547E+05	0.197995E+06	0.145992E+06	3	10
11	0.403324E+05	0.199717E+06	0.147630E+06	3	15
12	0.404074E+05	0.201439E+06	0.149270E+06	3	20

THIS TABLE IS DIRECTLY COMPUTED BY ABAQUS

STEP NO.	TOTAL BENDING MOMENT AT AUXILIARY NODE (LB-IN)	ROTATION ABOUT GLOBAL Y-AXIS (DEGREES)
1	0.454358E+07	0.948961E+00
2	0.461746E+07	0.103849E+01
3	0.467001E+07	0.112801E+01
4	0.471254E+07	0.121754E+01
5	0.484799E+07	0.238333E+01
6	0.484840E+07	0.246905E+01
7	0.484791E+07	0.255476E+01
8	0.484741E+07	0.258905E+01
9	0.484702E+07	0.260941E+01
10	0.484656E+07	0.262977E+01
11	0.484605E+07	0.265013E+01
12	0.484545E+07	0.267049E+01

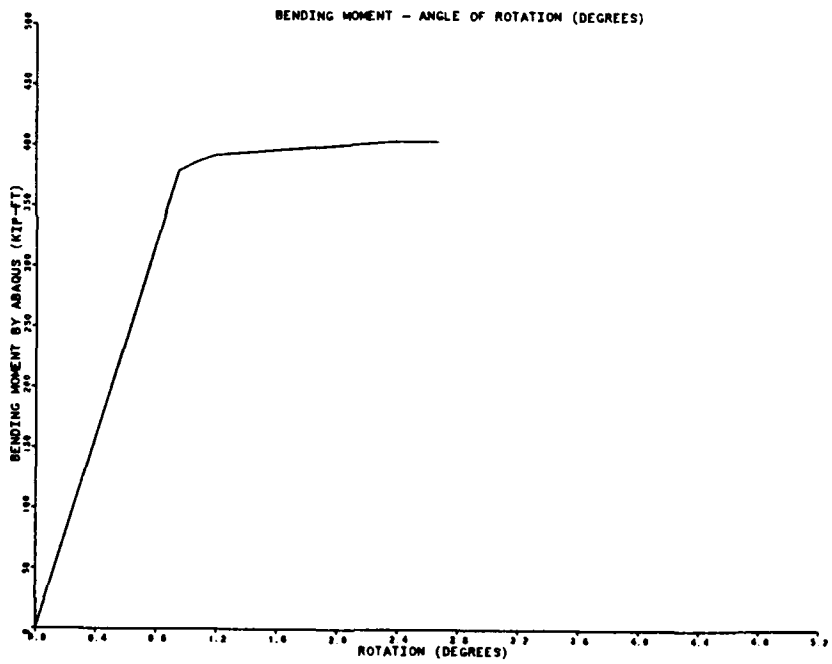

NOTE: MODEL 20AN

FIGURE 10. MOMENT VERSUS ANGLE OF ROTATION FOR MODEL 20AN

STEP NO 1 FOR STRESSES

ANGLE (DEGREES)	LONGITUDINAL MEMBRANE STRESS (PSI)	NONDIMENSIONAL MEMBRANE LONGITUDINAL STRESS	HOOP STRESS (PSI)	NONDIMENSIONAL HOOP STRESS
0.000	0.577263E+05	0.743560E-01	0.565043E+04	0.727820E-02
7.515	0.575137E+05	0.740825E-01	0.520929E+04	0.670997E-02
15.036	0.570501E+05	0.730715E-01	0.480631E+04	0.619090E-02
22.546	0.566981E+05	0.730316E-01	0.369790E+04	0.476318E-02
30.055	0.558863E+05	0.719860E-01	0.251018E+04	0.323371E-02
37.565	0.541005E+05	0.696857E-01	0.891396E+03	0.114811E-02
45.058	0.526970E+05	0.678779E-01	-.726330E+03	-.935570E-03
52.545	0.490866E+05	0.632274E-01	-.242899E+04	-.312873E-02
60.037	0.439330E+05	0.565891E-01	-.413699E+04	-.532877E-02
67.517	0.316974E+05	0.408287E-01	-.546495E+04	-.703928E-02
74.990	0.206613E+05	0.266134E-01	-.677433E+04	-.872587E-02
82.468	0.908372E+04	0.117005E-01	-.726358E+04	-.935607E-02
89.958	-.248360E+04	-.319908E-02	-.772615E+04	-.995199E-02
97.409	-.137537E+05	-.177158E-01	-.720813E+04	-.928463E-02
104.890	-.250179E+05	-.322250E-01	-.666339E+04	-.858296E-02
112.367	-.352456E+05	-.453991E-01	-.530551E+04	-.683391E-02
119.854	-.466403E+05	-.600764E-01	-.397324E+04	-.511785E-02
127.354	-.508741E+05	-.655298E-01	-.222103E+04	-.286096E-02
134.850	-.534266E+05	-.688179E-01	-.437958E+03	-.564175E-03
142.355	-.531554E+05	-.684683E-01	0.119954E+04	0.154510E-02
149.879	-.534160E+05	-.688040E-01	0.283921E+04	0.365712E-02
157.403	-.529533E+05	-.682080E-01	0.395456E+04	0.509379E-02
164.929	-.523780E+05	-.674670E-01	0.509771E+04	0.656625E-02
172.467	-.521716E+05	-.672011E-01	0.549798E+04	0.708183E-02
180.000	-.520033E+05	-.669843E-01	0.583635E+04	0.751768E-02

FIGURE 11. AXIAL AND HOOP STRESS DISTRIBUTION AT MIDLENGTH FOR MODEL 20AN AT THE FIRST LOAD STEP

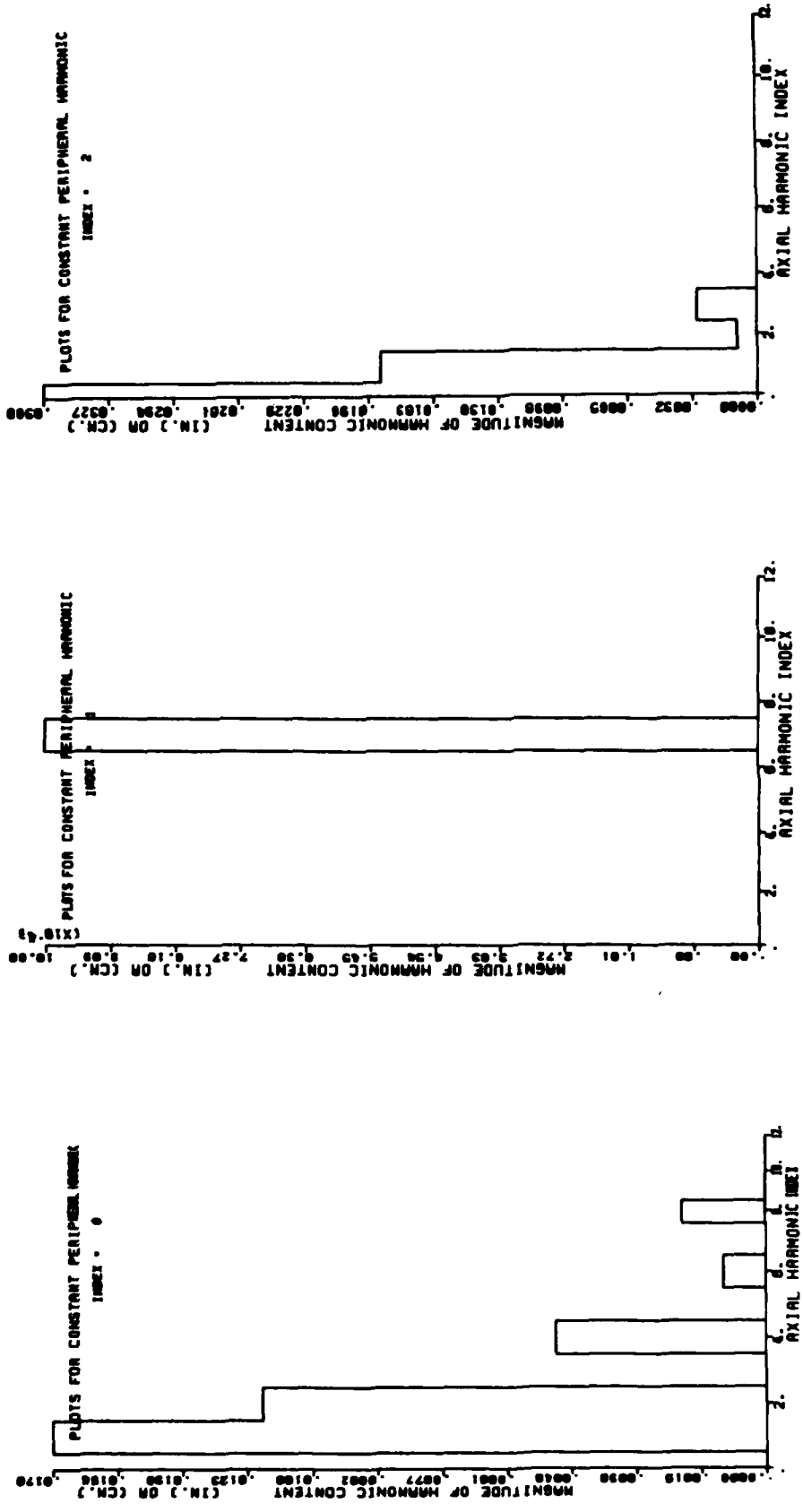

NOTE: MODEL 20A WITH IMPERFECTIONS

FOR CONSTANT PERIPHERAL HARMONIC INDEX = 0, 1, 2
PLOT OF MAGNITUDE OF AXIAL HARMONIC INDEX OF COSINE-COSINE COEFFICIENT

FIGURE 12. MAGNITUDE OF AXIAL HARMONICS (OF COSINE-COSINE TERMS) FOR MODEL 20A WITH IMPERFECTIONS

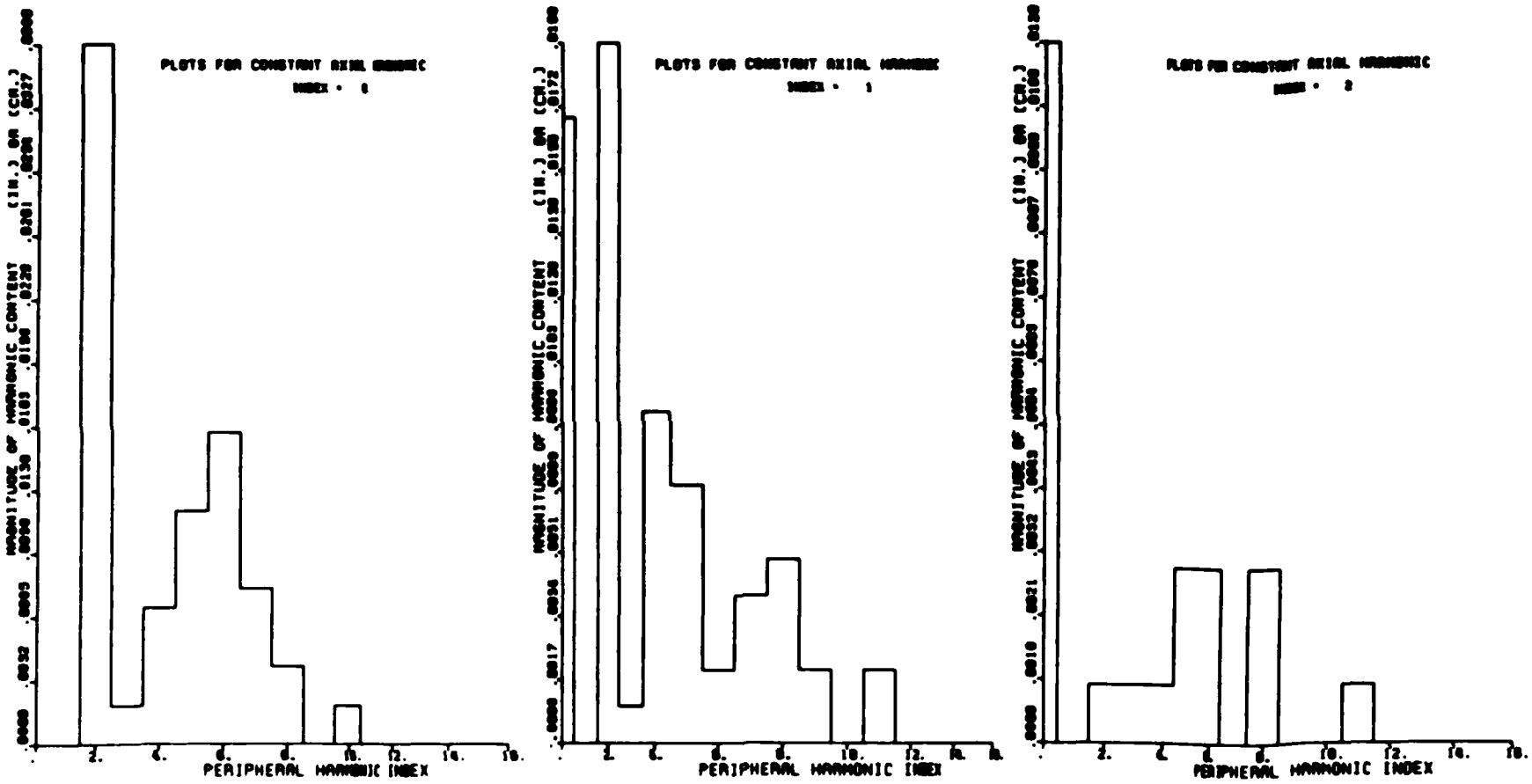

NOTE: MODEL 20A WITH IMPERFECTIONS

FOR CONSTANT AXIAL INDEX = 0, 1, 2
PLOT OF MAGNITUDE OF PERIPHERAL HARMONIC INDEX OF COSINE-COSINE COEFFICIENT

FIGURE 13. MAGNITUDE PERIPHERAL HARMONICS (OF COSINE-COSINE TERMS) FOR MODEL 20A WITH IMPERFECTIONS

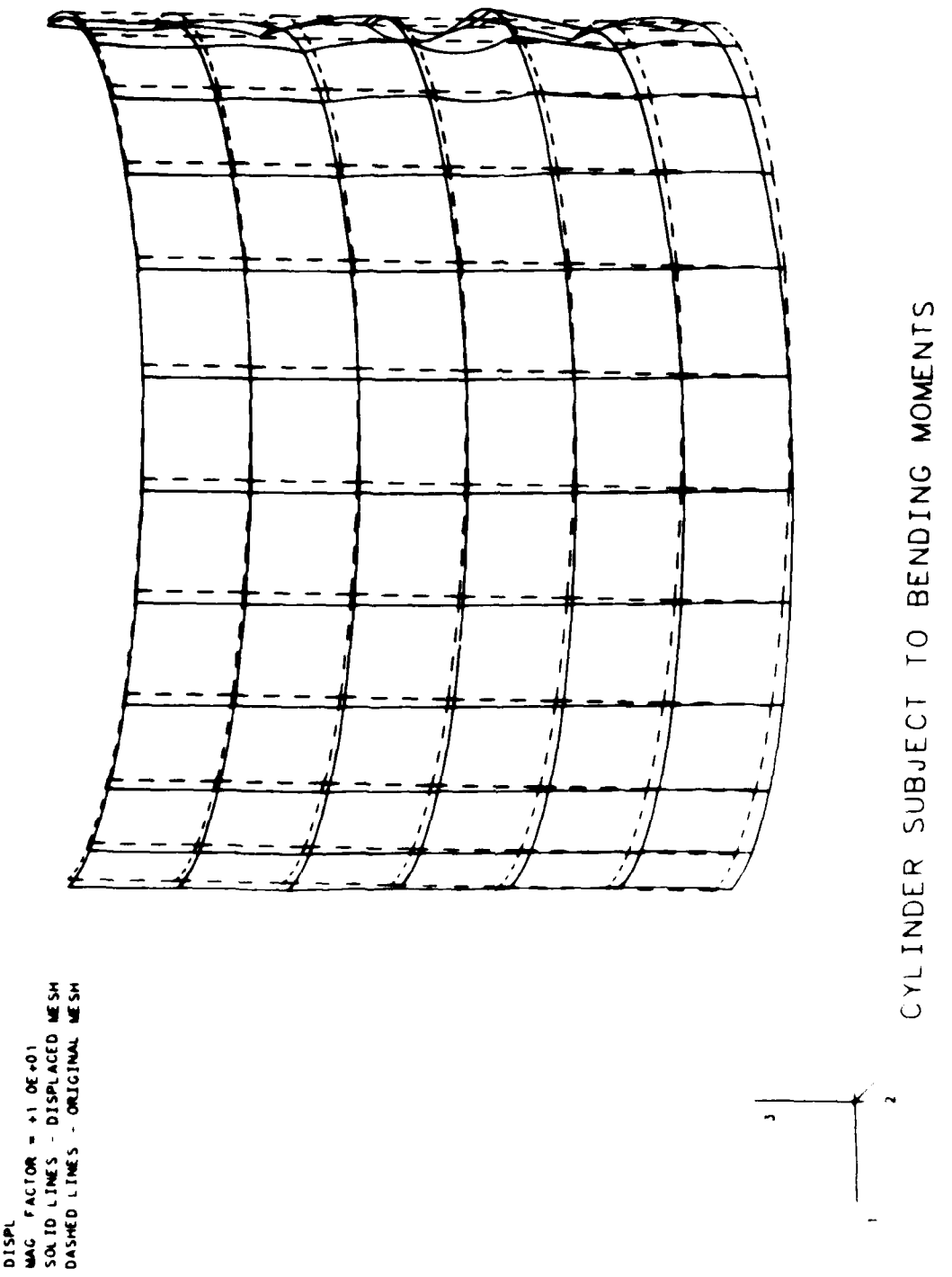

FIGURE 14. DEFORMED AND UNDEFORMED PROFILES FOR MODEL IC1 AT STEP 3, INCREMENT 30

STEP NO 1 PER STRESSEL

ANGLE (DEGREES)	LONGITUDINAL MEMBRANE STRESS (PSI)	NONDIMENSIONAL MEMBRANE LONGITUDINAL STRESS	HOOP STRESS (PSI)	NONDIMENSIONAL HOOP STRESS
0 000	0 801223E+03	0 939849E-02	0 128540E+01	0 150779E-04
7 501	0 787550E+03	0 923811E-02	0 978863E+00	0 114808E-04
14 999	0 773911E+03	0 907811E-02	0 124577E+01	0 146131E-04
22 499	0 733807E+03	0 860863E-02	0 910348E+00	0 106786E-04
30 000	0 693863E+03	0 813915E-02	0 111934E+01	0 131324E-04
37 500	0 630193E+03	0 739298E-02	0 789364E+00	0 921247E-05
45 000	0 566552E+03	0 664576E-02	0 912254E+00	0 107004E-04
52 499	0 483570E+03	0 567237E-02	0 603055E+00	0 707395E-05
59 999	0 400610E+03	0 469923E-02	0 653652E+00	0 766746E-05
67 500	0 303984E+03	0 356578E-02	0 379108E+00	0 444701E-05
75 000	0 207369E+03	0 243248E-02	0 339838E+00	0 398636E-05
82 499	0 103689E+03	0 121629E-02	0 131082E+00	0 153763E-05
90 000	- 117473E-02	- 137799E-07	0 690910E-02	0 810490E-07
97 500	- 103695E+03	- 121637E-02	- 126971E+00	- 148939E-05
104 999	- 207374E+03	- 243253E-02	- 327367E+00	- 384243E-05
112 499	- 303999E+03	- 356589E-02	- 375525E+00	- 440497E-05
120 000	- 400619E+03	- 469934E-02	- 645770E+00	- 757500E-05
127 500	- 483584E+03	- 567253E-02	- 600412E+00	- 704299E-05
135 000	- 566569E+03	- 664596E-02	- 910020E+00	- 106747E-04
142 499	- 630212E+03	- 739250E-02	- 783825E+00	919441E-05
149 999	- 693887E+03	- 813943E-02	- 112334E+01	- 131770E-04
157 500	- 733911E+03	- 860892E-02	- 909616E+00	- 106700E-04
165 000	- 773939E+03	- 907849E-02	- 125380E+01	- 147073E-04
172 499	- 787577E+03	- 923842E-02	- 978740E+00	- 114808E-04
180 000	- 801254E+03	- 939886E-02	- 129487E+01	- 151890E-04

MODEL IC1

STEP 1 INCREMENT 5
PLASTIC DISSIPATION = 0.0 lb-in
ANGLE OF ROTATION = 0.261×10^{-2} deg
TOTAL BENDING MOMENT = 0.302161×10^{6} lb-in

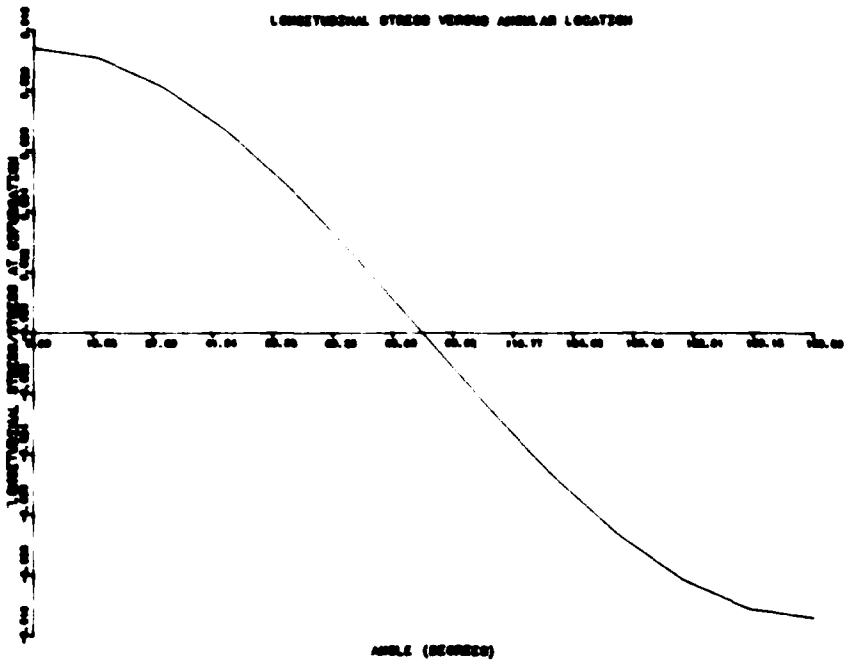

(A)

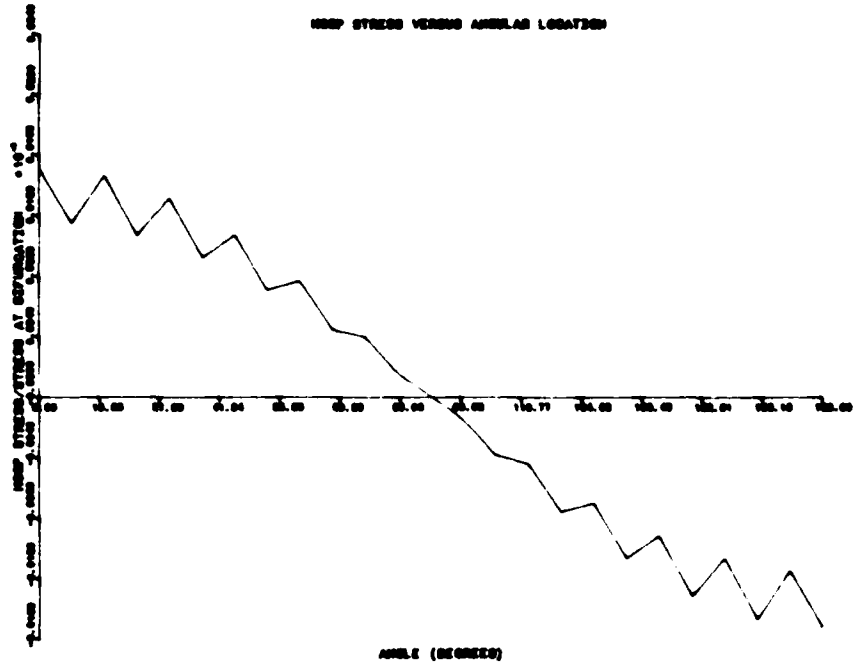

(B)

FIGURE 15. (A) DISTRIBUTION OF AXIAL STRESS AT MIDLENGTH FOR MODEL IC1
(B) DISTRIBUTION OF HOOP STRESS AT MIDLENGTH FOR MODEL IC1

INCREMENT NO	STRAIN ENERGY	EXTERNAL WORK DONE	PLASTIC DISSIPATION	ABAQUS STEP	ABAQUS INCREMENT
1	0.689298E+01	0.860693E+01	0.000000E+00	1	5
2	0.476726E+03	0.574620E+03	0.000000E+00	1	10
3	0.598167E+03	0.697774E+03	0.000000E+00	2	5
4	0.190540E+04	0.210104E+04	0.000000E+00	2	10
5	0.262736E+05	0.324433E+05	0.251876E+04	2	15
6	0.368287E+05	0.522000E+05	0.108556E+05	2	20
7	0.369008E+05	0.527348E+05	0.113174E+05	3	5
8	0.369705E+05	0.532687E+05	0.117807E+05	3	10
9	0.370218E+05	0.538017E+05	0.122615E+05	3	15
10	0.370689E+05	0.543335E+05	0.127454E+05	3	20
11	0.371399E+05	0.548644E+05	0.132045E+05	3	25
12	0.372179E+05	0.553944E+05	0.136556E+05	3	30

THIS TABLE IS DIRECTLY COMPUTED BY ABAQUS

STEP NO	TOTAL BENDING MOMENT AT AUXILIARY NODE (LB-IN)	ROTATION ABOUT GLOBAL Y-AXIS (DEGREES)
1	0.302161E+06	0.261412E-01
2	0.251283E+07	0.217399E-01
3	0.261474E+07	0.243521E-01
4	0.502345E+07	0.434634E-01
5	0.185971E+08	0.170019E+00
6	0.215742E+08	0.223410E+00
7	0.215440E+08	0.224831E+00
8	0.215113E+08	0.226252E+00
9	0.214690E+08	0.227674E+00
10	0.214354E+08	0.229095E+00
11	0.213872E+08	0.230516E+00
12	0.213542E+08	0.231937E+00

FIGURE 16. ENERGIES AND BENDING MOMENTS VERSUS ANGLE OF ROTATION FOR MODEL IC1

BENDING MOMENTS AT CUT NO 2

NODE NO	STEP 1 FORCE ZZ	STEP 1 ARM XX	STEP 2 FORCE ZZ	STEP 2 ARM XX	STEP 3 FORCE ZZ	STEP 3 ARM XX
301	0 142961E+03	0 295167E+02	0 118901E+04	0 295219E+02	0 133186E+04	0 295[illegible]E+02
302	0 562321E+03	0 292637E+02	0 467665E+04	0 292690E+02	0 523840E+04	0 292[illegible]E+02
303	0 276051E+03	0 285107E+02	0 229593E+04	0 285161E+02	0 257175E+04	0 285[illegible]E+02
304	0 524047E+03	0 272698E+02	0 435831E+04	0 272753E+02	0 488183E+04	0 272760E+02
305	0 247564E+03	0 255618E+02	0 205895E+04	0 255675E+02	0 230629E+04	0 255[illegible]E+02
306	0 449957E+03	0 234168E+02	0 374208E+04	0 234228E+02	0 419154E+04	0 234[illegible]E+02
307	0 202106E+03	0 208719E+02	0 168082E+04	0 208781E+02	0 188274E+04	0 208[illegible]E+02
308	0 345267E+03	0 179689E+02	0 287137E+04	0 179753E+02	0 321624E+04	0 179762E+02
309	0 142928E+03	0 147589E+02	0 118858E+04	0 147656E+02	0 133133E+04	0 147665E+02
310	0 217066E+03	0 112959E+02	0 180514E+04	0 113028E+02	0 202190E+04	0 113038E+02
311	0 739676E+02	0 763996E+01	0 615014E+03	0 764699E+01	0 688830E+03	0 764799E+01
312	0 740267E+02	0 385397E+01	0 615537E+03	0 386110E+01	0 689376E+03	0 386207E+01
313	-0 239628E-02	0 978430E-03	-0 172262E+00	0 813689E-02	-0 277421E+00	0 911449E-02
314	-0 740294E+02	-0 385203E+01	-0 615741E+03	-0 384490E+01	-0 689837E+03	-0 384393E+01
315	-0 739716E+02	-0 763804E+01	-0 615300E+03	-0 763100E+01	-0 689309E+03	-0 763004E+01
316	-0 217067E+03	-0 112941E+02	-0 180524E+04	-0 112872E+02	-0 202225E+04	-0 112868E+02
317	-0 142930E+03	-0 147571E+02	-0 118870E+04	-0 147504E+02	-0 133159E+04	-0 147498E+02
318	-0 345265E+03	-0 179671E+02	-0 287129E+04	-0 179606E+02	-0 321638E+04	-0 179597E+02
319	-0 202104E+03	-0 208701E+02	-0 168071E+04	-0 208639E+02	-0 188269E+04	-0 208630E+02
320	-0 449952E+03	-0 234152E+02	-0 374180E+04	-0 234091E+02	-0 419147E+04	-0 234083E+02
321	0 247559E+03	-0 255602E+02	-0 205862E+04	-0 255544E+02	-0 230597E+04	-0 255538E+02
322	-0 524040E+03	-0 272682E+02	-0 435785E+04	-0 272626E+02	-0 488153E+04	-0 272617E+02
323	-0 276044E+03	-0 285093E+02	-0 229542E+04	-0 285037E+02	-0 257120E+04	-0 285029E+02
324	0 562312E+03	-0 292623E+02	-0 467608E+04	-0 292568E+02	-0 523799E+04	-0 292560E+02
325	-0 142956E+03	-0 295153E+02	-0 118873E+04	-0 295099E+02	-0 133155E+04	-0 295091E+02
TOTAL OUT OF BALANCE FORCE ZZ	0 [illegible]61E 01		0 172876E+01		0 325928E-01	
TOTAL MOMENT	[illegible]1064E+06		0 125629E+07		0 140722E+07	
FORCE ZZ ON TOP QUARTER	[illegible]5826E+04		0 270974E+05		0 303521E+05	
FORCE ZZ IN BOTTOM QUARTER	[illegible]5823E+04		-0 270957E+05		-0 303521E+05	
POINT OF ZERO FORCE	[illegible]208E-02		0 854474E-02		0 100688E-01	
PERCENTAGE OUT OF BALANCE FORCE ZZ	[illegible]		0 [illegible]		0 00	

FIGURE 17. BENDING MOMENT COMPUTATION THROUGH CONSISTENT FORCES AT MIDDLE FOR MODEL IC1 (FOR HALF ONLY)

NODE No.

	STEP 4		STEP 5		STEP 6	
	FORCE ZZ	ARM XX	FORCE ZZ	ARM XX	FORCE ZZ	ARM XX
301	0.237718E+04	0.295276E+02	0.841004E+04	0.295528E+02	0.977909E+04	0.298643E+02
302	0.934944E+04	0.292747E+02	0.333018E+05	0.293005E+02	0.387082E+05	0.293121E+02
303	0.459020E+04	0.285219E+02	0.164759E+05	0.285494E+02	0.191513E+05	0.285614E+02
304	0.871299E+04	0.272813E+02	0.319176E+05	0.273114E+02	0.370607E+05	0.273241E+02
305	0.411632E+04	0.255738E+02	0.154755E+05	0.256071E+02	0.178924E+05	0.256210E+02
306	0.748095E+04	0.234294E+02	0.287473E+05	0.234658E+02	0.334288E+05	0.234814E+02
307	0.336022E+04	0.208850E+02	0.131363E+05	0.209243E+02	0.158489E+05	0.209417E+02
308	0.574014E+04	0.179826E+02	0.223486E+05	0.180244E+02	0.277174E+05	0.180431E+02
309	0.237597E+04	0.147732E+02	0.925426E+04	0.148170E+02	0.116494E+05	0.148365E+02
310	0.360845E+04	0.113106E+02	0.140275E+05	0.113561E+02	0.173187E+05	0.113760E+02
311	0.122914E+04	0.765498E+01	0.476350E+04	0.770164E+01	0.571041E+04	0.772199E+01
312	0.123016E+04	0.384919E+01	0.472064E+04	0.391648E+01	0.509588E+04	0.393646E+01
313	-0.818297E+00	0.162668E-01	-0.565243E+02	0.637684E-01	-0.681824E+03	0.837168E-01
314	-0.123139E+04	-0.383681E+01	-0.490931E+04	-0.378951E+01	-0.755634E+04	-0.376969E+01
315	-0.123055E+04	-0.762301E+01	-0.488038E+04	-0.757609E+01	-0.704983E+04	-0.755630E+01
316	-0.360933E+04	-0.112793E+02	-0.142026E+05	-0.112330E+02	-0.196266E+05	-0.112138E+02
317	-0.237672E+04	-0.147427E+02	-0.937282E+04	-0.146970E+02	-0.129274E+05	-0.146778E+02
318	-0.574040E+04	-0.179532E+02	-0.225035E+05	-0.179082E+02	-0.290652E+05	-0.178904E+02
319	-0.336005E+04	-0.208567E+02	-0.132248E+05	-0.208125E+02	-0.161187E+05	-0.207968E+02
320	-0.748050E+04	-0.234021E+02	-0.287240E+05	-0.233598E+02	-0.335145E+05	-0.233474E+02
321	-0.411525E+04	-0.255476E+02	-0.153948E+05	-0.255075E+02	-0.173049E+05	-0.254993E+02
322	-0.871189E+04	-0.272559E+02	-0.317266E+05	-0.272185E+02	-0.349604E+05	-0.272149E+02
323	-0.458841E+04	-0.284972E+02	-0.162852E+05	-0.284622E+02	-0.173475E+05	-0.284634E+02
324	-0.934797E+04	-0.292504E+02	-0.330061E+05	-0.292168E+02	-0.348229E+05	-0.292211E+02
325	-0.237617E+04	-0.295034E+02	-0.829117E+04	-0.294705E+02	-0.858502E+04	-0.294762E+02
TOTAL OUT OF BALANCE FORCE ZZ	0.173047E+01		0.917969E+00		0.273438E-01	
TOTAL MOMENT	0.251148E+07		0.929705E+07		0.107838E+08	
FORCE ZZ ON TOP QUARTER	0.541712E+05		0.202579E+06		0.239561E+06	
FORCE ZZ ON BOTTOM QUARTER	-0.541695E+05		-0.202578E+06		-0.239561E+06	
POINT OF ZERO FORCE	0.176146E-01		0.136130E+00		0.837101E+00	
PERCENTAGE OUT OF BALANCE FORCE ZZ	0.00		0.00		0.00	

FIGURE 17. (CONTINUED)

NODE NO	STEP 7 FORCE ZZ	STEP 7 ARM XX	STEP 8 FORCE ZZ	STEP 8 ARM XX	STEP 9 FORCE ZZ	STEP 9 ARM XX
301	0 979476E+04	0 295646E+02	0 980967E+04	0 295650E+02	0 982288E+04	0 295653E+02
302	0 387686E+05	0 293124E+02	0 388261E+05	0 293128E+02	0 388767E+05	0 293131E+02
303	0 191805E+05	0 285617E+02	0 192083E+05	0 285621E+02	0 192327E+05	0 285625E+02
304	0 371150E+05	0 273246E+02	0 371668E+05	0 273250E+02	0 372111E+05	0 273253E+02
305	0 179175E+05	0 256214E+02	0 179415E+05	0 256218E+02	0 179615E+05	0 256222E+02
306	0 336653E+05	0 234818E+02	0 336994E+05	0 234823E+02	0 337255E+05	0 234827E+02
307	0 158614E+05	0 209421E+02	0 158727E+05	0 209426E+02	0 158804E+05	0 209431E+02
308	0 277223E+05	0 180436E+02	0 277239E+05	0 180441E+02	0 277146E+05	0 180446E+02
309	0 116413E+05	0 148370E+02	0 116307E+05	0 148376E+02	0 116128E+05	0 148381E+02
310	0 172646E+05	0 113765E+02	0 172060E+05	0 113770E+02	0 171331E+05	0 113776E+02
311	0 566362E+04	0 772214E+01	0 561457E+04	0 772269E+01	0 555776E+04	0 772325E+01
312	0 496508E+04	0 393701E+01	0 483130E+04	0 393757E+01	0 468305E+04	0 393812E+01
313	-0 773211E+03	0 842585E-01	-0 865551E+03	0 848027E-01	-0 964874E+03	0 853474E-01
314	-0 776778E+04	-0 376916E+01	-0 798370E+04	-0 376863E+01	-0 821375E+04	-0 376810E+01
315	-0 718182E+04	-0 755577E+01	-0 731870E+04	-0 755522E+01	-0 746440E+04	-0 755467E+01
316	-0 198973E+05	-0 112130E+02	-0 201756E+05	-0 112124E+02	-0 204688E+05	-0 112117E+02
317	-0 130816E+05	-0 146772E+02	-0 132318E+05	-0 146765E+02	-0 133821E+05	-0 146758E+02
318	-0 292695E+05	-0 178897E+02	-0 294646E+05	-0 178889E+02	-0 296558E+05	-0 178881E+02
319	-0 161624E+05	-0 207960E+02	-0 162018E+05	-0 207953E+02	-0 162367E+05	-0 207945E+02
320	-0 335334E+05	-0 233468E+02	-0 335355E+05	-0 233463E+02	-0 335118E+05	-0 233458E+02
321	-0 172469E+05	-0 254992E+02	-0 171779E+05	-0 254992E+02	-0 170889E+05	-0 254992E+02
322	-0 346949E+05	-0 272153E+02	-0 344169E+05	-0 272157E+02	-0 341013E+05	-0 272162E+02
323	-0 171414E+05	-0 284642E+02	-0 169354E+05	-0 284649E+02	-0 167140E+05	-0 284657E+02
324	-0 343544E+05	-0 292221E+02	-0 338939E+05	-0 292230E+02	-0 334098E+05	-0 292239E+02
325	-0 845513E+04	-0 294772E+02	-0 832951E+04	-0 294782E+02	-0 819980E+04	-0 294790E+02
TOTAL OUT OF BALANCE FORCE ZZ	0 224609E-01		0 244141E-01		-0 976563E-02	
TOTAL MOMENT	0 107686E+08		0 107522E+08		0 107310E+08	
FORCE ZZ ON TOP QUARTER	0 239560E+06		0 239531E+06		0 239412E+06	
FORCE ZZ ON BOTTOM QUARTER	-0 239560E+06		-0 239531E+06		-0 239412E+06	
POINT OF ZERO FORCE	0 937547E+00		0 103749E+01		0 114473E+01	
PERCENTAGE OUT OF BALANCE FORCE ZZ	0 00				0 00	

FIGURE 17. (CONTINUED)

NODE NU

	STEP 10		STEP 11		STEP 12	
	FORCE ZZ	ARM XX	FORCE ZZ	ARM XX	FORCE ZZ	ARM XX
301	0.983531E+04	0.295656E+02	0.984903E+04	0.295659E+02	0.986307E+04	0.295662E+02
302	0.389243E+05	0.293135E+02	0.389772E+05	0.293138E+02	0.390314E+05	0.293141E+02
303	0.192556E+05	0.285629E+02	0.192814E+05	0.285632E+02	0.193077E+05	0.285635E+02
304	0.372524E+05	0.273257E+02	0.373002E+05	0.273261E+02	0.373493E+05	0.273265E+02
305	0.179800E+05	0.256227E+02	0.180021E+05	0.256231E+02	0.180249E+05	0.256235E+02
306	0.337486E+05	0.234832E+02	0.337791E+05	0.234836E+02	0.338113E+05	0.234841E+02
307	0.158868E+05	0.209436E+02	0.158965E+05	0.209440E+02	0.159070E+05	0.209445E+02
308	0.277010E+05	0.180451E+02	0.276975E+05	0.180456E+02	0.276963E+05	0.180461E+02
309	0.115918E+05	0.148386E+02	0.115774E+05	0.148392E+02	0.115643E+05	0.148397E+02
310	0.170541E+05	0.113781E+02	0.169877E+05	0.113787E+02	0.169237E+05	0.113792E+02
311	0.549748E+04	0.772380E+01	0.544361E+04	0.772434E+01	0.539072E+04	0.772489E+01
312	0.452830E+04	0.393867E+01	0.438642E+04	0.393921E+01	0.424729E+04	0.393975E+01
313	-0.106743E+04	0.858839E-01	-0.116312E+04	0.864172E-01	-0.125664E+04	0.869479E-01
314	-0.844984E+04	-0.376757E+01	-0.867290E+04	-0.376705E+01	-0.889164E+04	-0.376653E+01
315	-0.761241E+04	-0.755412E+01	-0.775336E+04	-0.755358E+01	-0.789261E+04	-0.755304E+01
316	-0.207627E+05	-0.112111E+02	-0.210434E+05	-0.112105E+02	-0.213235E+05	-0.112099E+02
317	-0.135281E+05	-0.146750E+02	-0.136666E+05	-0.146743E+02	-0.137963E+05	-0.146736E+02
318	-0.298355E+05	-0.178873E+02	-0.300060E+05	-0.178866E+02	-0.301658E+05	-0.178859E+02
319	-0.162641E+05	-0.207939E+02	-0.162900E+05	-0.207933E+02	-0.163182E+05	-0.207927E+02
320	-0.334661E+05	-0.233455E+02	-0.334270E+05	-0.233453E+02	-0.333886E+05	-0.233450E+02
321	-0.169890E+05	-0.254994E+02	-0.168993E+05	-0.254995E+02	-0.168117E+05	-0.254996E+02
322	-0.337758E+05	-0.272167E+02	-0.334841E+05	-0.272171E+02	-0.332019E+05	-0.272174E+02
323	-0.164941E+05	-0.284663E+02	-0.162974E+05	-0.284668E+02	-0.161084E+05	-0.284673E+02
324	-0.329361E+05	-0.292245E+02	-0.325126E+05	-0.292250E+02	-0.321063E+05	-0.292254E+02
325	-0.807435E+04	-0.294796E+02	-0.796243E+04	-0.294801E+02	-0.785544E+04	-0.294805E+02

TOTAL OUT OF BALANCE FORCE ZZ	0.327148E-01	-0.146484E-01	-0.341797E-02
TOTAL MOMENT	0.107082E+08	0.106900E+08	0.106729E+08
FORCE ZZ ON TOP QUARTER	0.239256E+06	0.239178E+06	0.239117E+06
FORCE ZZ ON BOTTOM QUARTER	-0.239256E+06	-0.239178E+06	-0.239117E+06
POINT OF ZERO FORCE	0.125476E+01	0.135584E+01	0.145438E+01
PERCENTAGE OUT OF BALANCE FORCE ZZ	0.00	0.00	0.00

FIGURE 17. (CONTINUED)

CRITICAL BENDING MOMENT (LB-IN)	CRITICAL BENDING MOMENT BY BRAZIER (LB-IN)	INERTIA OF UNDEFORMED CROSS-SECTION (IN**4)
0.323342E+08	0.176005E+08	0.111949E+05

CRITICAL CURVATURE ASSOCIATED WITH APPLIED MOMENT AT BIFURCATION (1/IN)	MAXIMUM STRESS AT BIFURCATION (LB/IN**2)
0.96276453E-04	0.85250141E+05

FULLY PLASTIC MOMENT BASED ON YIELD STRESS (LB-IN)	MAXIMUM AXIAL FORCE BASED ON YIELD STRESS (LBS)
0.196815E+08	0.104743E+07

NORMALIZED NET AXIAL FORCE

0.000000E+00

NEUTRAL AXIS AND OUTER FIBRE LOCATIONS ARE DERIVED
FROM CALCULATED LONGITUDINAL MEMBRANE FORCES
WHICH ARE COMPUTED FROM NODAL STRESSES

STEP NO	MEAN CURVATURE (1/IN)	CURVATURE AT 0 DEGREES (1/IN)	CURVATURE AT 180 DEGREES (1/IN)	M/MCRITICAL	M/MCRITICAL BRAZIER
1	0.904434E-06	0.904420E-06	0.904433E-06	0.934395E-02	0.171659E-01
2	0.752157E-05	0.752103E-05	0.752203E-05	0.777066E-01	0.142756E+00
3	0.842529E-05	0.842459E-05	0.842596E-05	0.870423E-01	0.159907E+00
4	0.150372E-04	0.150350E-04	0.150397E-04	0.155345E+00	0.285387E+00
5	0.573202E-04	0.574322E-04	0.572250E-04	0.575060E+00	0.105645E+01
6	0.680274E-04	0.731283E-04	0.631733E-04	0.667020E+00	0.122539E+01
7	0.677418E-04	0.735558E-04	0.622465E-04	0.666084E+00	0.122368E+01
8	0.674607E-04	0.739766E-04	0.613435E-04	0.665067E+00	0.122181E+01
9	0.671534E-04	0.744007E-04	0.603994E-04	0.663755E+00	0.121940E+01
10	0.668524E-04	0.748268E-04	0.594769E-04	0.662344E+00	0.121680E+01
11	0.665969E-04	0.752465E-04	0.586526E-04	0.661218E+00	0.121474E+01
12	0.663555E-04	0.756659E-04	0.578619E-04	0.660165E+00	0.121280E+01

FIGURE 18. PARAMETERS FOR MODEL IC1

M/MULTIM	STRAIN ENERGY (KIP-IN)	EXTERNAL WORK (KIP-IN)	PLASTIC DISSIPATION (KIP-IN)
0.153509E-01	0.489298E-02	0.860693E-02	0.000000E+00
0.127662E+00	0.476726E+00	0.574620E+00	0.000000E+00
0.143000E+00	0.598167E+00	0.697774E+00	0.000000E+00
0.255212E+00	0.190540E+01	0.210104E+01	0.000000E+00
0.944751E+00	0.267736E+02	0.324433E+02	0.251876E+01
0.109583E+01	0.368287E+02	0.522000E+02	0.108556E+02
0.109429E+01	0.369008E+02	0.527348E+02	0.113174E+02
0.109262E+01	0.369705E+02	0.532687E+02	0.117807E+02
0.109047E+01	0.370218E+02	0.538017E+02	0.122615E+02
0.108815E+01	0.370689E+02	0.543335E+02	0.127454E+02
0.108630E+01	0.371399E+02	0.548644E+02	0.132045E+02
0.108457E+01	0.372179E+02	0.553944E+02	0.136556E+02

STEP NO	MEAN CURVATURE (1/FT)	K/KCRITICAL	M/MULTIM	M/MCRITICAL	BENDING MOMENT (KIP-IN)	BENDING MOMENT (KIP-FT)
1	0.108532E-04	0.939414E-02	0.153509E-01	0.934395E-02	0.302129E+03	0.251774E+02
2	0.902588E-04	0.781247E-01	0.127662E+00	0.777066E-01	0.251258E+04	0.209381E+03
3	0.101104E-03	0.875115E-01	0.143000E+00	0.870423E-01	0.281444E+04	0.234537E+03
4	0.180447E-03	0.156188E+00	0.255212E+00	0.155345E+00	0.502295E+04	0.418580E+03
5	0.687843E-03	0.595371E+00	0.944751E+00	0.575060E+00	0.185941E+05	0.154951E+04
6	0.816328E-03	0.706584E+00	0.109583E+01	0.667020E+00	0.215675E+05	0.179729E+04
7	0.812902E-03	0.703618E+00	0.109429E+01	0.666084E+00	0.215373E+05	0.179477E+04
8	0.809528E-03	0.700698E+00	0.109262E+01	0.665067E+00	0.215044E+05	0.179203E+04
9	0.805841E-03	0.697506E+00	0.109047E+01	0.663755E+00	0.214619E+05	0.178850E+04
10	0.802228E-03	0.694379E+00	0.108815E+01	0.662344E+00	0.214163E+05	0.178470E+04
11	0.799163E-03	0.691726E+00	0.108630E+01	0.661218E+00	0.213799E+05	0.178166E+04
12	0.796265E-03	0.689218E+00	0.108457E+01	0.660165E+00	0.213459E+05	0.177882E+04

FIGURE 18. (CONTINUED)

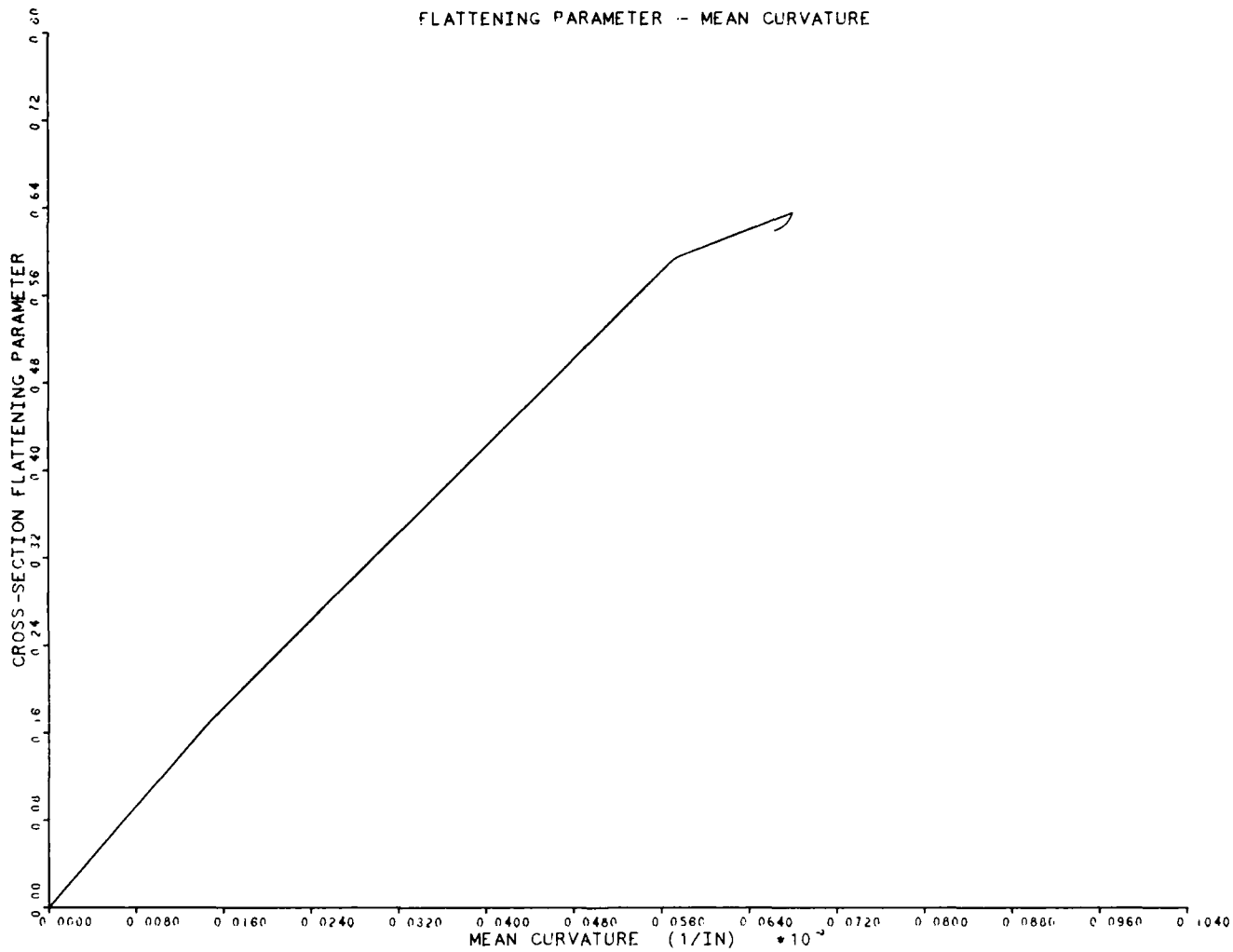

FIGURE 19. CROSS-SECTION FLATTENING PARAMETER $\Delta w/h$ VERSUS MEAN CURVATURE FOR MODEL IC1

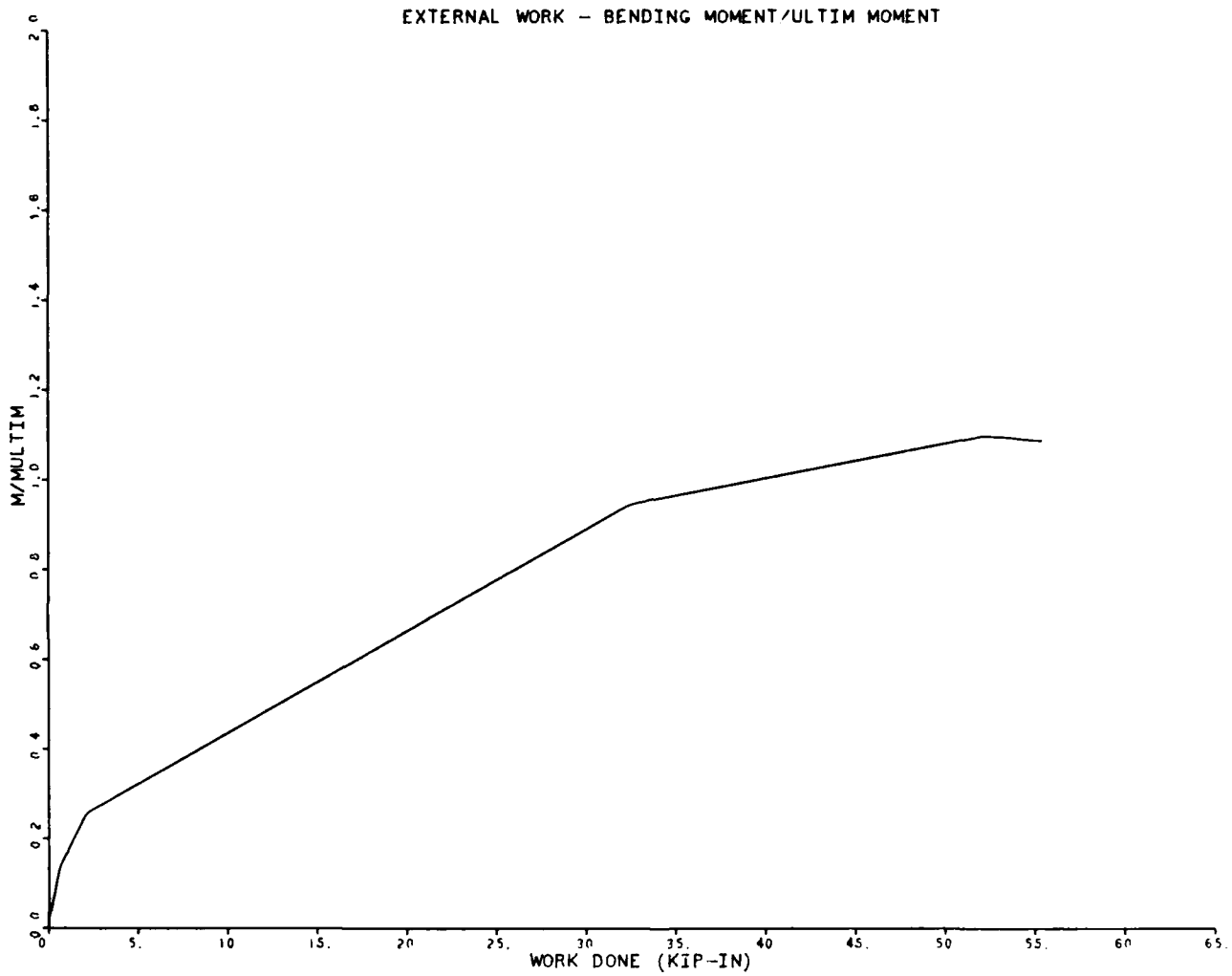

FIGURE 20. $M/M_{ULTIMATE}$ VERSUS WORK-DONE FOR MODEL IC1

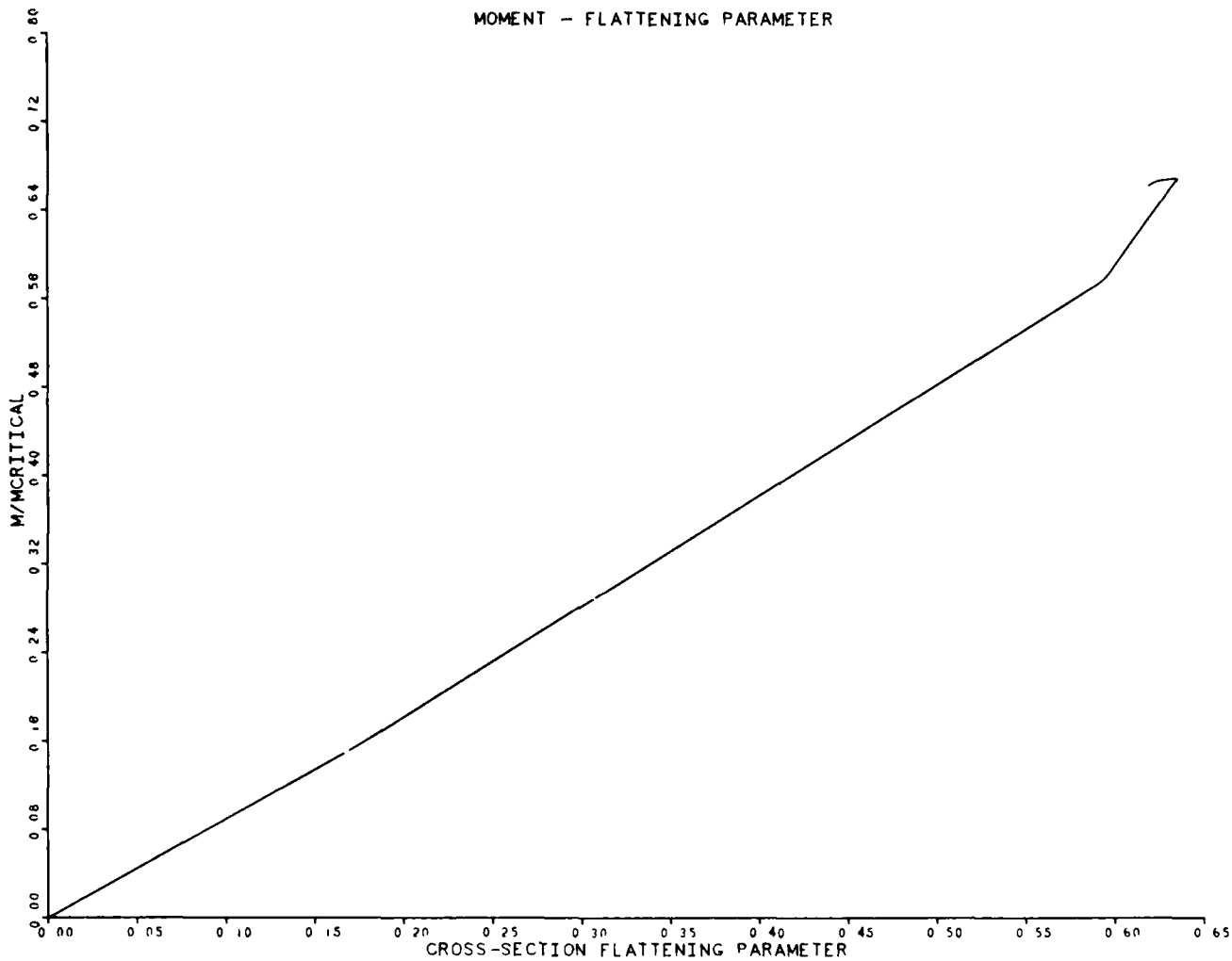

FIGURE 21. $M/M_{CRITICAL}$ VERSUS CROSS-SECTION FLATTENING PARAMETER $\Delta w/h$ FOR MODEL IC1

STEP NO 12 FOR STRESSES

ANGLE (DEGREES)	LONGITUDINAL MEMBRANE STRESS (PSI)	NONDIMENSIONAL MEMBRANE LONGITUDINAL STRESS	HOOP STRESS (PSI)	NONDIMENSIONAL HOOP STRESS
0.000	0.551415E+05	0.646820E+00	-.264942E+02	-.310782E-03
7.493	0.545596E+05	0.639994E+00	-.372192E+02	-.436588E-03
14.985	0.539987E+05	0.633414E+00	-.258313E+02	-.303005E-03
22.477	0.522130E+05	0.612471E+00	-.274028E+02	-.321792E-03
29.970	0.504176E+05	0.591407E+00	-.215333E+02	-.252590E-03
37.462	0.472706E+05	0.554528E+00	-.426591E+02	-.500399E-03
44.953	0.445144E+05	0.522163E+00	-.289669E+01	-.339787E-04
52.444	0.387356E+05	0.454376E+00	-.199684E+02	-.234233E-03
59.935	0.323764E+05	0.379781E+00	0.119622E+02	0.140319E-03
67.429	0.236825E+05	0.277801E+00	0.267256E+02	0.313497E-03
74.923	0.151808E+05	0.178073E+00	0.146263E+03	0.171570E-02
82.417	0.591246E+04	0.693543E-01	0.984448E+02	0.115478E-02
89.914	-.325298E+04	-.381581E-01	0.383160E+03	0.449454E-02
97.414	-.125727E+05	-.147480E+00	0.385080E+03	0.451706E-02
104.914	-.217663E+05	-.255323E+00	0.102120E+04	0.119789E-01
112.419	-.299974E+05	-.351876E+00	0.124724E+04	0.146304E-01
119.926	-.384329E+05	-.450825E+00	0.223845E+04	0.262575E-01
127.435	-.424396E+05	-.497824E+00	0.287815E+04	0.337612E-01
134.945	-.457414E+05	-.536555E+00	0.373761E+04	0.438428E-01
142.457	-.467050E+05	-.547858E+00	0.486330E+04	0.570475E-01
149.967	-.475568E+05	-.557850E+00	0.558036E+04	0.654587E-01
157.479	-.464296E+05	-.544628E+00	0.664683E+04	0.779686E-01
164.987	-.456964E+05	-.536028E+00	0.688194E+04	0.807265E-01
172.493	-.449120E+05	-.526826E+00	0.761090E+04	0.892772E-01
180.000	-.445802E+05	-.522957E+00	0.738390E+04	0.866145E-01

MODEL IC1 IN BENDING

STEP 3, INCREMENT 30
PLASTIC DISSIPATION = 13,655.6 lb-in
ANGLE OF ROTATION = 0.231937 deg
TOTAL BENDING MOMENT
= 2.13532×10^7 lb-in

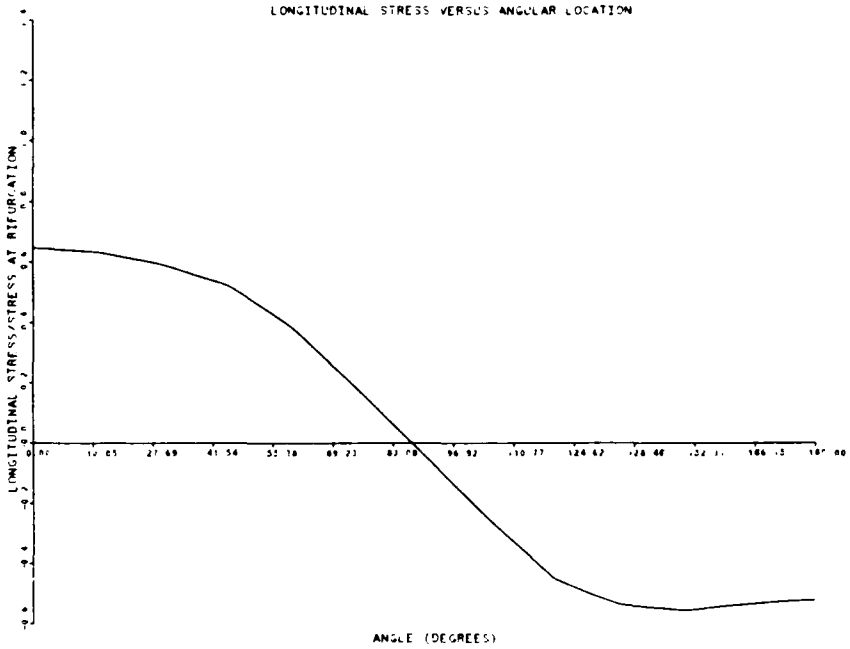

(A)

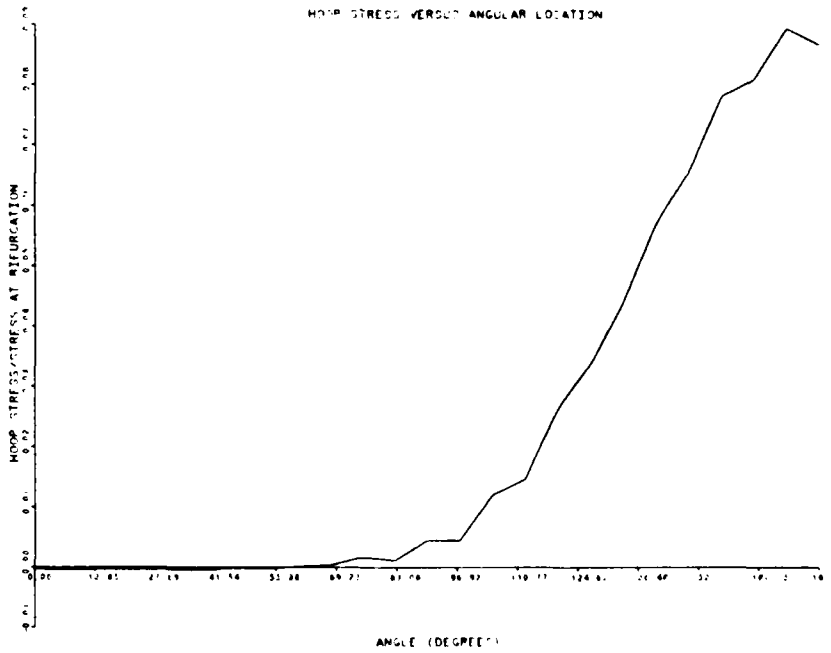

(B)

FIGURE 22. (A) AXIAL STRESS VERSUS PERIPHERAL LOCATION AT MIDLENGTH FOR MODEL IC1 (STEP 3, INCREMENT 30)
(B) HOOP STRESS VERSUS PERIPHERAL LOCATION AT MIDLENGTH FOR MODEL IC1 (STEP 3, INCREMENT 30)

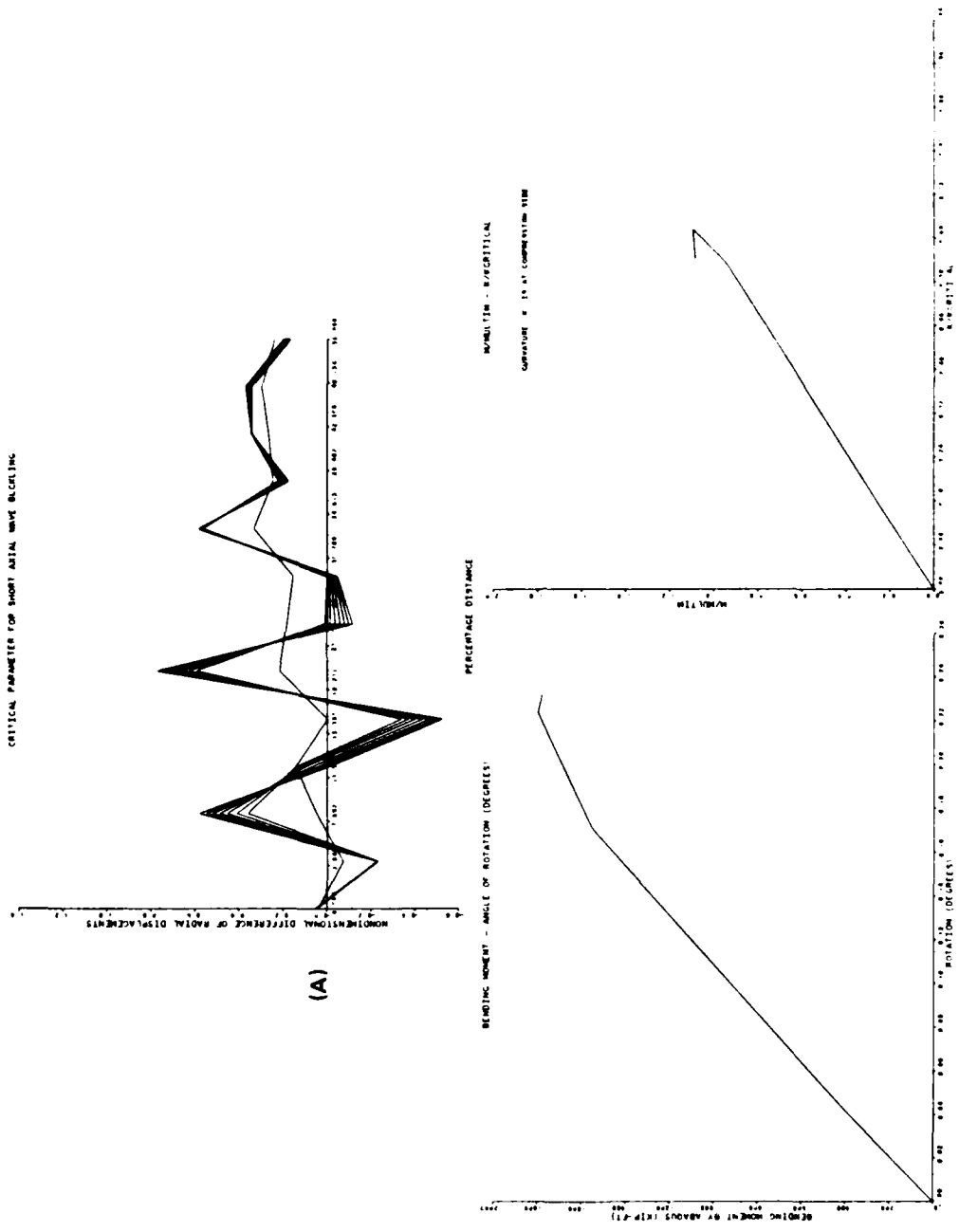

FIGURE 23. (A) CRITICAL PARAMETER $\delta w/h$ FOR SHORT AXIAL WAVE LENGTH BUCKLING FOR MODEL IC1
(B) BENDING MOMENT VERSUS ANGLE OF ROTATION FOR MODEL IC1
(C) $M/M_{ULTIMATE}$ VERSUS $K/K_{CRITICAL}$ FOR MODEL IC1

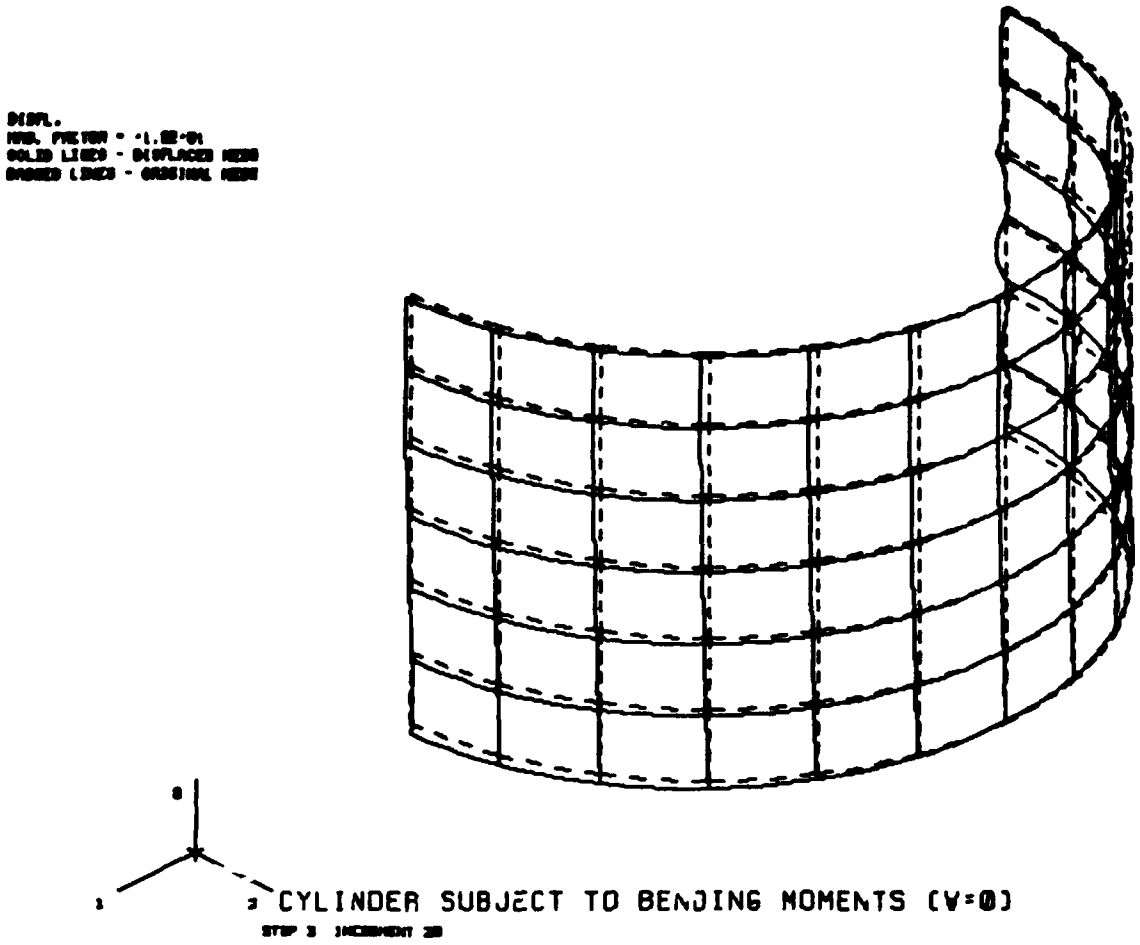

FIGURE 24. DEFORMED AND UNDEFORMED PROFILES FOR MODEL IC1 (WITH ADDITIONAL CONSTRAINT W = 0 AT END PLATE) FOR STEP 3, INCREMENT 20

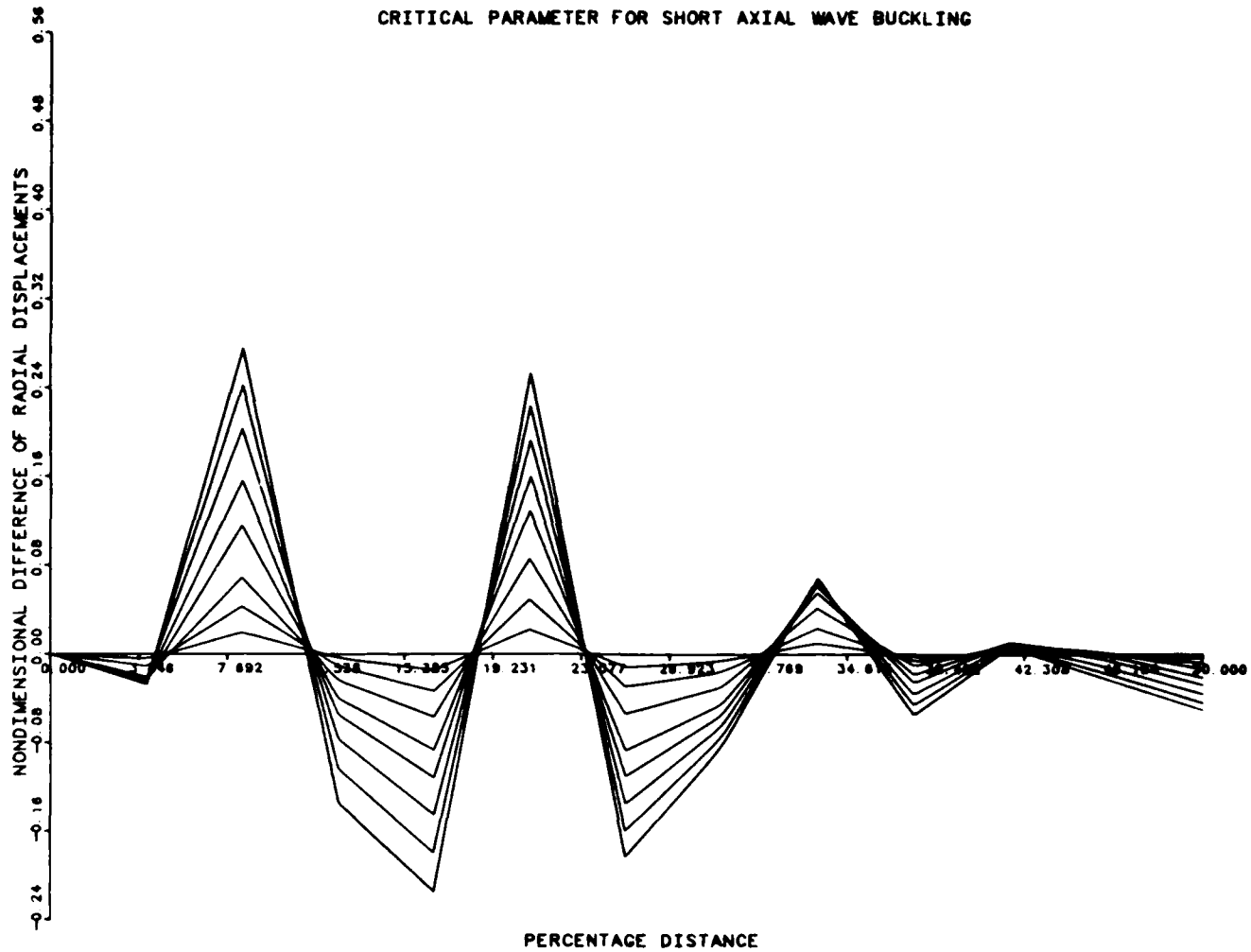

FIGURE 25. CRITICAL PARAMETER $\delta w/h$ FOR SHORT AXIAL WAVE LENGTH BUCKLING FOR MODEL 1C1 (WITH ADDITIONAL CONSTRAINT W = 0 AT LEFT END, WITH END PLATE) AT LOAD STEP 3, INCREMENT 4

STEP NO. 6 FOR STRESSES

ANGLE (DEGREES)	LONGITUDINAL MEMBRANE STRESS (PSI)	NONDIMENSIONAL MEMBRANE LONGITUDINAL STRESS	HOOP STRESS (PSI)	NONDIMENSIONAL HOOP STRESS
0.000	0.546760E+05	0.641359E+00	-.274158E+02	-.321592E-03
7.494	0.541877E+05	0.634693E+00	-.351538E+02	-.412351E-03
14.986	0.535632E+05	0.628306E+00	-.217131E+02	-.254699E-03
22.480	0.518898E+05	0.607739E+00	-.233789E+02	-.274238E-03
29.974	0.500496E+05	0.587091E+00	-.176325E+02	-.206832E-03
37.466	0.470184E+05	0.551534E+00	-.396939E+02	-.465617E-03
44.958	0.443551E+05	0.520294E+00	-.310132E+01	-.363790E-04
52.450	0.387641E+05	0.454710E+00	-.193796E+02	-.227326E-03
59.942	0.326110E+05	0.382533E+00	0.377450E+01	0.442756E-04
67.436	0.242396E+05	0.284335E+00	0.222544E+02	0.261048E-03
74.931	0.160379E+05	0.188120E+00	0.970598E+02	0.113852E-02
82.425	0.731838E+04	0.858994E-01	0.533516E+02	0.602364E-03
89.923	-.173031E+04	-.202968E-01	0.234678E+03	0.275272E-02
97.423	-.106595E+05	-.125038E+00	0.211273E+03	0.247827E-02
104.922	-.194725E+05	-.228415E+00	0.650811E+03	0.763414E-02
112.426	-.275895E+05	-.323629E+00	0.743166E+03	0.871748E-02
119.931	-.359974E+05	-.421883E+00	0.156554E+04	0.183641E-01
127.439	-.409004E+05	-.479770E+00	0.196758E+04	0.230791E-01
134.946	-.450875E+05	-.528885E+00	0.272689E+04	0.319869E-01
142.456	-.469886E+05	-.551246E+00	0.361946E+04	0.424569E-01
149.965	-.488630E+05	-.573172E+00	0.438925E+04	0.505483E-01
157.474	-.489287E+05	-.573943E+00	0.529877E+04	0.620617E-01
164.985	-.491819E+05	-.576913E+00	0.553256E+04	0.648977E-01
172.492	-.487287E+05	-.571597E+00	0.625805E+04	0.734083E-01
180.000	-.487593E+05	-.571956E+00	0.596368E+04	0.699551E-01

MODEL IC1 IN BENDING

STEP 2 INCREMENT 20
PLASTIC DISSIPATION = 10,855.6 lb-in
TOTAL BENDING MOMENT =
0.215742×10^8 lb-in

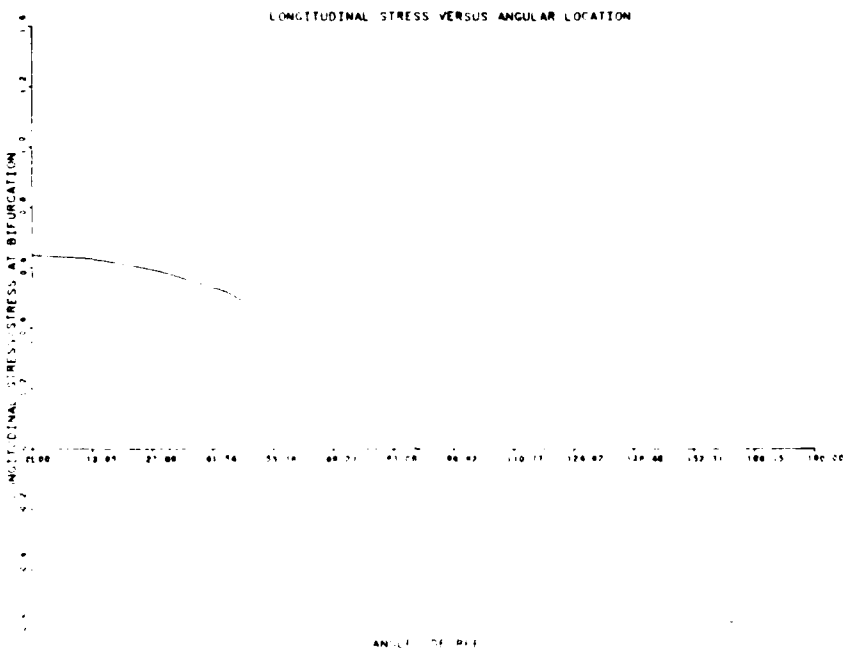

(A)

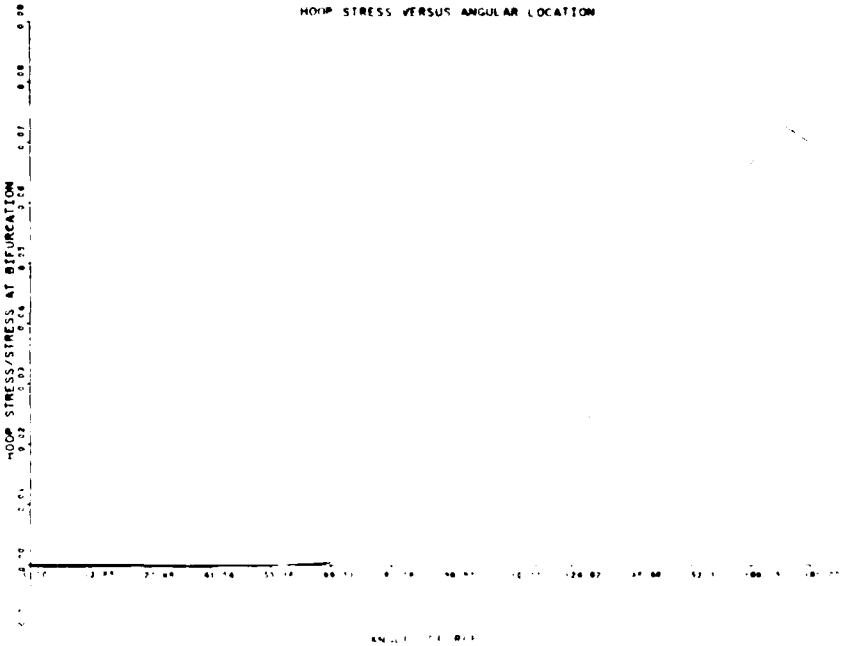

(B)

FIGURE 26. (A) DISTRIBUTION OF AXIAL STRESS AT MIDLENGTH FOR MODEL IC1
(B) DISTRIBUTION OF HOOP STRESS AT MIDLENGTH FOR MODEL IC1

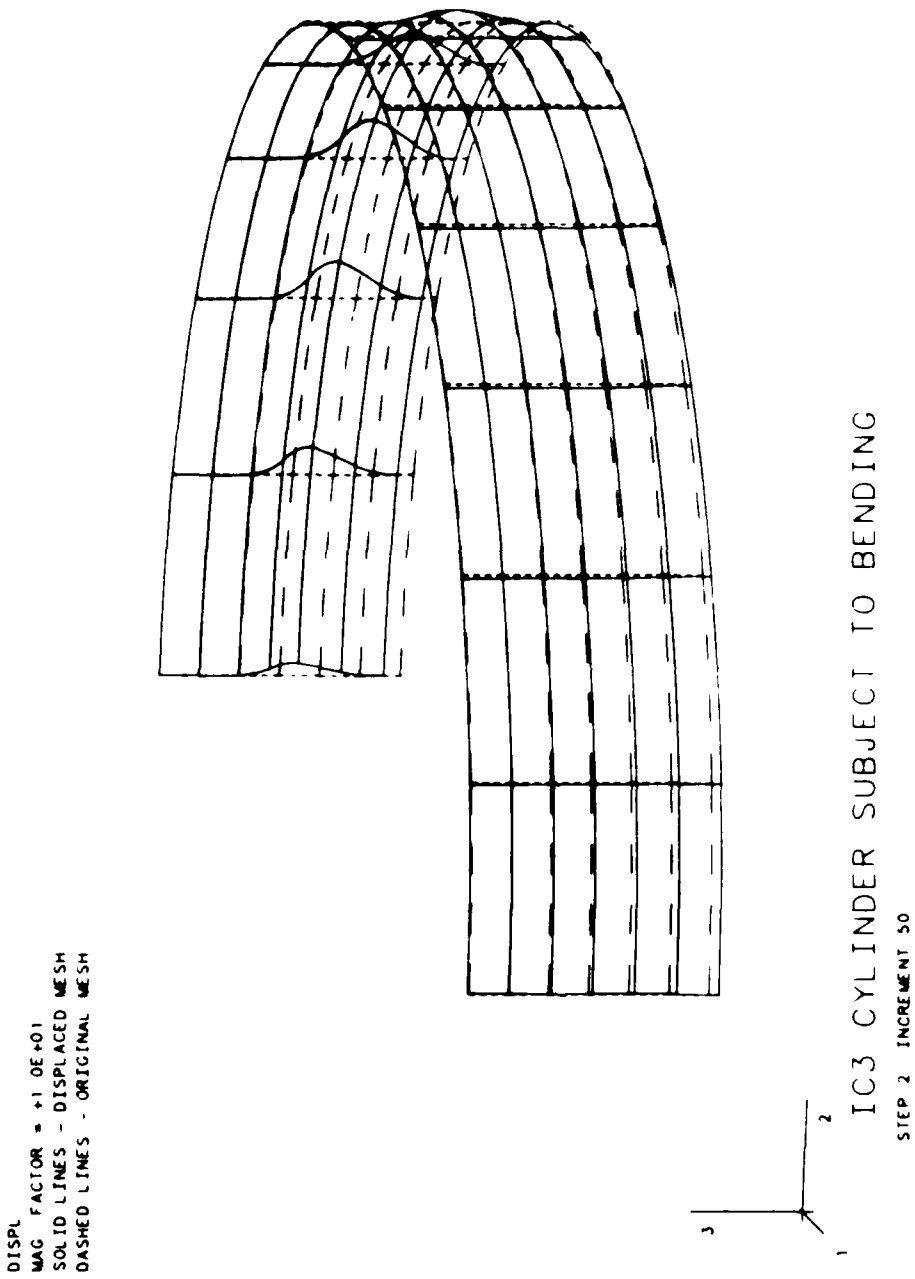

FIGURE 27. DEFORMED AND UNDEFORMED PROFILES FOR MODEL IC3 AT STEP 2, INCREMENT 50

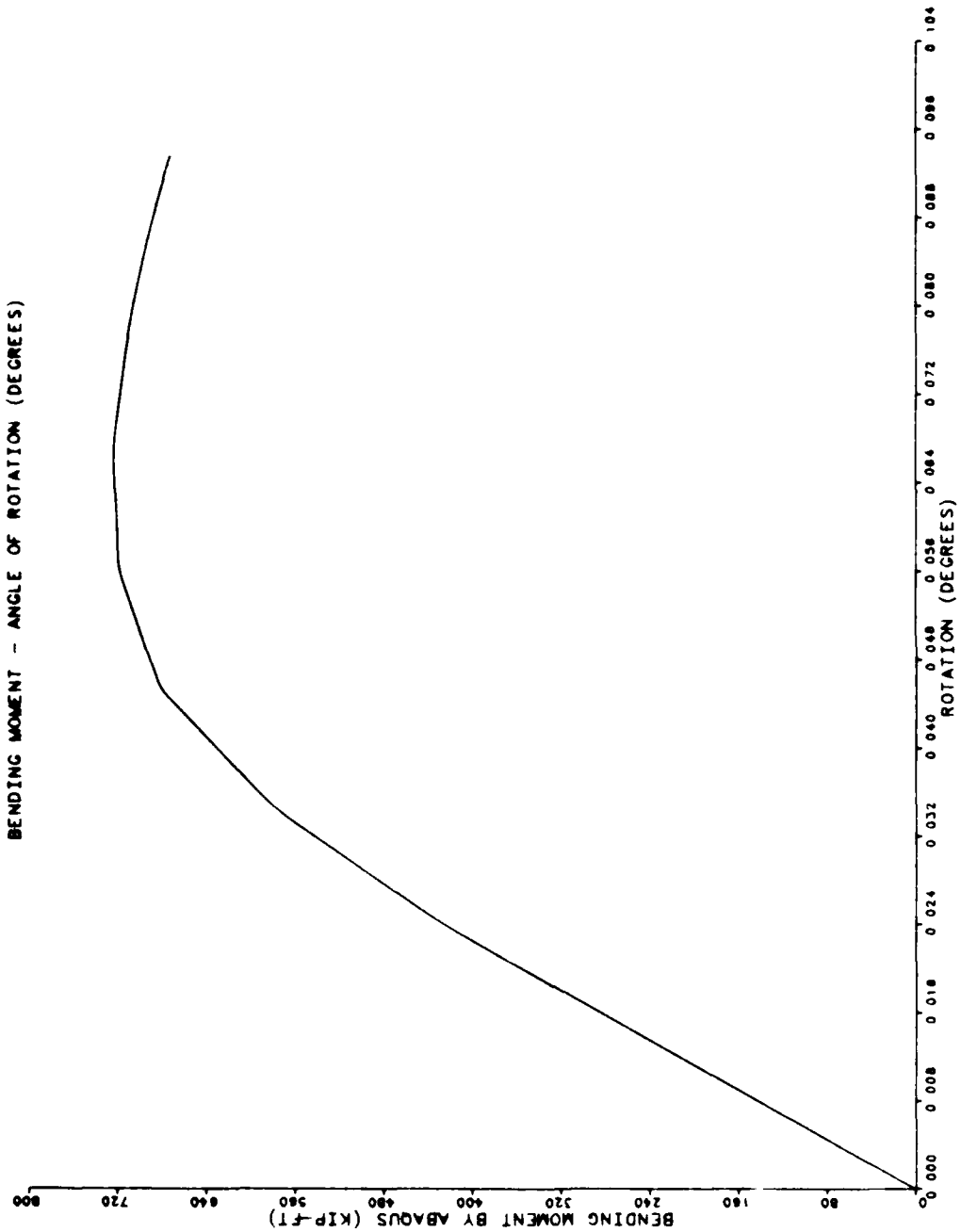

FIGURE 28. BENDING MOMENT VERSUS ROTATION FOR MODEL IC3

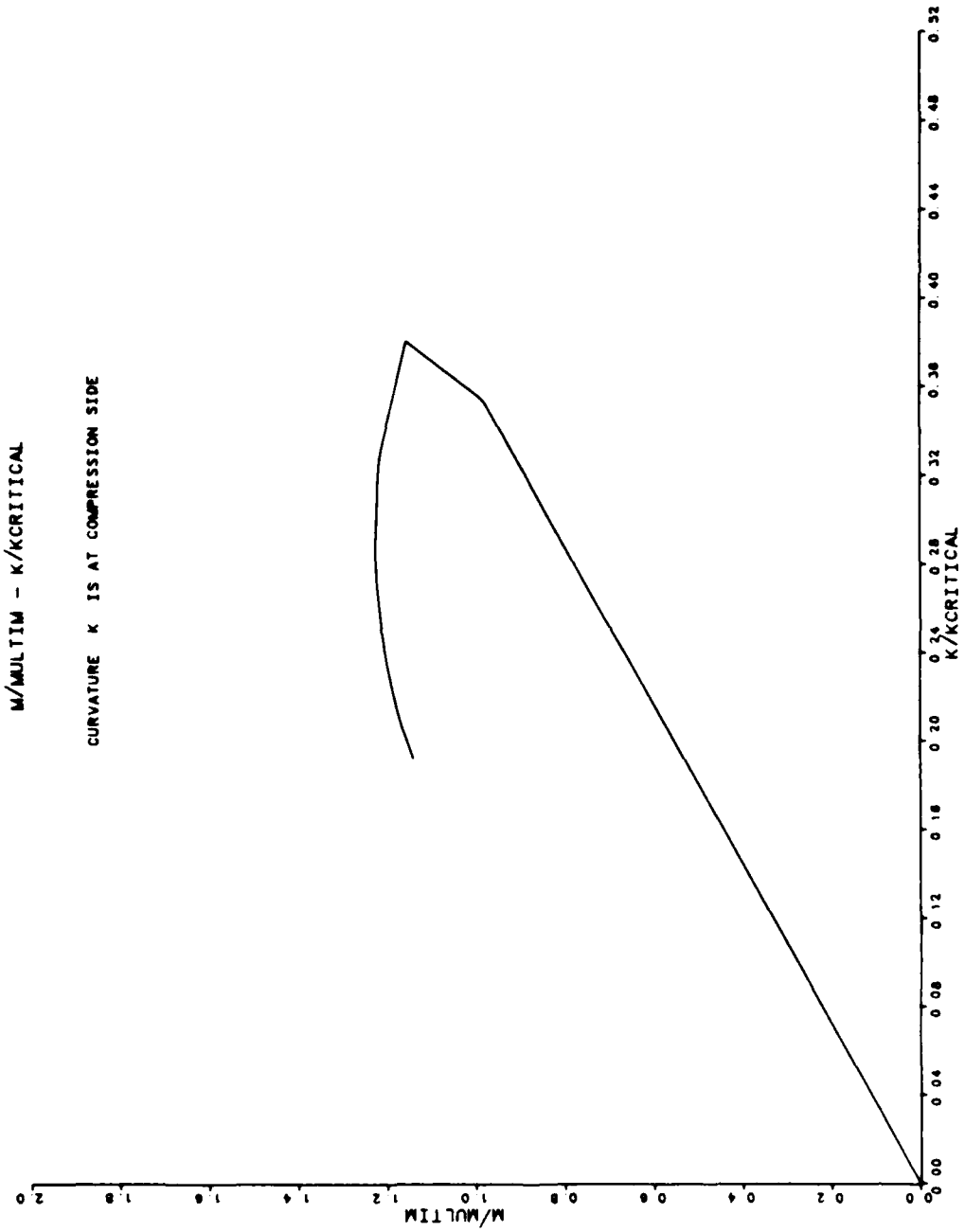

FIGURE 29. $M/M_{ULTIMATE}$ VERSUS $K/K_{CRITICAL}$ FOR MODEL IC3

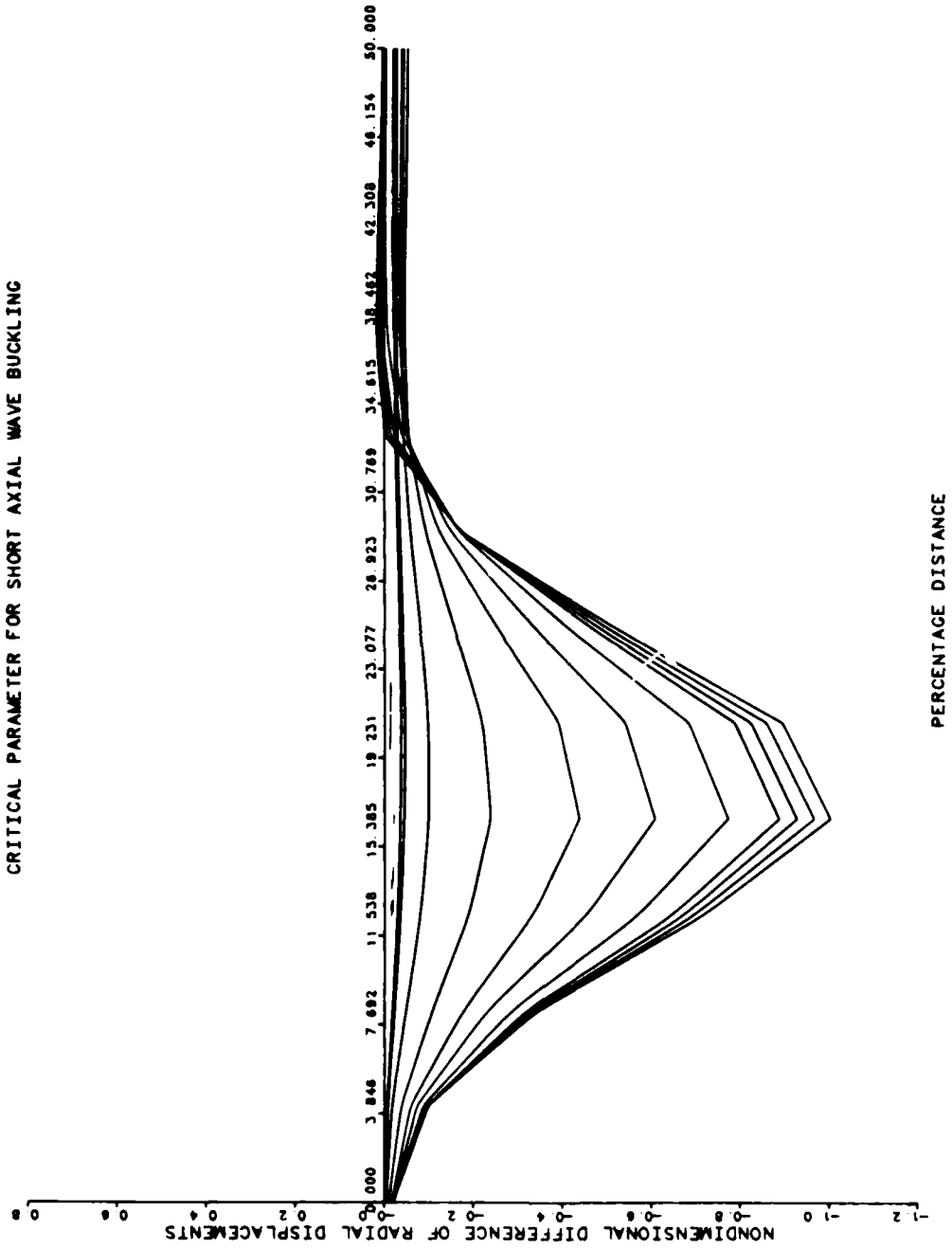

FIGURE 30. CRITICAL PARAMETER δ w/h PARAMETER FOR SHORT AXIAL WAVE LENGTH FOR MODEL IC3

STEP NO. 7 FOR STRESSES

ANGLE (DEGREES)	LONGITUDINAL MEMBRANE STRESS (PSI)	NONDIMENSIONAL MEMBRANE LONGITUDINAL STRESS	HOOP STRESS (PSI)	NONDIMENSIONAL HOOP STRESS
0.000	0.642829E+05	0.452112E+00	0.435281E+04	0.306084E-01
7.495	0.641384E+05	0.451096E+00	0.403149E+04	0.283558E-01
14.988	0.643147E+05	0.452336E+00	0.384566E+04	0.270472E-01
22.483	0.630562E+05	0.443484E+00	0.321140E+04	0.225863E-01
29.978	0.613694E+05	0.431621E+00	0.249204E+04	0.175269E-01
37.474	0.574819E+05	0.404280E+00	0.232071E+04	0.163219E-01
44.971	0.537099E+05	0.377750E+00	0.214385E+04	0.150781E-01
52.469	0.471512E+05	0.331622E+00	0.174196E+04	0.122515E-01
59.967	0.401487E+05	0.282316E+00	0.135938E+04	0.956075E-02
67.466	0.268998E+05	0.189191E+00	0.931924E+03	0.655438E-02
74.966	0.140946E+05	0.991298E-01	0.473285E+03	0.332872E-02
82.465	0.485719E+03	0.341614E-02	-.193002E+03	-.135741E-02
89.967	-.132608E+05	-.932641E-01	-.827576E+03	-.582048E-02
97.470	-.265623E+05	-.186817E+00	-.172850E+04	-.121568E-01
104.972	-.404118E+05	-.284223E+00	-.253223E+04	-.178096E-01
112.476	-.464233E+05	-.326503E+00	-.389303E+04	-.273803E-01
119.980	-.517245E+05	-.363787E+00	-.528597E+04	-.371771E-01
127.484	-.510259E+05	-.358874E+00	-.725029E+04	-.509922E-01
134.988	-.498552E+05	-.350640E+00	-.925388E+04	-.650840E-01
142.491	-.475650E+05	-.334532E+00	-.105549E+05	-.742344E-01
149.994	-.456008E+05	-.322125E+00	-.118748E+05	-.835174E-01
157.496	-.449183E+05	-.315918E+00	-.125786E+05	-.884688E-01
164.998	-.439901E+05	-.309389E+00	-.133677E+05	-.940176E-01
172.498	-.437164E+05	-.307464E+00	-.136191E+05	-.957854E-01
180.000	-.434515E+05	-.305601E+00	-.138563E+05	-.974540E-01

MODEL IC3 IN BENDING

STEP 2 INCREMENT 25
PLASTIC DISSIPATION = 3,152.01 lb-in
TOTAL BENDING MOMENT = 0.868945×10^7 lb-in

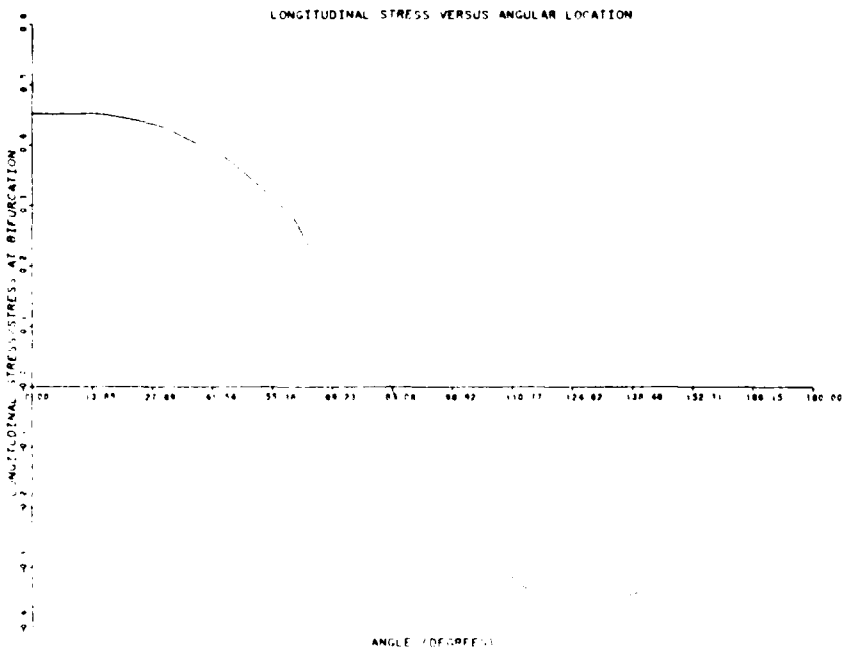

(A)

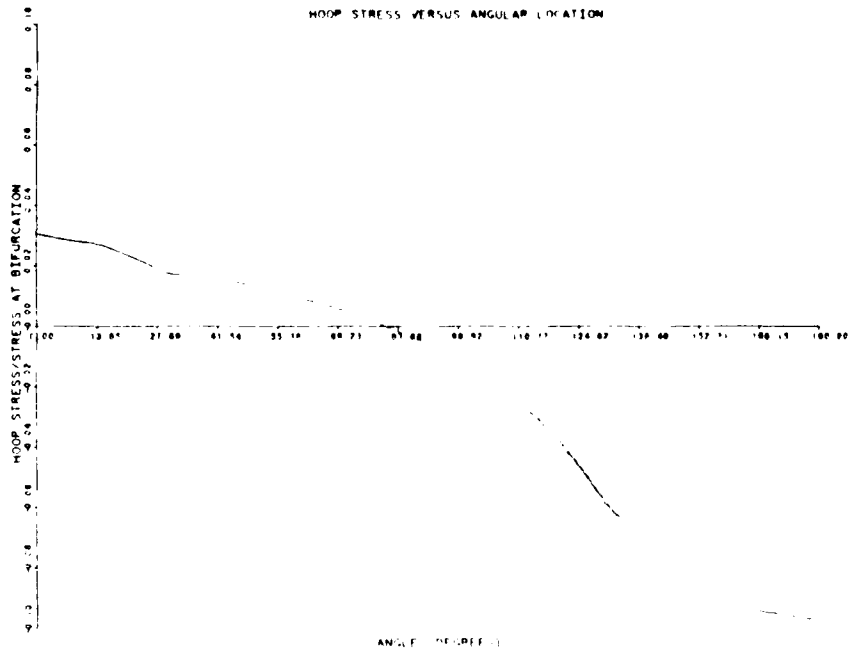

(B)

FIGURE 31. (A) DISTRIBUTION OF AXIAL STRESS AT MIDLENGTH FOR MODEL IC3
(B) DISTRIBUTION OF HOOP STRESS AT MIDLENGTH FOR MODEL IC3

STEP NO. 12 FOR STRESSES

ANGLE (DEGREES)	LONGITUDINAL MEMBRANE STRESS (PSI)	NONDIMENSIONAL MEMBRANE LONGITUDINAL STRESS	HOOP STRESS (PSI)	NONDIMENSIONAL HOOP STRESS
0.000	0.654667E+05	0.468438E+00	0.789911E+04	0.499292E-01
7.493	0.652734E+05	0.459079E+00	0.663773E+04	0.466842E-01
14.985	0.658952E+05	0.457825E+00	0.620868E+04	0.436667E-01
22.478	0.646418E+05	0.454636E+00	0.516952E+04	0.363581E-01
29.972	0.651009E+05	0.457865E+00	0.432425E+04	0.304132E-01
37.469	0.615252E+05	0.432717E+00	0.325049E+04	0.228613E-01
44.966	0.571421E+05	0.401890E+00	0.203543E+04	0.143155E-01
52.463	0.480645E+05	0.338046E+00	0.159484E+04	0.112168E-01
59.961	0.383461E+05	0.269695E+00	0.115506E+04	0.812374E-02
67.460	0.199373E+05	0.140222E+00	0.441526E+03	0.310533E-02
74.961	0.188934E+04	0.132880E-01	-.336616E+03	-.236748E-02
82.461	-.167151E+05	-.117560E+00	-.169295E+04	-.119068E-01
89.965	-.369538E+05	-.259902E+00	-.280733E+04	-.197444E-01
97.469	-.456780E+05	-.321261E+00	-.489050E+04	-.343957E-01
104.973	-.522075E+05	-.367184E+00	-.720659E+04	-.506852E-01
112.477	-.490960E+05	-.345300E+00	-.994273E+04	-.699289E-01
119.980	-.458160E+05	-.322232E+00	-.126014E+05	-.886275E-01
127.484	-.424628E+05	-.298648E+00	-.137211E+05	-.965028E-01
134.987	-.397175E+05	-.279340E+00	-.149320E+05	-.105019E+00
142.490	-.379854E+05	-.267158E+00	-.151686E+05	-.106683E+00
149.993	-.361818E+05	-.254473E+00	-.154127E+05	-.108400E+00
157.495	-.350507E+05	-.246517E+00	-.152087E+05	-.106965E+00
164.997	-.339118E+05	-.238508E+00	-.150392E+05	-.105773E+00
172.497	-.335384E+05	-.235881E+00	-.149262E+05	-.104979E+00
180.000	-.332055E+05	-.233540E+00	-.147879E+05	-.104006E+00

1 21 PLOTS HAVE BEEN GENERATED

MODEL IC3 IN BENDING

STEP 2 INCREMENT 50
PLASTIC DISSIPATION = 6,668.75 lb-in
TOTAL BENDING MOMENT =
0.807536×10^2 lb-in

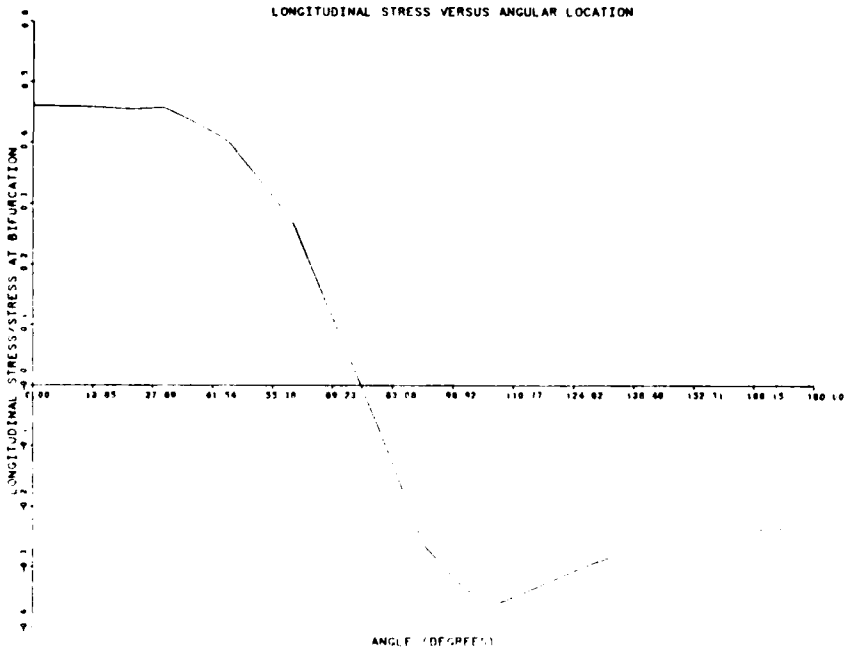

(A)

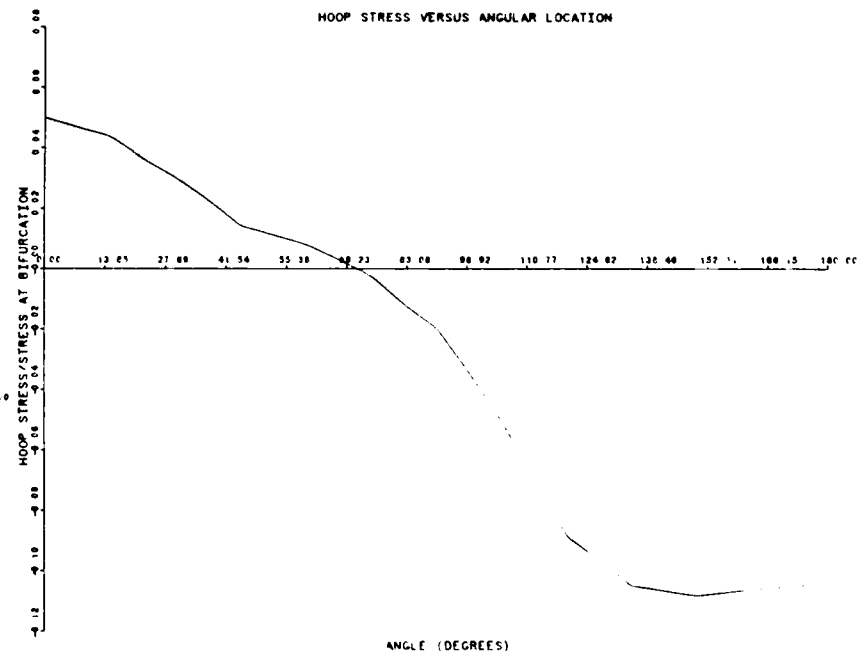

(B)

FIGURE 32. (A) DISTRIBUTION OF AXIAL STRESS AT MIDLENGTH FOR MODEL IC3
(B) DISTRIBUTION OF HOOP STRESS AT MIDLENGTH FOR MODEL IC3

INCREMENT NO.	STRAIN ENERGY	EXTERNAL WORK DONE	PLASTIC DISSIPATION	ABAQUS STEP	ABAQUS INCREMENT
1	0.127204E+02	0.158832E+02	0.000000E+00	1	5
2	0.879397E+03	0.105993E+04	0.798614E-01	1	10
3	0.110134E+04	0.128691E+04	0.199161E+01	2	5
4	0.198726E+04	0.240388E+04	0.201469E+03	2	10
5	0.281884E+04	0.387239E+04	0.813697E+03	2	15
6	0.336067E+04	0.548439E+04	0.187341E+04	2	20
7	0.372775E+04	0.713271E+04	0.315201E+04	2	25
8	0.396236E+04	0.876480E+04	0.455169E+04	2	30
9	0.407135E+04	0.988195E+04	0.556229E+04	2	35
10	0.409666E+04	0.102750E+05	0.593035E+04	2	40
11	0.411708E+04	0.106641E+05	0.629926E+04	2	45
12	0.413264E+04	0.110488E+05	0.666875E+04	2	50

THIS TABLE IS DIRECTLY COMPUTED BY ABAQUS

STEP NO.	TOTAL BENDING MOMENT AT AUXILIARY NODE (LB-IN)	ROTATION ABOUT GLOBAL Y-AXIS (DEGREES)
1	0.557606E+06	0.261412E-02
2	0.463408E+07	0.217399E-01
3	0.518505E+07	0.243521E-01
4	0.694606E+07	0.344965E-01
5	0.817855E+07	0.453655E-01
6	0.863034E+07	0.562345E-01
7	0.868945E+07	0.671034E-01
8	0.852624E+07	0.779724E-01
9	0.833801E+07	0.855807E-01
10	0.825516E+07	0.882980E-01
11	0.816751E+07	0.910152E-01
12	0.807536E+07	0.937325E-01

FIGURE 33. ENERGIES AND BENDING MOMENTS VERSUS ANGLE OF ROTATION FOR MODEL IC3

BENDING MOMENTS ARE BASED ON AN AXIS THROUGH POINT OF ZERO AXIAL FORCE

ARMS AND POINT OF ZERO AXIAL FORCE ARE IN TERMS OF ORIGINAL COORDINATE SYSTEM
FORCES ARE EXTRACTED FROM REACTIONS

BENDING MOMENTS AT CUT NO. 2

NODE NO.	STEP 1		STEP 2		STEP 3	
	FORCE ZZ	ARM XX	FORCE ZZ	ARM XX	FORCE ZZ	ARM XX
301	0.440351E+03	0.176965E+02	0.366822E+04	0.176931E+02	0.410359E+04	0.176926E+02
302	0.173102E+04	0.175445E+02	0.144185E+05	0.175411E+02	0.161327E+05	0.175407E+02
303	0.850367E+03	0.170936E+02	0.708220E+04	0.170904E+02	0.792625E+04	0.170900E+02
304	0.161307E+04	0.163496E+02	0.134300E+05	0.163468E+02	0.150352E+05	0.163465E+02
305	0.762537E+03	0.153257E+02	0.634631E+04	0.153233E+02	0.710668E+04	0.153231E+02
306	0.138518E+04	0.140398E+02	0.115217E+05	0.140380E+02	0.129012E+05	0.140378E+02
307	0.622550E+03	0.125138E+02	0.517450E+04	0.125126E+02	0.579350E+04	0.125125E+02
308	0.106264E+04	0.107729E+02	0.882386E+04	0.107723E+02	0.987691E+04	0.107722E+02
309	0.440034E+03	0.884799E+01	0.364891E+04	0.884792E+01	0.408311E+04	0.884793E+01
310	0.667644E+03	0.677205E+01	0.552530E+04	0.677246E+01	0.618002E+04	0.677252E+01
311	0.227585E+03	0.458010E+01	0.187631E+04	0.458087E+01	0.209682E+04	0.458098E+01
312	0.227361E+03	0.231014E+01	0.185587E+04	0.231113E+01	0.206884E+04	0.231127E+01
313	-0.241966E+00	0.145859E-03	-0.204352E+02	0.121435E-02	-0.279679E+02	0.136388E-02
314	-0.228264E+03	-0.230986E+01	-0.193263E+04	-0.230888E+01	-0.217444E+04	-0.230874E+01
315	-0.228001E+03	-0.457990E+01	-0.191185E+04	-0.457914E+01	-0.214601E+04	-0.457903E+01
316	-0.668292E+03	-0.677195E+01	-0.558205E+04	-0.677155E+01	-0.626050E+04	-0.677149E+01
317	-0.440263E+03	-0.884801E+01	-0.366981E+04	-0.884809E+01	-0.411399E+04	-0.884809E+01
318	-0.106285E+04	-0.107731E+02	-0.884561E+04	-0.107737E+02	-0.991365E+04	-0.107738E+02
319	-0.622527E+03	-0.125142E+02	-0.517537E+04	-0.125154E+02	-0.579958E+04	-0.125155E+02
320	-0.138488E+04	-0.140402E+02	-0.115027E+05	-0.140421E+02	-0.128845E+05	-0.140423E+02
321	-0.762258E+03	-0.153263E+02	-0.632680E+04	-0.153287E+02	-0.708394E+04	-0.153290E+02
322	-0.161232E+04	-0.163504E+02	-0.133745E+05	-0.163532E+02	-0.149589E+05	-0.163536E+02
323	-0.849902E+03	-0.170944E+02	-0.704598E+04	-0.170976E+02	-0.787210E+04	-0.170981E+02
324	-0.173002E+04	-0.175455E+02	-0.143376E+05	-0.175489E+02	-0.160028E+05	-0.175494E+02
325	-0.440085E+03	-0.176975E+02	-0.364633E+04	-0.177010E+02	-0.406651E+04	-0.177015E+02
TOTAL OUT OF BALANCE FORCE ZZ	0.456970E+00		0.185547E-01		0.200195E-01	
TOTAL MOMENT	0.278819E+06		0.231717E+07		0.259268E+07	
FORCE ZZ ON TOP QUARTER	0.100303E+05		0.833717E+05		0.933049E+05	
FORCE ZZ ON BOTTOM QUARTER	-0.100299E+05		-0.833716E+05		-0.933049E+05	
POINT OF ZERO FORCE	0.502889E-02		0.508149E-01		0.619815E-01	
PERCENTAGE OUT OF BALANCE FORCE ZZ	0.00		0.00		0.00	

FIGURE 34. BENDING MOMENT COMPUTATION THROUGH CONSISTENT FORCES AT MIDDLE FOR MODEL IC3 (FOR HALF ONLY)

NODE NO.	STEP 4 FORCE ZZ	STEP 4 ARM XX	STEP 5 FORCE ZZ	STEP 5 ARM XX	STEP 6 FORCE ZZ	STEP 6 ARM XX
301	0.527693E+04	0.176905E+02	0.619564E+04	0.176892E+02	0.670997E+04	0.176889E+02
302	0.208766E+05	0.175387E+02	0.245094E+05	0.175374E+02	0.266127E+05	0.175372E+02
303	0.103285E+05	0.170881E+02	0.121203E+05	0.170869E+02	0.132035E+05	0.170868E+02
304	0.199849E+05	0.163449E+02	0.234314E+05	0.163438E+02	0.256510E+05	0.163438E+02
305	0.967432E+04	0.153218E+02	0.113097E+05	0.153210E+02	0.124432E+05	0.153211E+02
306	0.179420E+05	0.140369E+02	0.212325E+05	0.140363E+02	0.233027E+05	0.140366E+02
307	0.819252E+04	0.125120E+02	0.998510E+04	0.125117E+02	0.108478E+05	0.125121E+02
308	0.138744E+05	0.107721E+02	0.174629E+05	0.107721E+02	0.192315E+05	0.107726E+02
309	0.572986E+04	0.884801E+01	0.733979E+04	0.884830E+01	0.823641E+04	0.884889E+01
310	0.864412E+04	0.677282E+01	0.108413E+05	0.677328E+01	0.115996E+05	0.677394E+01
311	0.291331E+04	0.458144E+01	0.357155E+04	0.458202E+01	0.350920E+04	0.458272E+01
312	0.281583E+04	0.231183E+01	0.318571E+04	0.231248E+01	0.211365E+04	0.231316E+01
313	-0.971087E+02	0.196034E-02	-0.385615E+03	0.261973E-02	-0.138705E+04	0.323324E-02
314	-0.319325E+04	-0.230818E+01	-0.470638E+04	-0.230758E+01	-0.764950E+04	-0.230707E+01
315	-0.309503E+04	-0.457859E+01	-0.431977E+04	-0.457811E+01	-0.632498E+04	-0.457773E+01
316	-0.896872E+04	-0.677123E+01	-0.122700E+05	-0.677093E+01	-0.164894E+05	-0.677076E+01
317	-0.587306E+04	-0.884806E+01	-0.802115E+04	-0.884797E+01	-0.999914E+04	-0.884803E+01
318	-0.140964E+05	-0.107740E+02	-0.182213E+05	-0.107743E+02	-0.211197E+05	-0.107745E+02
319	-0.824794E+04	-0.125161E+02	-0.100832E+05	-0.125168E+02	-0.111559E+05	-0.125170E+02
320	-0.178464E+05	-0.140433E+02	-0.210701E+05	-0.140442E+02	-0.219048E+05	-0.140442E+02
321	-0.953775E+04	-0.153304E+02	-0.109947E+05	-0.153315E+02	-0.107425E+05	-0.153312E+02
322	-0.196265E+05	-0.163553E+02	-0.221677E+05	-0.163566E+02	-0.209439E+05	-0.163558E+02
323	-0.101135E+05	-0.171001E+02	-0.111696E+05	-0.171014E+02	-0.102664E+05	-0.171001E+02
324	-0.204061E+05	-0.175515E+02	-0.222265E+05	-0.175528E+02	-0.204016E+05	-0.175512E+02
325	-0.515157E+04	-0.177037E+02	-0.554938E+04	-0.177050E+02	-0.507633E+04	-0.177032E+02
TOTAL OUT OF BALANCE FORCE ZZ	0.312500E-01		0.439453E-02		0.371094E-01	
TOTAL MOMENT	0.347327E+07		0.408963E+07		0.431560E+07	
FORCE ZZ ON TOP QUARTER	0.126253E+06		0.151185E+06		0.163461E+06	
FORCE ZZ ON BOTTOM QUARTER	-0.126253E+06		-0.151185E+06		-0.163461E+06	
POINT OF ZERO FORCE	0.150878E+00		0.452507E+00		0.131500E+01	
PERCENTAGE OUT OF BALANCE FORCE ZZ	0.00		0.00		0.00	

FIGURE 34. (CONTINUED)

NODE NO.	STEP 7 FORCE ZZ	STEP 7 ARM XX	STEP 8 FORCE ZZ	STEP 8 ARM XX	STEP 9 FORCE ZZ	STEP 9 ARM XX
301	0.689778E+04	0.176875E+02	0.697909E+04	0.176854E+02	0.700815E+04	0.176844E+02
302	0.275205E+05	0.175358E+02	0.278077E+05	0.175339E+02	0.279327E+05	0.175330E+02
303	0.138012E+05	0.170856E+02	0.138582E+05	0.170840E+02	0.139215E+05	0.170833E+02
304	0.270087E+05	0.163431E+02	0.275475E+05	0.163418E+02	0.276494E+05	0.163413E+02
305	0.131523E+05	0.153209E+02	0.137226E+05	0.153201E+02	0.139226E+05	0.153198E+02
306	0.246825E+05	0.140367E+02	0.256113E+05	0.140364E+02	0.260998E+05	0.140363E+02
307	0.115097E+05	0.125124E+02	0.119150E+05	0.125127E+02	0.120836E+05	0.125128E+02
308	0.202139E+05	0.107731E+02	0.207409E+05	0.107736E+02	0.208605E+05	0.107739E+02
309	0.860393E+04	0.884948E+01	0.866585E+04	0.885006E+01	0.855367E+04	0.885045E+01
310	0.115236E+05	0.677457E+01	0.107738E+05	0.677517E+01	0.988175E+04	0.677557E+01
311	0.301807E+04	0.458334E+01	0.220468E+04	0.458389E+01	0.145031E+04	0.458423E+01
312	0.204944E+03	0.231372E+01	-0.235562E+04	0.231416E+01	-0.448867E+04	0.231442E+01
313	-0.283797E+04	0.369054E-02	-0.466547E+04	0.400909E-02	-0.621277E+04	0.416721E-02
314	-0.113564E+05	-0.230675E+01	-0.152039E+05	-0.230656E+01	-0.175410E+05	-0.230650E+01
315	-0.862614E+04	-0.457753E+01	-0.102864E+05	-0.457744E+01	-0.109392E+05	-0.457743E+01
316	-0.198458E+05	-0.677069E+01	-0.213224E+05	-0.677062E+01	-0.215504E+05	-0.677054E+01
317	-0.110443E+05	-0.884799E+01	-0.109740E+05	-0.884776E+01	-0.104873E+05	-0.884751E+01
318	-0.218021E+05	-0.107743E+02	-0.205515E+05	-0.107736E+02	-0.193969E+05	-0.107730E+02
319	-0.106541E+05	-0.125165E+02	-0.971903E+04	-0.125152E+02	-0.911569E+04	-0.125144E+02
320	-0.203133E+05	-0.140431E+02	-0.185999E+05	-0.140414E+02	-0.174717E+05	-0.140404E+02
321	-0.978744E+04	-0.153294E+02	-0.894518E+04	-0.153273E+02	-0.836545E+04	-0.153264E+02
322	-0.191746E+05	-0.163535E+02	-0.174981E+05	-0.163513E+02	-0.162926E+05	-0.163504E+02
323	-0.939466E+04	-0.170975E+02	-0.854779E+04	-0.170953E+02	-0.793382E+04	-0.170944E+02
324	-0.186590E+05	-0.175485E+02	-0.169447E+05	-0.175462E+02	-0.156773E+05	-0.175454E+02
325	-0.464127E+04	-0.177005E+02	-0.421237E+04	-0.176982E+02	-0.389128E+04	-0.176974E+02
TOTAL OUT OF BALANCE FORCE ZZ	0.123047E+00		0.854492E-01		0.285645E-01	
TOTAL MOMENT	0.434517E+07		0.426357E+07		0.416954E+07	
FORCE ZZ ON TOP QUARTER	0.168137E+06		0.169827E+06		0.169364E+06	
FORCE ZZ ON BOTTOM QUARTER	-0.168137E+06		-0.169826E+06		-0.169364E+06	
POINT OF ZERO FORCE	0.223210E+01		0.310462E+01		0.369498E+01	
PERCENTAGE OUT OF BALANCE FORCE ZZ	0.00		0.00		0.00	

FIGURE 34. (CONTINUED)

NODE NO.	STEP 10 FORCE ZZ	STEP 10 ARM XX	STEP 11 FORCE ZZ	STEP 11 ARM XX	STEP 12 FORCE ZZ	STEP 12 ARM XX
301	0.701600E+04	0.176842E+02	0.702250E+04	0.176839E+02	0.702849E+04	0.176837E+02
302	0.279653E+05	0.175327E+02	0.279943E+05	0.175325E+02	0.280204E+05	0.175322E+02
303	0.139375E+05	0.170830E+02	0.139548E+05	0.170828E+02	0.139706E+05	0.170826E+02
304	0.276861E+05	0.163411E+02	0.277171E+05	0.163410E+02	0.277458E+05	0.163408E+02
305	0.139509E+05	0.153196E+02	0.139678E+05	0.153196E+02	0.139753E+05	0.153195E+02
306	0.262140E+05	0.140363E+02	0.263036E+05	0.140363E+02	0.263694E+05	0.140362E+02
307	0.121461E+05	0.125129E+02	0.122016E+05	0.125130E+02	0.122499E+05	0.125131E+02
308	0.208223E+05	0.107740E+02	0.207484E+05	0.107741E+02	0.206423E+05	0.107742E+02
309	0.846381E+04	0.885059E+01	0.834606E+04	0.885072E+01	0.820603E+04	0.885084E+01
310	0.947316E+04	0.677571E+01	0.901882E+04	0.677583E+01	0.852528E+04	0.677595E+01
311	0.113376E+04	0.458434E+01	0.785728E+03	0.458444E+01	0.410271E+03	0.458452E+01
312	-0.533759E+04	0.231450E+01	-0.623029E+04	0.231455E+01	-0.715349E+04	0.231459E+01
313	-0.679569E+04	0.420166E-02	-0.735703E+04	0.421232E-02	-0.788878E+04	0.421213E-02
314	-0.183030E+05	-0.230650E+01	-0.189602E+05	-0.230651E+01	-0.195251E+05	-0.230653E+01
315	-0.110670E+05	-0.457743E+01	-0.111291E+05	-0.457745E+01	-0.111461E+05	-0.457746E+01
316	-0.214285E+05	-0.677049E+01	-0.212282E+05	-0.677045E+01	-0.209778E+05	-0.677040E+01
317	-0.102559E+05	-0.884740E+01	-0.100207E+05	-0.884728E+01	-0.978534E+04	-0.884715E+01
318	-0.189784E+05	-0.107729E+02	-0.185590E+05	-0.107727E+02	-0.181409E+05	-0.107725E+02
319	-0.890659E+04	-0.125141E+02	-0.869612E+04	-0.125139E+02	-0.848933E+04	-0.125136E+02
320	-0.170518E+05	-0.140402E+02	-0.166317E+05	-0.140400E+02	-0.162257E+05	-0.140397E+02
321	-0.815033E+04	-0.153261E+02	-0.793836E+04	-0.153260E+02	-0.773567E+04	-0.153257E+02
322	-0.158468E+05	-0.163502E+02	-0.153997E+05	-0.163501E+02	-0.149617E+05	-0.163498E+02
323	-0.770396E+04	-0.170943E+02	-0.747796E+04	-0.170942E+02	-0.725039E+04	-0.170940E+02
324	-0.152089E+05	-0.175453E+02	-0.147670E+05	-0.175452E+02	-0.143122E+05	-0.175451E+02
325	-0.377442E+04	-0.176973E+02	-0.366539E+04	-0.176973E+02	-0.355132E+04	-0.176972E+02
TOTAL OUT OF BALANCE FORCE ZZ	0.119629E-01		0.283203E-01		0.317383E-01	
TOTAL MOMENT	0.412816E+07		0.408440E+07		0.403838E+07	
FORCE ZZ ON TOP QUARTER	0.168809E+06		0.168061E+06		0.167144E+06	
FORCE ZZ ON BOTTOM QUARTER	-0.168809E+06		-0.168061E+06		-0.167144E+06	
POINT OF ZERO FORCE	0.390993E+01		0.413010E+01		0.435400E+01	
PERCENTAGE OUT OF BALANCE FORCE ZZ	0.00		0.00		0.00	

FIGURE 34. (CONTINUED)

CRITICAL BENDING MOMENT (LB-IN)	CRITICAL BENDING MOMENT BY BRAZIER (LB-IN)	INERTIA OF UNDEFORMED CROSS-SECTION (IN**4)
0.193869E+08	0.105529E+08	0.241300E+04

CRITICAL CURVATURE ASSOCIATED WITH APPLIED MOMENT AT BIFURCATION (1/IN)	MAXIMUM STRESS AT BIFURCATION (LB/IN**2)
0.26781092E-03	0.14218350E+06

FULLY PLASTIC MOMENT BASED ON YIELD STRESS (LB-IN)	MAXIMUM AXIAL FORCE BASED ON YIELD STRESS (LBS)
0.707537E+07	0.628014E+06

NORMALIZED NET AXIAL FORCE

0.000000E+00

NEUTRAL AXIS AND OUTER FIBRE LOCATIONS ARE DERIVED
FROM CALCULATED LONGITUDINAL MEMBRANE FORCES
WHICH ARE COMPUTED FROM NODAL STRESSES

STEP NO.	MEAN CURVATURE (1/IN)	CURVATURE AT 0 DEGREES (1/IN)	CURVATURE AT 180 DEGREES (1/IN)	M/MCRITICAL	M/MCRITICAL BRAZIER
1	0.765756E-05	0.766210E-05	0.765303E-05	0.287637E-01	0.528423E-01
2	0.635679E-04	0.639701E-04	0.631679E-04	0.239046E+00	0.439155E+00
3	0.709734E-04	0.715983E-04	0.703528E-04	0.267467E+00	0.491369E+00
4	0.977347E-04	0.100676E-03	0.948439E-04	0.358311E+00	0.658260E+00
5	0.115071E-03	0.128881E-03	0.101959E-03	0.421897E+00	0.775074E+00
6	0.117500E-03	0.152515E-03	0.873649E-04	0.445209E+00	0.817901E+00
7	0.132361E-03	0.206900E-03	0.746054E-04	0.448259E+00	0.823505E+00
8	0.145444E-03	0.261993E-03	0.638259E-04	0.439842E+00	0.808041E+00
9	0.150137E-03	0.292058E-03	0.574143E-04	0.430141E+00	0.790220E+00
10	0.151309E-03	0.301938E-03	0.553728E-04	0.425872E+00	0.782377E+00
11	0.152388E-03	0.311808E-03	0.534846E-04	0.421357E+00	0.774083E+00
12	0.153306E-03	0.321827E-03	0.515270E-04	0.416610E+00	0.765362E+00

FIGURE 35. PARAMETERS FOR MODEL IC3

TABLE 1. GEOMETRICAL AND MATERIAL PROPERTIES OF MODELS

MODEL No.	RADIUS R (in)	THICKNESS h (in)	YOUNG'S MODULUS E (ksi)	POISSON'S RATIO ν	YIELD STRESS σ_y (ksi)	HALF LENGTH USED IN COMPUTATION L/2 (in)	R/h	L/R
10A	5.258	0.233	28,947.0	0.3	50.000	108.0	22.566	41.08
16A	7.870	0.260	30,000.0	0.3	45.272	162.0	30.629	41.17
20A	9.873	0.255	28,947.0	0.3	50.000	162.0	38.717	32.82
10AN	5.258	0.233	28.947.0	0.3	50.000	36.0	22.566	13.69
16AN	7.870	0.260	30,000.0	0.3	45.272	54.0	30.629	13.72
20AN	9.873	0.255	28,947.0	0.3	50.000	54.0	38.717	10.94

TABLE 2. CHARACTERISTIC PARAMETERS OF MODELS

MODEL No.	(1) σ_{CR} (ksi)	(2) M_{CR} (k-in)	(3) K_{CR} (l/in)	(4) M_{BR} (k-in)	(5) M_o (k-in)	(6) F_o (k)	(7) I (in^4)
10A, 10AN	776.35	15,711.0	0.510074×10^{-2}	8,552.0	1.288.33	384.88	106.40
16A, 16AN	599.84	30,346.7	0.254063×10^{-2}	16,518.6	2,916.17	582.04	398.15
20A, 20AN	452.49	35,334.7	0.158329×10^{-2}	19,233.8	4,971.28	790.93	770.97

NOTES:

(1) CRITICAL STRESS AT BIFURCATION $\sigma_{CR} = \frac{E}{\sqrt{3(1-\nu^2)}}\left(\frac{h}{R}\right)$

(2) CRITICAL MOMENT AT BIFURCATION $M_{CR} = \frac{\pi E}{\sqrt{3(1-\nu^2)}} Rh^2$

(3) CRITICAL CURVATURE AT BIFURCATION $k_{CR} = \frac{1}{\sqrt{3(1-\nu^2)}} \frac{h}{R^2}$

(4) CRITICAL BRAZIER MOMENT $M_{BR} = \frac{2\sqrt{2}}{9\sqrt{(1-\nu^2)}} \pi E R h^2$

(5) PLASTIC MOMENT BASED ON YIELD STRESS $M_o = 4R^2 h \sigma_y$

(6) AXIAL FORCE BASED ON YIELD STRESS $F_o = 2Rh\sigma_y$

(7) MOMENT OF INERTIA OF UNDEFORMED CROSS-SECTION $I = \pi R^3 h$

TABLE 3. IMPERFECTION ORDINATES FOR MODEL 20A

ORDINATES

THETA

X/LT	192.000	204.000	216.000	228.000	240.000	252.000	264.000	276.000
0.000000	0.922800E-02	0.532703E-01	0.381276E-01	0.412373E-03	0.534936E-02	0.213324E-01	0.419134E-01	0.702429E-01
0.050000	-0.273508E-02	0.932986E-01	0.572972E-01	-0.236208E-01	-0.249254E-01	0.322901E-01	0.974046E-01	0.144907E+00
0.100000	-0.139790E-02	0.733454E-01	0.285544E-01	-0.497528E-01	-0.524496E-01	0.197428E-01	0.934740E-01	0.131047E+00
0.150000	0.882598E-02	0.840378E-01	0.415471E-01	-0.513955E-01	-0.768519E-01	0.174032E-01	0.111029E+00	0.118654E+00
0.200000	0.294119E-01	0.759007E-01	0.366844E-01	-0.572088E-01	-0.947356E-01	0.146194E-01	0.121397E+00	0.971359E-01
0.250000	0.569420E-01	0.107125E+00	0.630434E-01	-0.432427E-01	-0.803275E-01	0.283931E-01	0.122307E+00	0.833171E-01
0.300000	0.587691E-01	0.120308E+00	0.695473E-01	-0.426944E-01	-0.759875E-01	0.282439E-01	0.104548E+00	0.674163E-01
0.350000	0.947675E-01	0.161512E+00	0.101975E+00	-0.115966E-01	-0.566820E-01	0.310283E-01	0.970720E-01	0.751401E-01
0.400000	0.106320E+00	0.189066E+00	0.122558E+00	0.107897E-01	-0.306189E-01	0.303510E-01	0.741759E-01	0.593443E-01
0.450000	0.170502E+00	0.277381E+00	0.198644E+00	0.535319E-01	-0.869295E-02	0.279644E-01	0.774208E-01	0.799139E-01
0.500000	0.957271E-01	0.148977E+00	0.107577E+00	0.335628E-01	0.227757E-02	0.156684E-01	0.432331E-01	0.429463E-01
0.550000	-0.123206E-01	-0.167471E-01	-0.144291E-01	-0.426024E-02	0.945580E-04	-0.276715E-02	-0.222974E-02	-0.111400E-01
0.600000	0.861964E-02	0.136528E-01	0.107085E-01	0.797027E-02	0.294433E-02	0.913069E-03	0.101755E-01	0.835536E-02
0.650000	-0.804689E-02	-0.462000E-02	-0.106954E-01	-0.531462E-02	0.452551E-03	-0.727634E-03	0.501528E-02	-0.536140E-03
0.700000	0.943419E-02	0.602955E-02	0.193869E-02	0.565529E-02	0.175125E-03	-0.661598E-02	0.531096E-02	0.272419E-02
0.750000	-0.340602E-03	-0.173567E-02	-0.194810E-02	-0.780460E-03	0.633975E-03	-0.451005E-02	0.167308E-02	0.923504E-03
0.800000	-0.107[illegible]7E-02	0.337440E-02	0.348815E-02	-0.268060E-02	0.179798E-02	-0.746664E-03	-0.471455E-02	-0.922013E-03
0.850000	0.301870E-02	-0.724911E-02	-0.117893E-02	-0.146546E-02	-0.275021E-02	0.246292E-02	-0.580020E-03	-0.263397E-02
0.900000	-0.685521E-03	-0.361017E-03	0.791710E-02	0.234172E-02	-0.293859E-02	0.682932E-02	0.540418E-02	-0.281658E-02
0.950000	0.374156E-02	-0.943986E-02	-0.715384E-02	-0.345909E-02	0.486302E-02	-0.119939E-02	-0.141946E-01	-0.130689E-01
1.000000	0.922800E-02	0.532703E-01	0.381276E-01	0.412373E-03	0.534936E-02	0.213324E-01	0.419134E-01	0.702429E-01

X/LT	288.000	300.000	312.000	324.000	336.000	348.000	360.000
0.000000	0.339874E-01	-0.233634E-01	-0.929431E-02	0.280505E-02	0.133777E-01	-0.307670E-02	-0.720000E-01
0.050000	0.447923E-01	-0.691457E-01	-0.473118E-01	-0.115513E-01	0.140462E-01	-0.203953E-01	-0.166540E+00
0.100000	0.138384E-01	-0.909785E-01	-0.548253E-01	-0.119753E-01	0.181868E-02	-0.405532E-01	-0.163133E+00
0.150000	-0.353654E-02	-0.947255E-01	-0.582822E-01	-0.221260E-01	-0.183314E-01	-0.594349E-01	-0.155891E+00
0.200000	-0.225653E-01	-0.975983E-01	-0.489259E-01	-0.187670E-01	-0.268823E-01	-0.598588E-01	-0.119344E+00
0.250000	-0.172601E-01	-0.810596E-01	-0.316570E-01	0.920460E-02	-0.815232E-02	-0.679257E-01	-0.107000E+00
0.300000	-0.188396E-01	-0.750899E-01	-0.305303E-01	0.243841E-01	-0.448614E-02	-0.859771E-01	-0.110079E+00
0.350000	0.505112E-02	-0.457155E-01	-0.818294E-02	0.385764E-01	0.398301E-02	-0.418180E-01	-0.562947E-01
0.400000	0.955542E-02	-0.297037E-01	0.605738E-02	0.452052E-01	0.125429E-01	-0.632942E-02	-0.251874E-01
0.450000	0.540593E-01	0.249353E-01	0.446672E-01	0.624779E-01	0.359596E-01	0.343128E-01	0.268397E-01
0.500000	0.355676E-01	0.235263E-01	0.302055E-01	0.363815E-01	0.276074E-01	0.314202E-01	0.320000E-01
0.550000	-0.578116E-02	-0.529331E-02	-0.859608E-02	-0.517567E-02	-0.120009E-02	-0.451463E-02	0.102403E-03
0.600000	0.903013E-02	0.123038E-01	0.210536E-02	0.306918E-02	0.443904E-02	-0.644643E-02	0.623500E-02
0.650000	-0.100456E-01	-0.340113E-02	-0.422872E-02	0.197954E-02	-0.156417E-02	-0.119917E-01	-0.495014E-02
0.700000	-0.109241E-01	-0.452152E-02	0.229372E-02	0.582345E-03	-0.673183E-02	0.259112E-02	0.900227E-02
0.750000	0.857054E-02	-0.509808E-02	-0.383000E-02	0.717949E-03	0.916219E-03	-0.931781E-04	0.300000E-02
0.800000	0.151503E-04	0.211804E-02	-0.689787E-02	-0.125794E-02	0.735488E-02	-0.203997E-02	-0.470314E-02
0.850000	0.277311E-02	0.376730E-02	-0.135285E-03	-0.263556E-02	0.405142E-03	0.190366E-02	0.168021E-02
0.900000	0.659875E-03	0.450033E-02	-0.115069E-03	-0.610589E-02	-0.443105E-02	-0.754055E-03	-0.279045E-02
0.950000	-0.157556E-02	-0.906532E-04	0.763751E-02	0.285364E-02	-0.125292E-02	-0.106732E-02	0.908296E-02
1.000000	0.339874E-01	-0.233634E-01	-0.929431E-02	0.280505E-02	0.133777E-01	-0.307670E-02	-0.720000E-01

TABLE 3. (CONTINUED)

ORDINATES THETA

X/LT	0.000	12.000	24.000	36.000	48.000	60.000	72.000	84.000
0.000000	-0.720000E-01	-0.113378E+00	-0.776086E-01	-0.131789E-01	0.378943E-01	0.753634E-01	0.634422E-01	0.544707E-01
0.050000	0.166540E+00	-0.251353E+00	-0.176173E+00	-0.411795E-01	0.586236E-01	0.120011E+00	0.101057E+00	0.843301E-01
0.100000	-0.163133E+00	-0.229562E+00	-0.146952E+00	-0.231671E-01	0.387240E-01	0.638396E-01	0.500868E-01	0.394747E-01
0.150000	-0.155891E+00	-0.219361E+00	-0.148599E+00	-0.159239E-01	0.382066E-01	0.434023E-01	0.313674E-01	0.385024E-01
0.200000	-0.119344E+00	-0.174053E+00	-0.117815E+00	0.794235E-02	0.373361E-01	0.223385E-01	0.928574E-02	0.440409E-01
0.250000	-0.107000E+00	-0.140954E+00	-0.969389E-01	0.306019E-01	0.583836E-01	0.280596E-01	0.952505E-02	0.721317E-01
0.300000	-0.110079E+00	-0.117931E+00	-0.771922E-01	0.389349E-01	0.643833E-01	0.112513E-01	-0.141357E-01	0.759331E-01
0.350000	0.562947E-01	-0.760206E-01	-0.439329E-01	0.478687E-01	0.782650E-01	0.191157E-01	-0.967166E-02	0.103124E+00
0.400000	-0.251874E-01	-0.528193E-01	-0.172699E-01	0.508513E-01	0.740548E-01	0.130102E-01	-0.142277E-01	0.110350E+00
0.450000	0.258397E-01	0.354039E-02	0.324595E-01	0.841546E-01	0.826911E-01	0.601090E-02	-0.590374E-02	0.151[illegible]E+00
0.500000	0.320000E-01	0.200127E-01	0.320849E-01	0.533135E-01	0.413304E-01	0.447372E-02	0.332380E-03	0.000907E-01
0.550000	0.102407E-03	-0.177568E-02	-0.681081E-02	-0.543518E-02	-0.103839E-01	-0.281882E-02	-0.270208E-02	-0.129541E-01
0.600000	0.623500E-02	0.118385E-01	-0.901983E-03	0.225634E-02	-0.963443E-03	-0.306927E-02	0.815087E-02	0.954071E-02
0.650000	-0.478014E-02	0.349389E-03	0.655679E-03	-0.618280E-03	-0.307285E-02	-0.690269E-02	0.187799E-02	-0.370974E-02
0.700000	0.900227E-02	0.597525E-02	0.628516E-02	0.317565E-02	0.550077E-02	0.209951E-02	0.310314E-02	0.263906E-02
0.750000	0.300000E-02	0.815634E-02	0.665811E-02	0.351812E-02	0.538488E-02	-0.901924E-03	-0.213766E-02	-0.111567E-02
0.800000	-0.470314E-02	0.774176E-03	-0.264617E-02	-0.163066E-02	0.224563E-02	-0.139929E-02	-0.208736E-04	-0.720904E-03
0.850000	0.158021E-02	0.477379E-02	0.949819E-02	0.704987E-02	-0.359161E-02	-0.122750E-01	-0.929230E-02	-0.687976E-02
0.900000	-0.279045E-02	-0.779145E-02	-0.743221E-02	-0.204840E-02	0.459637E-03	0.919244E-03	0.464286E-02	0.105747E-01
0.950000	0.908296E-02	0.184659E-01	0.138550E-01	0.641330E-02	-0.354084E-02	-0.487423E-02	-0.342046E-02	-0.317834E-03
1.000000	-0.720000E-01	-0.113378E+00	-0.776086E-01	-0.131789E-01	0.378943E-01	0.753634E-01	0.634422E-01	0.544707E-01

X/LT	96.000	108.000	120.000	132.000	144.000	156.000	168.000	180.000
0.000000	0.760176E-01	0.890414E-01	0.486506E-01	-0.643463E-02	-0.435572E-01	-0.925067E-01	-0.120528E+00	-0.700000E-01
0.050000	0.137575E+00	0.151006E+00	0.652131E-01	-0.507779E-01	-0.125749E+00	-0.218559E+00	-0.266129E+00	-0.167936E+00
0.100000	0.690340E-01	0.100111E+00	0.358213E-01	-0.555694E-01	-0.112357E+00	-0.198956E+00	-0.231300E+00	-0.138107E+00
0.150000	0.869653E-01	0.100554E+00	0.321004E-01	-0.729127E-01	-0.135774E+00	-0.214392E+00	-0.237822E+00	-0.135367E+00
0.200000	0.924832E-01	0.893262E-01	0.183193E-01	-0.753532E-01	-0.136705E+00	-0.201682E+00	-0.213263E+00	-0.102144E+00
0.250000	0.133858E+00	0.109800E+00	0.253275E-01	-0.580898E-01	-0.133348E+00	-0.199362E+00	-0.189742E+00	-0.730000E-01
0.300000	0.140093E+00	0.110389E+00	0.747101E-02	-0.629626E-01	-0.189920E+00	-0.193041E+00	-0.143941E+00	-0.676638E-01
0.350000	0.211102E+00	0.140359E+00	0.633012E-02	-0.758237E-01	-0.135268E+00	-0.194080E+00	-0.134603E+00	-0.167497E-01
0.400000	0.228882E+00	0.151985E+00	0.219996E-02	-0.763120E-01	-0.125509E+00	-0.190456E+00	-0.100624E+00	0.676823E-02
0.450000	0.313374E+00	0.243964E+00	0.489307E-01	-0.733350E-01	-0.145956E+00	-0.184575E+00	-0.709596E-01	0.524156E-01
0.500000	0.155103E+00	0.135637E+00	0.317224E-01	-0.296957E-01	-0.685773E-01	-0.863142E-01	-0.254919E-01	0.380000E-01
0.550000	-0.209299E-01	-0.155433E-01	-0.128269E-01	0.190446E-02	0.776570E-02	0.307241E-02	0.989188E-03	-0.480439E-02
0.600000	0.136124E-01	0.154646E-01	0.307133E-02	-0.330123E-02	-0.543087E-02	-0.647403E-03	0.384598E-02	0.275151E-02
0.650000	0.653840E-02	-0.576129E-02	-0.824028E-02	-0.140016E-02	0.429038E-02	0.445119E-02	0.116847E-02	-0.687659E-02
0.700000	0.626253E-02	0.102799E-01	0.418071E-02	0.139122E-02	0.205960E-03	-0.298559E-02	-0.410836E-02	0.200321E-02
0.750000	0.250659E-02	0.427398E-02	0.236603E-02	0.680747E-02	0.465630E-02	0.483787E-02	0.393123E-02	0.100000E-02
0.800000	0.340659E-02	0.419086E-03	0.302156E-02	0.720332E-02	-0.598687E-02	-0.651715E-02	-0.168912E-02	-0.237614E-02
0.850000	-0.623722E-02	-0.138757E-01	-0.503752E-02	0.301100E-02	0.257891E-02	0.101744E-01	0.792418E-02	0.739[illegible]E-02
0.900000	0.977811E-02	0.523995E-02	-0.724054E-04	-0.133822E-01	-0.143289E-01	-0.536727E-02	-0.129390E-01	-0.923010E-02
0.950000	0.941322E-02	-0.598532E-02	-0.273349E-04	0.620817E-02	0.146373E-01	0.179582E-01	0.151846E-01	0.159264E-01
1.000000	0.760176E-01	0.890414E-01	0.486506E-01	-0.643463E-02	-0.435572E-01	-0.925067E-01	-0.120528E+00	-0.700000E-01

NOTE: MODEL 20A WITH IMPERFECTIONS

FULL FOURIER COEFFICIENTS ARE CALCULATED BASED ON ORDINATES

TABLE 4. FOURIER COEFFICIENTS OF MODEL 20A WITH IMPERFECTIONS

COSINE-SINE FOURIER COEFFICIENTS

PERIPHERAL HARMONICS

AXIAL HARMONIC	0	1	2	3	4	5	6	7
0	0.000000E+00	0.000000E+00	0.170000E-01	-0.300000E-01	0.190000E-01	-0.840000E-01	-0.400000E-02	-0.000001E-00
1	0.000000E+00	0.000000E+00	-0.500000E-02	0.599997E-02	-0.140000E-01	-0.140000E-01	0.000000E+00	0.999999E-03
2	0.000000E+00	0.108819E-07	0.000000E+00	-0.000002E-02	0.300001E-02	0.300001E-02	-0.400000E-02	-0.200001E-02
3	0.000000E+00	0.200000E-02	0.000000E+00	0.000000E+00	-0.300000E-02	0.110483E-07	0.100001E-02	0.000000E+00
4	0.000000E+00	0.200001E-02	0.000000E+00	-0.199999E-02	0.199999E-02	0.357790E-07	0.000000E+00	0.000000E+00
5	0.000000E+00	0.000000E+00	0.000000E+00	0.000000E+00	-0.100000E-02	0.000000E+00	0.000000E+00	0.000000E+00
6	0.000000E+00	0.000000E+00	0.000000E+00	0.000000E+00	0.100000E-02	0.000000E+00	0.000000E+00	0.000000E+00
7	0.000000E+00	0.000000E+00	0.000000E+00	0.000000E+00	0.000000E+00	0.000000E+00	0.000000E+00	0.000000E+00
8	0.000000E+00	0.000000E+00	0.000000E+00	0.000000E+00	0.000000E+00	0.000000E+00	0.000000E+00	0.000000E+00
9	0.000000E+00	0.000000E+00	0.000000E+00	0.137[illegible]0E-07	0.000000E+00	-0.130221E-07	0.223645E-07	0.000000E+00
10	0.000000E+00	0.000000E+00	0.000000E+00	0.000000E+00	0.000000E+00	0.000000E+00	0.000000E+00	0.000000E+00

PERIPHERAL HARMONICS

AXIAL HARMONIC	8	9	10	11	12	13	14	15
0	0.200000E-02	0.000000E+00	-0.200001E-02	0.104333E-07	-0.120331E-07	0.100001E-02	0.000000E+00	0.000000E+00
1	0.000000E+00	-0.599999E-02	0.000000E+00	-0.200001E-02	0.200001E-02	0.000000E+00	0.000000E+00	0.000000E+00
2	0.100001E-02	0.000000E+00	-0.300001E-02	0.000000E+00	-0.100000E-02	0.000000E+00	0.000000E+00	0.000000E+00
3	0.199999E-02	0.100002E-02	0.000000E+00	0.103896E-07	0.000000E+00	0.129011E-07	0.000000E+00	0.000000E+00
4	0.000000E+00	0.119635E-07	0.000000E+00	0.000000E+00	0.137873E-07	0.999997E-03	0.000000E+00	0.000000E+00
5	0.000000E+00	0.000000E+00	0.000000E+00	0.100155E-07	-0.157937E-07	0.000000E+00	0.000000E+00	0.000000E+00
6	0.000000E+00	-0.108133E-07	0.000000E+00	0.000000E+00	0.137351E-07	-0.125890E-07	0.000000E+00	0.000000E+00
7	0.000000E+00	0.000000E+00	0.120000E-07	0.000000E+00	0.177028E-07	-0.153790E-07	0.000000E+00	0.000000E+00
8	0.000000E+00	0.000000E+00	0.000000E+00	0.150497E-07	0.000000E+00	0.000000E+00	0.000000E+00	0.000000E+00
9	0.000000E+00	0.000000E+00	0.110105E-07	0.000000E+00	0.000000E+00	0.000000E+00	0.000000E+00	0.000000E+00
10	0.000000E+00	0.000000E+00	0.000000E+00	0.000000E+00	0.000000E+00	0.000000E+00	0.000000E+00	0.000000E+00

COSINE-COSINE FOURIER COEFFICIENTS

PERIPHERAL HARMONICS

AXIAL HARMONIC	0	1	2	3	4	5	6	7
0	0.000000E+00	0.000000E+00	-0.360000E-01	-0.200000E-02	0.700000E-02	-0.120000E-01	-0.160000E-01	0.000000E-02
1	-0.170000E-01	0.000000E+00	-0.190000E-01	-0.100000E-02	-0.900001E-02	0.700000E-02	0.199999E-02	-0.400000E-02
2	0.120000E-01	0.000000E+00	-0.100001E-02	0.999990E-03	0.100000E-02	0.299998E-02	0.300001E-02	-0.134664E-07
3	0.000000E+00	0.000000E+00	-0.299997E-02	-0.100001E-02	-0.200000E-02	0.000000E+00	0.000000E+00	0.000000E+00
4	0.500001E-02	0.000000E+00	0.158359E-07	0.100001E-02	0.223252E-07	0.000000E+00	0.100000E-02	0.000000E+00
5	0.000000E+00	0.000000E+00	0.191609E-07	0.000000E+00	0.000000E+00	0.100002E-02	0.999997E-03	0.000000E+00
6	0.999993E-03	0.148764E-07	-0.175040E-07	0.000000E+00	0.000000E+00	0.000000E+00	0.000000E+00	0.106482E-07
7	0.000000E+00	-0.100000E-02	0.000000E+00	0.000000E+00	-0.999994E-03	0.000000E+00	0.000000E+00	0.000000E+00
8	0.200000E-02	0.000001E+00	0.000000E+00	0.000000E+00	0.000000E+00	0.000000E+00	0.000000E+00	0.000000E+00
9	0.000000E+00	0.000000E+00	0.000000E+00	0.000000E+00	-0.104416E-07	0.140844E-07	0.000000E+00	-0.234976E-07
10	0.000000E+00	0.000000E+00	0.000000E+00	0.000000E+00	0.000000E+00	0.000000E+00	0.000000E+00	0.183284E-07

PERIPHERAL HARMONICS

AXIAL HARMONIC	8	9	10	11	12	13	14	15
0	0.400001E-02	0.000000E+00	0.200000E-02	0.000000E+00	0.000000E+00	0.000000E+00	-0.129926E-07	0.000000E+00
1	-0.500000E-02	0.200000E-02	0.000000E+00	-0.200000E-02	0.000000E+00	-0.157816E-07	0.000000E+00	0.000000E+00
2	-0.300000E-02	-0.187898E-07	0.000000E+00	-0.100000E-02	-0.109696E-07	0.000000E+00	0.000000E+00	0.000000E+00
3	0.000000E+00	0.000000E+00	0.000000E+00	0.000000E+00	0.000000E+00	0.000000E+00	0.000000E+00	0.000000E+00
4	0.000000E+00	0.000000E+00	-0.165504E-07	0.173294E-07	0.000000E+00	0.000000E+00	0.000000E+00	0.000000E+00
5	0.000000E+00	0.117855E-07	0.000000E+00	0.000000E+00	0.000000E+00	0.161146E-07	0.000000E+00	0.000000E+00
6	0.000000E+00	0.000000E+00	0.000000E+00	0.138192E-07	0.000000E+00	0.000000E+00	0.168503E-07	0.000000E+00
7	0.000000E+00	0.000000E+00	0.000000E+00	0.000000E+00	0.000000E+00	0.000000E+00	0.000000E+00	0.000000E+00
8	0.000000E+00	0.000000E+00	0.000000E+00	-0.139401E-07	-0.101513E-07	0.000000E+00	0.000000E+00	-0.134614E-07
9	0.138682E-07	0.000000E+00	0.000000E+00	-0.191065E-07	0.000000E+00	0.000000E+00	0.000000E+00	0.000000E+00
10	0.000000E+00	0.000000E+00	0.000000E+00	0.000000E+00	0.000000E+00	0.000000E+00	0.000000E+00	0.000000E+00

TABLE 4. (CONTINUED)

SINE-SINE FOURIER COEFFICIENTS

PERIPHERAL HARMONICS

AXIAL HARMONIC	0	1	2	3	4	5	6	7
0	0.000000E+00	0.000000E+00	0.000000E+00	0.000000E+00	0.000000E+00	0.000000E+00	0.000000E+00	0.000000E+00
1	0.000000E+00	-0.100000E-02	0.210000E-01	-0.350000E-01	0.220000E-01	-0.350000E-01	-0.399999E-02	-0.200001E-02
2	0.000000E+00	-0.100000E-02	-0.400000E-02	0.499999E-02	-0.100000E-01	-0.120000E-01	-0.150311E-07	0.200000E-02
3	0.000000E+00	0.000000E+00	0.700000E-02	-0.170000E-01	0.900002E-02	-0.100000E-01	-0.500002E-02	-0.200001E-02
4	0.000000E+00	0.000000E+00	-0.200000E-02	0.200000E-02	-0.600000E-02	-0.499999E-02	0.000000E+00	0.000000E+00
5	0.000000E+00	0.000000E+00	0.400000E-02	-0.999997E-02	0.599999E-02	-0.499998E-02	-0.199999E-02	-0.100000E-02
6	0.000000E+00	0.000000E+00	0.000000E+00	0.100000E-02	-0.400000E-02	-0.300000E-02	0.000000E+00	0.000000E+00
7	0.000000E+00	0.000000E+00	0.300000E-02	-0.700001E-02	0.499997E-02	-0.299999E-02	-0.200000E-02	-0.100113E-07
8	0.000000E+00	0.000000E+00	0.000000E+00	-0.136716E-07	-0.299999E-02	-0.199999E-02	-0.180997E-07	0.000000E+00
9	0.000000E+00	-0.185028E-07	0.200001E-02	-0.499999E-02	0.299999E-02	-0.200000E-02	-0.999990E-03	0.000000E+00
10	0.000000E+00	0.000000E+00	0.000000E+00	0.000000E+00	0.000000E+00	0.000000E+00	0.000000E+00	0.000000E+00

PERIPHERAL HARMONICS

AXIAL HARMONIC	8	9	10	11	12	13	14	15
0	0.000000E+00	0.000000E+00	0.000000E+00	0.000000E+00	0.000000E+00	0.000000E+00	0.000000E+00	0.000000E+00
1	0.200000E-02	0.000000E+00	-0.200000E-02	-0.999986E-03	-0.163400E-07	0.200001E-02	0.000000E+00	0.000000E+00
2	0.000000E+00	-0.600000E-02	0.000000E+00	-0.141944E-07	0.100002E-02	-0.119051E-07	0.000000E+00	0.000000E+00
3	0.200000E-02	0.000000E+00	-0.400001E-02	0.000000E+00	-0.100002E-02	0.000000E+00	-0.100000E-02	0.000000E+00
4	0.999998E-03	0.163758E-07	0.000000E+00	0.000000E+00	0.100001E-02	0.000000E+00	0.000000E+00	0.000000E+00
5	0.000000E+00	0.187622E-07	-0.100000E-02	0.000000E+00	0.000000E+00	0.128295E-07	0.000000E+00	0.000000E+00
6	0.000000E+00	-0.199999E-02	-0.123413E-07	-0.999987E-03	-0.200311E-07	0.158511E-07	0.000000E+00	0.000000E+00
7	0.000000E+00	0.000000E+00	0.000000E+00	-0.186314E-07	0.125957E-07	0.000000E+00	0.000000E+00	0.000000E+00
8	0.000000E+00	0.000000E+00	0.000000E+00	0.000000E+00	0.127937E-07	-0.108845E-07	0.000000E+00	0.000000E+00
9	0.000000E+00	0.107298E-07	0.000000E+00	0.000000E+00	0.000000E+00	0.000000E+00	0.000000E+00	0.000000E+00
10	0.000000E+00	0.000000E+00	0.000000E+00	0.000000E+00	0.000000E+00	0.000000E+00	0.000000E+00	0.000000E+00

SINE-COSINE FOURIER COEFFICIENTS

PERIPHERAL HARMONICS

AXIAL HARMONIC	0	1	2	3	4	5	6	7
0	0.000000E+00	0.000000E+00	0.000000E+00	0.000000E+00	0.000000E+00	0.000000E+00	0.000000E+00	0.000000E+00
1	-0.600000E-02	0.000000E+00	-0.460000E-01	-0.400000E-02	0.000000E-02	-0.160000E-01	-0.210000E-01	0.100000E-01
2	-0.140000E-01	0.000000E+00	-0.150000E-01	0.000000E+00	-0.600001E-02	0.599999E-02	0.999990E-03	-0.300000E-02
3	0.599999E-02	0.000000E+00	-0.150000E-01	0.000000E+00	0.299999E-02	-0.300002E-02	-0.500000E-02	0.299999E-02
4	-0.600000E-02	0.000000E+00	-0.799999E-02	-0.100001E-02	-0.400000E-02	0.199999E-02	0.000000E+00	-0.200000E-02
5	0.500001E-02	0.000000E+00	0.899999E-02	0.000000E+00	0.200001E-02	-0.200000E-02	-0.300000E-02	0.199999E-02
6	-0.400000E-02	0.999998E-03	-0.399998E-02	0.000000E+00	-0.100001E-02	0.200001E-02	0.999998E-03	0.110649E-07
7	0.299999E-02	0.147951E-07	-0.700001E-02	0.000000E+00	0.200001E-02	-0.100000E-02	-0.200000E-02	0.200001E-02
8	-0.400000E-02	-0.107538E-07	-0.400001E-02	0.000000E+00	-0.199999E-02	0.999989E-03	0.000000E+00	0.232573E-07
9	0.299999E-02	0.000000E+00	-0.399999E-02	0.000000E+00	0.999995E-03	0.000000E+00	0.000000E+00	0.999985E-03
10	0.000000E+00	0.000000E+00	0.000000E+00	0.000000E+00	0.000000E+00	0.000000E+00	0.000000E+00	0.000000E+00

PERIPHERAL HARMONICS

AXIAL HARMONIC	8	9	10	11	12	13	14	15
0	0.000000E+00	0.000000E+00	0.000000E+00	0.000000E+00	0.000000E+00	0.000000E+00	0.000000E+00	0.000000E+00
1	0.600001E-02	0.000000E+00	0.300000E-02	0.000000E+00	0.000000E+00	-0.141341E-07	0.000000E+00	0.000000E+00
2	-0.400000E-02	0.200000E-02	0.000000E+00	-0.999990E-03	0.000000E+00	-0.120254E-07	0.000000E+00	0.000000E+00
3	0.000000E+00	-0.170083E-07	0.000000E+00	-0.100001E-02	0.000000E+00	0.000000E+00	0.000000E+00	0.000000E+00
4	-0.200000E-02	0.000000E+00	0.000000E+00	0.000000E+00	0.000000E+00	-0.231379E-07	0.000000E+00	0.000000E+00
5	0.124986E-07	-0.118791E-07	0.000000E+00	0.000000E+00	0.000000E+00	0.000000E+00	-0.214629E-07	0.113553E-07
6	0.000000E+00	0.000000E+00	0.000000E+00	0.000000E+00	0.000000E+00	0.000000E+00	0.000000E+00	0.102461E-07
7	0.000000E+00	0.000000E+00	0.000000E+00	0.108716E-07	0.000000E+00	0.000000E+00	0.000000E+00	0.000000E+00
8	-0.100002E-02	0.000000E+00	-0.101068E-07	0.175758E-07	0.000000E+00	-0.122515E-07	0.119226E-07	0.000000E+00
9	0.000000E+00	0.000000E+00	0.000000E+00	0.000000E+00	-0.100493E-07	0.134368E-07	0.000000E+00	0.000000E+00
10	0.000000E+00	0.000000E+00	0.000000E+00	0.000000E+00	0.000000E+00	0.000000E+00	0.000000E+00	0.000000E+00

TABLE 5. GEOMETRICAL AND MATERIAL PROPERTIES USED FOR MODELS

MODEL NO.	RADIUS R (in)	CENTER PANEL THICKNESS h_1 (in)	END PANEL THICKNESS h_2 (in)	YOUNG'S MODULUS E (ksi)	POISSON'S RATIO ν	MATERIAL 43 YIELD STRESS σ_y (ksi)	MATERIAL 50 YIELD STRESS σ_y (ksi)	ULTIMATE STRESS FOR MATERIAL 43 (ksi)	ULTIMATE STRESS FOR MATERIAL 50 (ksi)	HALF LENGTH USED IN COMPUTATION L/2 (in)
IC1	29.516	0.138582	0.112992	30,000	0.3	40.755	50.183	62.221	74.259	44.291
IC3	17.697	0.138582	0.112992	30,000	0.3	40.755	50.183	62.221	74.259	5.315

MODEL NO.	R/h BASED ON CENTER PANEL h GRADE 43	L/R	FRAME SPACING (in)	INTERNAL STIFFENER GRADE 43 $d_w \times t_w$ (in x in)	END PLATE THICKNESS GRADE 43 (in)	CENTER PANEL (GRADE 43) FAILURE STRESS FOR PURE COMPRESSION (REF. 26)	CENTER PANEL FAILURE LOAD FOR PURE COMPRESSION (KIPS) (REF. 26)
IC1	212.985	3.000	29.516	1.8897 x 0.138582	0.3149606	25.671	660.7
IC3	127.700	0.600	3.543	0.94488 x 0.138582	0.3149606	36.404	560.0

TABLE 6. CHARACTERISTICS OF MODELS OF TABLE 5

MODEL NO.	CENTER PANEL σ_{CR} (ksi)	END PANEL σ_{CR} (ksi)	CENTER PANEL M_{CR} (k-in)	END PANEL M_{CR} (k-in)	CENTER PANEL K_{CR} (1/in)	END PANEL K_{CR} (1/in)	CENTER PANEL M_{BR} (k-in)	END PANEL M_{BR} (k-in)	I (in^4)	CENTER PANEL M_o (k-in)	END PANEL M_o (k-in)
IC1	85.250	69.507	32,334.2	21,495.3	9.6276458×10^{-5}	7.8496698×10^{-5}	17,600.5	11,700.56	11,194.9	19,681.7	19,759.6
IC3	142.184	115.928	19,386.4	12,887.80	2.678096×10^{-4}	2.183569×10^{-4}	10,552.763	7,015.327	2,412.91	7,075.3	7,103.3

REFERENCES

1. Moussouros, M., An Analysis of Explosion-Induced Bending Damage in Submerged Shell Targets, NSWC TR 84-380, Dec 1984.

2. Moussouros, M., "Finite Element Modeling Techniques for Buckling Analysis of Cylindrical Shells under Bending Loads," Paper No. 11, presented at International Conference on "Advances in Marine Structures," Admiralty Research Establishment, Scotland, 20-23 May 1986.

3. Axelrad, E.L. and Emmerling, F.A., "Elastic Tubes," Applied Mechanics Reviews, Vol. 37, No. 7, Jul 1984, pp. 891-897.

4. Axelrad, E.L., "Schalentheorie," B.G. Teubner, Stuttgart, 1983, pp. 171-175, 195-201.

5. Emmerling, F.A., "Nonlinear Bending of Curved Tubes," in Flexible Shells, Theory and Applications, edited by E.L. Axelrad and F.A. Emmerling, Berlin, Springer Verlag, 1984.

6. Sobel, L.H. and Newman, S.Z., "Comparison of Experimental and Simplified Analytical Results for In-Plane Plastic Bending of an Elbow," Journal of Pressure Vessel Technology, Vol. 102, Nov 1980, pp. 400-409.

7. Bolt, S.E. and Greenstreet, W.L., "Experimental Determinations of Plastic Collapse Loads for Pipe Elbows," 71-PVP-37 paper, Pressure Vessel and Piping Conference (ASME), San Francisco, CA, 10-12 May 1971.

8. Calladine, C.K., "Plastic Buckling of Tubes in Pure Bending," in Collapse, the Buckling of Structures in Theory and Practice, edited by J.M.T. Thompson and G.W. Huant, Symposium, University College, London, 31 Aug-3 Sep 1982, pp. 111-124.

9. Funk, P., "Ueber ein Stabilitaetsproblem bei den durch Kruemmungs steif gemischten Messbaendern," Oesterreichischer Ingenieur Archiv, Vol. 5, 1951, pp. 388-397.

10. Seaman, W.J. and Wan, F.Y.M., "Lateral Bending and Twisting of Thin-Walled Curved Tubes," Studies in Applied Mathematics, Vol. LIII, No. 1, Mar 1974, pp. 73-89.

11. Mallett, R.L. and Wan, F.Y.M., "The Static-Geometric Duality and Staggered Mesh Scheme in the Numerical Solution of Some Shell Problems," Studies in Applied Mathematics, Vol. LII, No. 1, Mar 1973, pp. 21-38.

REFERENCES (Cont.)

12. Chen, W.F. and Atsuta, T., "Theory of Beam-Columns," Space Behavior and Design, Vol. 2, McGraw-Hill Co., 1977.

13. Chen, W.F. and Han, D.J., "Tubular Members in Offshore Structures," Pitman Advanced Publishing Program, 1985.

14. Basar, Y. and Kraetzig, W.B., "Mechanik der Flaechentragwerke," F. Vieweg und Sohn Verlag, Braunschweig, 1985.

15. Dikmen, M., "Theory of Thin Elastic Shells," Pitman Advanced Publishing Program, 1982.

16. Calladine, C.R., "Theory of Shell Structures," Cambridge University Press, 1983, Chapter 16, pp. 595-625.

17. Møllmann, H., Introduction to the Theory of Thin Shells, J. Wiley & Sons, 1981.

18. Niordson, F.I., Shell Theory, Elsevier Publishers, 1985.

19. Bushnell, D., Computerized Buckling Analysis of Shells, Martinus Nijhoff Publishers, 1985.

20. Yamaki, N., Elastic Stability of Circular Cylindrical Shells, Elsevier Publishers, 1984.

21. Gould, P.L., Finite Element Analysis of Shells of Revolution, Pitman Advanced Publishing Program, 1985.

22. Kolar, V.; Kratochvil, J.; Leitner, F.; and Zeniser, A., "Berechnung von Flaechen- und Raumtragwerken nach der Methode der finiten Elemente," Springer Verlag Wien, 1975.

23. Burns, C.S. and Parks, T.W., DFT/FFT and Convolution Algorithms, Theory and Implementation, J. Wiley & Sons, 1985.

24. Zurmuehl, R., "Praktische Mathematik fuer Ingenieure und Physiker," Springer Verlag, 1965, pp. 360-364.

25. Hibbitt, Karlsson, and Sorensen, ABAQUS User's Manual, Version 4, Jul 1982, and "ABAQUS Example Problems," Oct 1982.

26. Dowling, P.J.; Harding, J.E.; Fahy, W.; and Agelidis, N., "Report on the Testing of Large and Small Scale Stiffened Shells Under Axial Compression," Engineering Structures Laboratories, Imperial College, London, CESLIC Report SS1, Aug 1981.

27. Harding, J.E., Personal Communication, 8 Jan 1985.

NOMENCLATURE

$\underset{\sim}{E}, \underset{\sim}{F}, \underset{\sim}{G}, \underset{\sim}{H}$	=	Matrices whose coefficients are given by E_{iJ}, F_{iJ}, G_{iJ}, H_{iJ}
E_{iJ}, F_{iJ}, G_{iJ}, H_{iJ}	=	Form of coefficients defined in Equations (A-41) - (A-49), (A-50) - (A-54), (A-55) - (A-59), and (A-60) - (A-64) respectively.
F_0	=	Axial Force based on yield stress ($2Rh\sigma_y$)
$f^*(t_n, \theta\mu)$	=	Defined in equations (A-30), (A-31) and (A-32)
$F(x,y,z)$	=	Symbolic representation of the surface of the cylinder ($F = x^2 + y^2 - R^2$)
h	=	Shell thickness
I	=	Moment of inertia of undeformed cross-section ($\pi R^3 h$)
K_{CR}	=	Critical curvature at bifurcation $\left(\frac{E}{\sqrt{3(1-\nu^2)}}\right)\frac{h}{R^2}$
ℓ	=	Total length of shell
$2L$	=	Total length of shell
M	=	Upper bound in axial wave numbers (If only a sinusoidal distribution is used, then there will be M points, otherwise, M+1)
M_{BR}	=	Critical Brazier moment $\frac{2\sqrt{2}}{9\sqrt{(1-\nu^2)}}\pi ERh^2$
M_{CR}	=	Critical moment at bifurcation $\left(\frac{\pi E}{\sqrt{3(1-\nu^2)}}\right)Rh^2$
M_0	=	Plastic Moment based on yield stress ($4R^2h\sigma_y$), where R is mean radius

N	=	Upper bound in peripheral wave numbers. (There is a total of N+1 points peripherally)
$\underset{\sim}{n}$	=	Outward normal to cylindrical surface
(N_x, N_y, N_z)	=	Components of $\underset{\sim}{n}$ in global Cartesian system (x, y, z)
R	=	Actual radius of cylindrical shell including imperfections (In formulae for σ_{CR}, M_{CR}, K_{CR}, M_{BR}, M_0, F_0, and I, R is the mean radius as given by R_0)
R_0	=	Mean radius of circular cylindrical shell (perfect shell or radius of imperfect shell prior to introduction of imperfections)
(R, θ, z)	=	Cylindrical frame of reference
t_k	=	$\frac{\pi}{(M-1)} k$
(x, y, z)	=	Global Cartesian system of reference
σ_{CR}	=	Critical stress at bifurcation $\frac{\pi E}{\sqrt{3(1-\nu^2)}} \frac{h}{R}$
∇F	=	Gradient of function F, i.e., (F_x, F_y, F_z) or $\left(\frac{\partial F}{\partial x}, \frac{\partial F}{\partial y}, \frac{\partial F}{\partial z}\right)$
δ_{mk}	=	Imperfection coefficients (usually of small amplitude compared to R_0)
θ_μ	=	$\frac{2\pi}{(K-1)} \mu$, where K is the total number of points including the 0 and 2π points (K is odd)
σ_y	=	Yield stress
$\lvert\nabla F\rvert$	=	Magnitude of gradient of F, i.e., $(F_x^2 + F_y^2 + F_z^2)^{1/2}$

APPENDIX A

ANALYSIS OF A NEARLY CYLINDRICAL SURFACE

In this section we consider the definition of a nearly cylindrical surface based on a cylindrical frame of reference (R,θ,z). The object is to obtain the perturbed cylindrical surface from an ideal one of mean radius R_0 and total length 2L.

Two types of perturbations will be considered for the imperfections:

(1) <u>No imperfections at $z = 0$ and $z = 2L$.</u>

Symmetrical imperfections peripherally. Therefore, the local radius R is given by

$$R = R_0 + \sum_{m=1}^{M} \sum_{k=0}^{N} \delta_{mk} \sin\left[\frac{m\pi}{2L} z\right] \cos[k\theta] \tag{A-1}$$

where δ_{mk} are the imperfection coefficients. The equation of the surface F of the thin hollow cylindrical shell is:

$$F(x,y,z) = x^2 + y^2 - R^2 =$$

$$x^2 + y^2 - 2R_0 \sum_{m=1}^{M} \sum_{k=0}^{N} \delta_{mk} \sin\left[\frac{m\pi}{2L} z\right] \cos[k\theta] \tag{A-2}$$

$$\left\{ \sum_{m=1}^{M} \sum_{k=0}^{N} \delta_{mk} \sin\left[\frac{m\pi}{2L}\right] z \cos[k\theta] \right\}^2$$

and

$$\left.\begin{aligned} x &= R\cos\theta \\ y &= R\sin\theta \\ z &= z \end{aligned}\right\} \tag{A-3}$$

Next, we need to define the outward normals $\underset{\sim}{n} = (n_x, n_y, n_z)$ to the perturbed surface. This can be accomplished by obtaining the gradient of the function, which defines $F(x,y,z)$.

We must obtain ∇F, where

$$\nabla F = \left(\frac{\partial F}{\partial x}, \frac{\partial F}{\partial y}, \frac{\partial F}{\partial z}\right) = \left(F_x, F_y, F_z\right) \tag{A-4}$$

$$|\nabla F| = \left(F_x^2 + F_y^2 + F_z^2\right)^{1/2} \tag{A-5}$$

and

$$n = \left(n_x, n_y, n_z,\right) = \left(F_x, F_y, F_z\right) \Big/ |\nabla F| \tag{A-6}$$

To calculate the components of ∇F we employ the form of the function as given by Equation (A-2), i.e.

$$\frac{\partial F}{\partial x} = 2x - 2R\frac{\partial R}{\partial x} \tag{A-7}$$

$$\frac{\partial F}{\partial y} = 2y - 2R\frac{\partial R}{\partial x} \tag{A-8}$$

$$\frac{\partial F}{\partial z} = -2R\frac{\partial R}{\partial z} \tag{A-9}$$

However, $R = R(z, \theta)$ and since z is independent of x and y

$$\frac{\partial R}{\partial x} = \frac{\partial R}{\partial z}\frac{\partial z}{\partial x} + \frac{\partial R}{\partial \theta}\frac{\partial \theta}{\partial x} = \frac{\partial \theta}{\partial x}\frac{\partial R}{\partial \theta} \tag{A-10}$$

$$\frac{\partial R}{\partial y} = \frac{\partial R}{\partial z}\frac{\partial z}{\partial y} + \frac{\partial R}{\partial \theta}\frac{\partial \theta}{\partial y} = \frac{\partial \theta}{\partial y}\frac{\partial R}{\partial \theta} \tag{A-11}$$

$$\text{But } \theta = \cot^{-1}\left[\frac{x}{y}\right] \tag{A-12}$$

and

$$\frac{\partial \theta}{\partial x} = -\frac{\sin\theta}{R} \tag{A-13}$$

$$\frac{\partial \theta}{\partial y} = \frac{\cos\theta}{R} \tag{A-14}$$

Substituting Equations (A-13) in (A-10) and (A-14) in (A-11) we get

$$\frac{\partial R}{\partial x} = -\frac{\sin\theta}{R}\frac{\partial R}{\partial \theta} \tag{A-15}$$

$$\frac{\partial R}{\partial y} = -\frac{\cos\theta}{R}\frac{\partial R}{\partial \theta} \tag{A-16}$$

and thus Equations (A-7) - (A-9) become, in view of (A-15), (A-16) and (A-3).

$$\frac{\partial F}{\partial x} = 2R\left[\cos\theta + \frac{\sin\theta}{R}\frac{\partial R}{\partial \theta}\right] \tag{A-17}$$

$$\frac{\partial F}{\partial y} = 2R\left[\sin\theta + \frac{\cos\theta}{R}\frac{\partial R}{\partial \theta}\right] \tag{A-18}$$

$$\frac{\partial F}{\partial z} = -\ 2R\ \frac{\partial R}{\partial z} \tag{A-19}$$

From A.1

$$\frac{\partial R}{\partial \theta} = -\sum_{m=1}^{M}\sum_{k=0}^{N} k\ \delta_{mk}\ \sin\left[\frac{m\pi}{2L}z\right]\ \cos\ [k\theta] \tag{A-20}$$

$$\frac{\partial R}{\partial z} = \sum_{m=1}^{M}\sum_{k=0}^{N}\left(\frac{m\pi}{2L}\right)\ \delta_{mk}\ \cos\left[\frac{m\pi}{2L}z\right]\ \cos\ [k\theta] \tag{A-21}$$

and finally Equations (A-17) through (A-19) become

$$\frac{\partial F}{\partial x} = 2R\left[\cos\theta - \sin\theta\sum_{m=1}^{M}\sum_{k=0}^{N} k\left(\frac{\delta_{mk}}{R}\right)\ \sin\left[\frac{m\pi}{2L}\right]z\ \ \sin\ (k\theta)\right] \tag{A-22}$$

$$\frac{\partial F}{\partial y} = 2R\left[\sin\theta + \cos\theta\sum_{m=1}^{M}\sum_{k=0}^{N} k\left(\frac{\delta_{mk}}{R}\right)\ \sin\left[\frac{m}{2L}\right]z\ \ \sin\ (k\theta)\right] \tag{A-23}$$

$$\frac{\partial F}{\partial z} = -2R\sum_{m=1}^{M}\sum_{k=0}^{N}\left(\frac{m\pi}{2L}\right)\ \delta_{mk}\ \cos\left[\frac{m\pi}{2L}z\right]\ \cos\ [k\theta] \tag{A-24}$$

and

$$|\nabla F| = 2R\left[1 + \left(\sum_{m=1}^{M}\sum_{k=0}^{N}\left(\frac{m\pi}{2L}\right)\delta_{mk}\ \cos\left[\frac{m\pi}{2L}z\right]\ \cos\ (k\theta)\right)^2 + \right.$$
$$\left. + \left(\sum_{m=1}^{M}\sum_{k=0}^{N}\left(\frac{k}{R}\right)\ \delta_{mk}\ \sin\left[\frac{m\pi}{2L}z\right]\ \sin\ (k\theta)\right)^2\right]^{1/2} \tag{A-25}$$

The axial interval 2L (or π) is divided in (M-1) equal segments $t_k = \frac{\pi}{(M-1)}k$ The peripheral interval 2π is divided in K-1 equal angles $\theta_\mu = \frac{2}{(K-1)}\mu$, where K is total number of points including the 0 and 2π ends (K=odd). Setting f for the portion of Equation A-1 to be represented by the series and

$$t = \frac{\pi}{2L}z$$

$$f\left(t_k, \theta_\mu\right) = \sum_{m=1}^{M} \sum_{k=0}^{N} \delta_{mk} \sin\left[\frac{m\pi}{2L} z_k\right] \cos\left[k\theta_\mu\right] = \tag{A-26}$$

$$= \sum_{m=1}^{M} \sum_{k=0}^{N} \delta_{mk} \sin\left[m\, t_k\right] \cos\left[k\theta_\mu\right]$$

The coefficients $\delta_{m,\lambda}$ are given by

$$\delta_{m,\lambda} = \frac{2}{(M-1)} \frac{4}{(K-1)} \sum_{n=1}^{n=M-2} \sum_{\mu=0}^{\mu=\frac{K-1}{2}} f^*\left(t_n, \theta_\mu\right) \sin\left[m\frac{\pi}{(M-1)}n\right] \cdot \cos\left[\lambda \cdot \frac{2\pi}{(K-1)}\mu\right] \tag{A-27}$$

and

$$\lambda = 1,2,3,\ldots \frac{(K-1)}{2} - 1$$

$$m = 1,2,\ldots, M-2$$

$$\delta_{m,0} = \frac{2}{(M-1)} \cdot \frac{2}{(K-1)} \sum_{n=1}^{n=M-2} \sum_{\mu=0}^{\mu=\frac{K-1}{2}} f^*\left(t_n, \theta_\mu\right) \sin\left[m\frac{\pi}{(M-1)}n\right] \tag{A-28}$$

for $m = 1,2,\ldots, M-2$

$$\delta_{m,\,\frac{K-1}{2}} = \frac{2}{(M-1)}\;\frac{2}{(K-1)}\sum_{n=1}^{M-1}\;\sum_{k=0}^{\frac{K-1}{2}} f^{*}\left(t_n, \theta_k\right)\left(-1\right)^{k}\;\sin\left[m\frac{\pi}{(M-1)}n\right] \tag{A-29}$$

for $m = 1,2,\ldots, M-2$

and

$$f^{*}\left(t_n\,,\,\theta_o\right) = \frac{1}{2}\;f\left(t_n\,,\,\theta_0\right) \qquad \text{for} \quad n \neq 0 \quad \text{and } M-1 \tag{A-30}$$

$$f^{*}\left(t_n\,,\,\theta_{\frac{K-1}{2}}\right) = \frac{1}{2}\;f\left(t_n\,,\,\theta_{\frac{K-1}{2}}\right) \qquad \text{for } n \neq 0,\ M-1 \tag{A-31}$$

due to the effect of the trapezoidal rule during integration. Also note that, if the terms corresponding to t_o were needed, then

$$f^{*}\left(t_o\,,\,\theta_o\right) = \frac{1}{4}\;f\left(t_o\,,\,\theta_o\right) \tag{A-32}$$

and similarly for the other 3 points

$$f^{*}\left(t_{M-1}\,,\,\theta_0\right),\ f^{*}\left(t_0\,,\,\theta_{\frac{K-1}{2}}\right),\ f^{*}\left(t_{M-1}\,,\,\theta_{\frac{K-1}{2}}\right)$$

(2) <u>General type of imperfection</u>.

In the general type of imperfection, the cylindrical surface in the axial $(0, \ell)$ and peripheral $(0, 2\pi)$ intervals is given by

$$R = R_0 + f(z,\theta) = R_0 + \sum_{m=0}^{M}\;\sum_{k=0}^{N}\Bigg\{E_{mk}\;\cos\left(\frac{2m\pi z}{\ell}\right)\cos\,(k\theta) +$$

$$+\;F_{mk}\;\cos\left(\frac{2m\pi z}{\ell}\right)\;\sin k\theta\;+$$

$$+\;G_{mk}\;\sin\left(\frac{2m\pi z}{\ell}\right)\;\sin k\theta\;+$$

$$+\;H_{mk}\;\sin\left(\frac{2m\pi z}{\ell}\right)\;\sin k\theta\Bigg\} \tag{A-33}$$

where $\ell = 2L$

The total number of equidistant points axially is 2M + 1 and the total number of points peripherally is 2N + 1, including end points.

Discretizing and setting

$$z_p = \frac{\ell}{2M}\, p \qquad \text{for } p = 0,1,2, \ldots, 2M \tag{A-34}$$

$$\theta_q = \frac{2\pi}{2N}\, q = \frac{\pi}{N}\, q \qquad \text{for } q = 0,1, \ldots, 2N-1 \tag{A-35}$$

We can abbreviate

$$\frac{2m\pi}{\ell}\, z_p = \left(\frac{2m\pi}{\ell}\right)\cdot\left(\frac{\ell}{2M}\, p\right) = m\left(\frac{\pi}{M}\, p\right) = m\varphi_p \tag{A-36}$$

so that

$$f\left(z_p, \theta_q\right) = f\left(p,q\right) = \sum_{m=0}^{M} \sum_{k=0}^{N} \Bigg\{ E_{mk} \cos(m\varphi_p) \cos(k\theta_q) + F_{mk} \cos(m\varphi_p) \sin(k\theta_q) + G_{mk} \sin(m\varphi_q) \cos(k\theta_q) + H_{mk} \sin(m\varphi_p) \sin(k\theta_q) \Bigg\} \tag{A-37}$$

The Fourier coefficients E_{mk}, F_{mk}, G_{mk}, and H_{mk} can be obtained if we multiply Equation (A-37) in turn with a product of either

$\cos(\ell\varphi_p)$ or $\sin(\ell\varphi_p)$

and

$\cos(\lambda\theta_q)$ or $\sin(\lambda\theta_q)$

and sum in both directions (double sums), while invoking certain orthogonality conditions such as

$$\sum_{p=0}^{2M-1} \cos(\ell\varphi_p) \cos(m\varphi_p) = \begin{cases} 0 & \text{for } \ell \neq m \\ M & \text{for } \ell = m \neq M \\ 2M & \text{for } \ell = m = M \end{cases} \tag{A-38}$$

$$\sum_{p=0}^{2M-1} \sin(\ell\varphi_p) \sin(m\varphi_p) = \begin{cases} 0 & \text{for } \ell \neq m \\ M & \text{for } \ell = m \neq M \\ 0 & \text{for } \ell = m = M \end{cases} \tag{A-39}$$

$$\sum_{p=0}^{2M-1} \sin(m\varphi_p) \cos(m\varphi_p) = 0 \text{ for all } \ell, m \tag{A-40}$$

They are as follows:

$$E_{0,0} = \frac{1}{2N} \cdot \frac{1}{2M} \sum_{p=0}^{2M-1} \sum_{q=0}^{2N-1} f(p,q) \tag{A-41}$$

$$E_{0,N} = \frac{1}{2N} \cdot \frac{1}{2M} \sum_{p=0}^{p=2M-1} \sum_{q=0}^{2N-1} (-1)^q f(p,q) \tag{A-42}$$

$$E_{M,0} = \frac{1}{2N} \cdot \frac{1}{2M} \sum_{p=0}^{2M-1} \sum_{q=0}^{2N-1} (-1)^q f(p,q) \tag{A-43}$$

$$E_{M,N} = \frac{1}{2N} \cdot \frac{1}{2M} \sum_{p=0}^{2M-1} \sum_{q=0}^{2N-1} (-1)^{p+q} f(p,q) \tag{A-44}$$

$$E_{0,k} = \frac{1}{N} \cdot \frac{1}{2M} \sum_{p=0}^{2M-1} \sum_{q=0}^{2N-1} f(p,q) \cos(k\theta_q) \tag{A-45}$$

$$k = 1,2, \ldots N-1$$

$$E_{m,0} = \frac{1}{2N} \cdot \frac{1}{M} \sum_{p=0}^{2M-1} \sum_{q=0}^{2N-1} f(p,q) \cos(m\varphi_p) \tag{A-46}$$

$$m = 1,2, \ldots M-1$$

$$E_{m,k} = \frac{1}{N} \cdot \frac{1}{M} \sum_{p=0}^{2M-1} \sum_{q=0}^{2N-1} f(p,q) \cos(m\varphi_p) \cos(k\theta_q) \tag{A-47}$$

$$E_{m,N} = \frac{1}{2N} \cdot \frac{1}{M} \sum_{p=0}^{2M-1} \sum_{q=0}^{2N-1} (-1)^q f(p,q) \cos(m\varphi_p) \tag{A-48}$$

$$\text{for } m = 1,2, \ldots M-1$$

$$E_{M,k} = \frac{1}{2M} \cdot \frac{1}{N} \sum_{p=0}^{p=2M-1} \sum_{q=0}^{2N-1} (-1)^p f(p,q) \cos(k\theta_p) \tag{A-49}$$

$$\text{for } k = 1,2, \ldots , N-1$$

$$F_{m,0} = 0 \quad \text{for} \quad m = 0, 1, 2, \ldots , M \tag{A-50}$$

$$F_{m,N} = 0 \quad \text{for} \quad m = 0, 1, \ldots , M \tag{A-51}$$

$$F_{M,k} = \frac{1}{N} \cdot \frac{1}{M} \sum_{p=0}^{2M-1} \sum_{q=0}^{2N-1} f(p,q) \cos(m\varphi_p) \sin(k\theta_q) \tag{A-52}$$

$$m = 1,2, \ldots , M-1$$
$$k = 1,2, \ldots , N-1$$

$$F_{0,k} = \frac{1}{2M} \cdot \frac{1}{N} \sum_{p=0}^{2M-1} \sum_{q=0}^{2N-1} f(p,q) \sin(k\theta_q) \tag{A-53}$$

$$k = 1,2, \ldots , N-1$$

$$F_{M,k} = \frac{1}{2M} \cdot \frac{1}{N} \sum_{p=0}^{2M-1} \sum_{q=0}^{2N-1} (-1)^p f(p,q) \sin(k\theta_q) \qquad k = 1,2, \ldots , N-1 \tag{A-54}$$

$$G_{0,k} = 0 \quad \text{for} \quad k = 0,1, \ldots , N \tag{A-55}$$

$$G_{M,k} = 0 \quad \text{for} \quad k = 0,1, \ldots , N \tag{A-56}$$

$$G_{m,k} = \frac{1}{M} \cdot \frac{1}{N} \sum_{p=0}^{2M-1} \sum_{q=0}^{2N-1} f(p,q) \sin(m\varphi_p) \cos(k\theta_q) \qquad \text{for } m = 1,2, \ldots , M-1 \quad k = 1,2, \ldots , N-1 \tag{A-57}$$

$$G_{m,n} = \frac{1}{2N} \cdot \frac{1}{M} \sum_{p=0}^{2M-1} \sum_{q=0}^{2N-1} (-1)^q f(p,q) \sin(m\varphi_p) \qquad \text{for } m = 1,2, \ldots , M-1 \tag{A-58}$$

$$G_{m,o} = \frac{1}{2N} \cdot \frac{1}{M} \sum_{p=0}^{2M-1} \sum_{q=0}^{2N-1} f(p,q) \sin(m\varphi_p) \qquad \text{for } m = 1,2, \ldots , M-1 \tag{A-59}$$

$$H_{m,o} = 0 \quad \text{for} \quad m = 0,1,2 \ldots , M \tag{A-60}$$

$$H_{m,N} = 0 \quad \text{for} \quad m = 0,1, \ldots , M \tag{A-61}$$

$$H_{0,k} = 0 \quad \text{for} \quad k = 1,2 \ldots , N-1 \tag{A-62}$$

$$H_{M,k} = 0 \quad \text{for} \quad k = 1,2 \ldots , N-1 \tag{A-63}$$

$$H_{m,k} = \frac{1}{N} \cdot \frac{1}{M} \sum_{p=0}^{2M-1} \sum_{q=0}^{2N-1} f(p,q) \sin(m\varphi_p) \sin(k\theta_q) \qquad \text{for } m = 1,2, \ldots , M-1 \quad k = 1,2, \ldots , N-1 \tag{A-64}$$

Equations (A-41)-(A-49), (A-50)-(A-54), (A-55)-(A-59), and (A-60)-(A-64) for the matrix of coefficients $\underset{\sim}{E}$, $\underset{\sim}{F}$, $\underset{\sim}{G}$, and $\underset{\sim}{H}$ are displayed below indicating the zero elements only. The size is $(\underset{\sim}{M}+1)(\underset{\sim}{N}+1)$, where 2M+1 indicates the total number of axial points, while 2N+1 the corresponding peripheral number.

By Equation (A-33) we obtain that the equation of the "almost" circularly cylindrical surface (F(x,y,z) is:

$$F(x,y,z) = x^2 + y^2 - R^2 =$$

$$= x^2 + y^2 - \Bigg\{ R_o^2 + \left(\sum_{m=0}^{M} \sum_{k=0}^{N} E_{mk} \cos(m\varphi_p)\cos(k\theta_q) \right)^2 +$$

$$+ \left(\sum_{m=0}^{M} \sum_{k=0}^{N} F_{mk} \cos(m\varphi_p)\sin(k\theta_q) \right)^2 +$$

$$+ \left(\sum_{m=0}^{M} \sum_{k=0}^{N} G_{mk} \sin(m\varphi_p)\cos(k\theta_q) \right)^2 +$$

$$+ \left(\sum_{m=0}^{M} \sum_{k=0}^{N} H_{mk} \sin(m\varphi_p)\sin(k\theta_q) \right)^2 +$$

$$+ 2R_o \Bigg[\sum_{m=0}^{M} \sum_{k=0}^{N} E_{mk} \cos(m\varphi_p)\cos(k\theta_q) +$$

$$+ \sum_{m=0}^{M} \sum_{k=0}^{N} F_{mk} \cos(m\varphi_p)\sin(k\theta_q) +$$

$$+ \sum_{m=0}^{M} \sum_{k=0}^{N} G_{mk} \sin(m\varphi_p)\cos(k\theta_q) +$$

$$+ \sum_{m=0}^{M} \sum_{k=0}^{N} H_{mk} \sin(m\varphi_p)\sin(k\theta_q) \Bigg] +$$

$$+ 2 \left(\sum_{m=0}^{M} \sum_{k=0}^{N} E_{mk} \cos(m\varphi_p)\cos(k\theta_q) \right) \left(\sum_{m=0}^{M} \sum_{k=0}^{N} F_{mk} \cos(m\varphi_p)\sin(k\theta_q) \right)$$

$$+ 2 \left(\sum_{m=0}^{M} \sum_{k=0}^{N} E_{mk} \cos(m\varphi_p)\cos(k\theta_q) \right) \left(\sum_{m=0}^{M} \sum_{k=0}^{N} G_{mk} \sin(m\varphi_p)\cos(k\theta_q) \right)$$

$$+ 2 \left(\sum_{m=0}^{M} \sum_{k=0}^{N} E_{mk} \cos(m\varphi_p)\cos(k\theta_q) \right) \left(\sum_{m=0}^{M} \sum_{k=0}^{N} H_{mk} \sin(m\varphi_p)\sin(k\theta_q) \right)$$

$$+ 2\left(\sum_{m=0}^{M}\sum_{k=0}^{N} F_{mk}\cos(m\varphi_p)\sin(k\theta_q)\right)\left(\sum_{m=0}^{M}\sum_{k=0}^{N} G_{mk}\sin(m\varphi_p)\cos(k\theta_q)\right)$$

$$+ 2\left(\sum_{m=0}^{M}\sum_{k=0}^{N} F_{mk}\cos(m\varphi_p)\sin(k\theta_q)\right)\left(\sum_{m=0}^{M}\sum_{k=0}^{N} H_{mk}\sin(m\varphi_p)\sin(k\theta_q)\right)$$

$$+ 2\left(\sum_{m=0}^{M}\sum_{k=0}^{N} G_{mk}\sin(m\varphi_p)\cos(k\theta_q)\right)\left(\sum_{m=0}^{M}\sum_{k=0}^{N} H_{mk}\sin(m\varphi_p)\sin(k\theta_q)\right) \tag{A-69}$$

where

$$\begin{aligned} x &= R\cos\theta \\ y &= R\sin\theta \\ z &= z \end{aligned} \tag{A-70}$$

Furthermore, Equations (A-7) through (A-9) or (A-17) through (A-19) are still valid in defining the gradient to the surface F, i.e.,

$$\frac{\partial F}{\partial x} = 2R\left[\cos\theta + \frac{\sin\theta}{R}\frac{\partial R}{\partial\theta}\right] \tag{A-71}$$

$$\frac{\partial F}{\partial y} = 2R\left[\sin\theta - \frac{\cos\theta}{R}\frac{\partial R}{\partial\theta}\right] \tag{A-72}$$

$$\frac{\partial F}{\partial z} = 2R\frac{\partial R}{\partial\theta} \tag{A-73}$$

and

$$\frac{\partial R}{\partial\theta} = \sum_{m=0}^{M}\sum_{k=0}^{N}\left\{-k\,E_{mk}\cos\left(\frac{2m\pi}{\ell}z\right)\sin(k\theta) + k\,F_{mk}\cos\left(\frac{2m\pi}{\ell}z\right)\cos(k\theta) - \right.$$

$$\left. - k\,G_{mk}\sin\left(\frac{2m\pi}{\ell}z\right)\sin(k\theta) + k\,H_{mk}\sin\left(\frac{2m\pi}{\ell}z\right)\cos(k\theta)\right\} \tag{A-74}$$

$$\frac{\partial R}{\partial z} = \sum_{m=0}^{M}\sum_{k=0}^{N}\left(\frac{2m\pi}{\ell}\right)\left\{-E_{mk}\sin\left(\frac{2m\pi}{\ell}z\right)\cos(k\theta) - F_{mk}\sin\left(\frac{2m\pi}{\ell}z\right)\sin(k\theta) + \right.$$

$$\left. + G_{mk}\cos\left(\frac{2m\pi}{\ell}z\right)\cos(k\theta) + H_{mk}\cos\left(\frac{2m\pi}{\ell}z\right)\sin(k\theta)\right\} \tag{A-75}$$

$$\frac{\partial F}{\partial x} = 2R\left[\cos\theta + \frac{\sin\theta}{R}\left\{\sum_{m=0}^{M}\sum_{k=0}^{N} k\left[-E_{mk}\cos(m\varphi_p)\sin(k\theta_q) + \right.\right.\right.$$

$$+ F_{mk}\cos(m\varphi_p)\cos(k\theta_q) - G_{mk}\sin(m\varphi_p)\sin(k\theta_q) +$$

$$\left.\left.\left. + H_{mk}\sin(m\varphi_p)\cos(k\theta_q)\right]\right\}\right] \qquad \text{(A-76)}$$

$$\frac{\partial F}{\partial y} = 2R\left[\sin\theta - \frac{\cos\theta}{R}\left\{\sum_{m=0}^{M}\sum_{k=0}^{N} k\left[-E_{mk}\cos(m\varphi_p)\sin(k\theta_q) + \right.\right.\right.$$

$$+ F_{mk}\cos(m\varphi_p)\cos(k\theta_q) - G_{mk}\sin(m\varphi_p)\sin(k\theta_q) +$$

$$\left.\left.\left. + H_{mk}\sin(m\varphi_p)\cos(k\theta_q)\right]\right\}\right] \qquad \text{(A-77)}$$

$$\frac{\partial F}{\partial z} = -2R\sum_{m=0}^{M}\sum_{k=0}^{N}\left(\frac{2m\pi}{\ell}\right)\left\{-E_{mk}\sin(m\varphi_p)\cos(k\theta_q) - F_{mk}\sin(m\varphi_p)\sin(k\theta_q) + \right.$$

$$\left. + G_{mk}\cos(m\varphi_p)\cos(k\theta_q) + H_{mk}\cos(m\varphi_p)\sin(k\theta_q)\right\} \qquad \text{(A-78)}$$

$$\left[F_x^2+F_y^2+F_z^2\right]^{1/2} = 2R\left[1+\left\{\sum_{m=0}^{M}\sum_{k=0}^{N}\left(\frac{k}{R}\right)\left[-E_{mk}\cos(m\varphi_p)\sin(k\theta_q)+F_{mk}\cos(m\varphi_p)\cos(k\theta_q)-\right.\right.\right.$$

$$\left.\left. -G_{mk}\sin(m\varphi_p)\sin(k\theta_q)+H_{mk}\sin(m\varphi_p)\cos(k\theta_q)\right]\right\}^2 +$$

$$+\left\{\sum_{m=0}^{M}\sum_{k=0}^{N}\left(\frac{2m\pi}{\ell}\right)\left[-E_{mk}\sin(m\varphi_p)\cos(k\theta_q)-F_{mk}\sin(m\varphi_p)\sin(k\theta_q)+\right.\right.$$

$$\left.\left.\left. + G_{mk}\cos(m\varphi_p)\cos(k\theta_q)+H_{mk}\cos(m\varphi_p)\sin(k\theta_q)\right]\right\}^2\right]^{1/2} \qquad \text{(A-79)}$$

[illegible] unit normal to the surface is given by Equations (A-5) and [illegible] Equations (A-76) through (A-79).

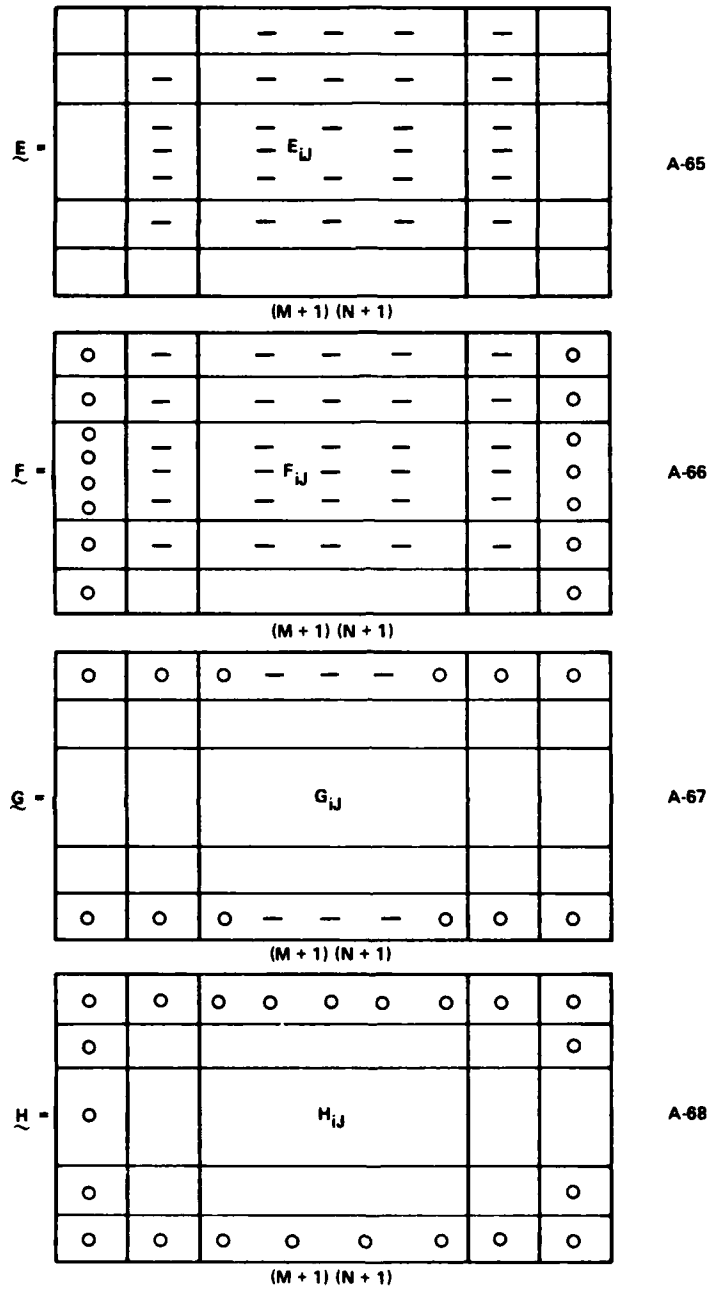

FIGURE A-1. FORM OF DOUBLE FOURIER COEFFICIENTS IS DISPLAYED SCHEMATICALLY

APPENDIX B

SUBROUTINE TO RUN ABAQUS BEND BUCKLING ANALYSIS

```
C
C     MPC SUBROUTINE FOR BEND-BUCKLING PROBLEMS
C
      SUBROUTINE MPC(UE,A,JDOF,N,JTYPE,X,U)
      IMPLICIT DOUBLE PRECISION (A-H,O-Z)
      DIMENSION A(N),JDOF(N),X(6,N),U(6,N)
      DIMENSION BIGAS(3),AS(3),A3(2)
C
C     XXXXXXXXXXXXXXXXXXXXXXXXXXXXXXXXXXXXXXXXXXXXXXXXXXXXXXXXXXXXXXXXXX
C     XXXXXXXXXXXXXXXXXXXXXXXXXXXXXXXXXXXXXXXXXXXXXXXXXXXXXXXXXXXXXXXXXX
C     XXXXXXXXXXXXXXXXX  N O T E S  XXXXXXXXXXXXXXXXXXXXXXXXXXXXXXXXXXX
C     XXXXXXXXXXXXXXXXXXXXXXXXXXXXXXXXXXXXXXXXXXXXXXXXXXXXXXXXXXXXXXXXXX
C
C
C
C     XXXX  UE       =  VALUE OF TOTAL DISPLACEMENT AT ELIMINATED D.O.F.X
C
C     XXXX  A(N)     =  ARRAY OF DERIVATIVES OF CONSTRAINT FUNCTIONS   XX
C
C     XXXX  JDOF(N)  =  ARRAY OF D.O.F. IDENTIFIERS AT NODES INVOLVED  XX
C     XXXX              IN   CONSTRAINTS                               XX
C
C     XXXX  N        =  NUMBER OF D.O.F. INVOLVED IN CONSTRAINTS       XX
C     XXXX              WHEN JTYPE=1, N IS THE NUMBER OF ELEMENTS FOR  XX
C     XXXX              WHICH THE VERTICAL RIGID BODY MOTION WILL BE   XX
C     XXXX              REMOVED                                        XX
C     XXXX              NOTE THAT WHEN JTYPE=1, ALL OTHER INTEGERS     XX
C     XXXX              APPEARING IN THE MPC CARD ARE  N               XX
C
C     XXXX  JTYPE    =  CONSTRAINT IDENTIFIER GIVEN ON CORRESPONDING   XX
C     XXXX              *MPC DATA CARD  (FIRST ENTRY)                  XX
C
C     XXXX  X(6,N)   =  ARRAY OF ORIGINAL COORDINATES AT THE NODES IN  XX
C     XXXX              THE CONSTRAINT                                 XX
C
C     XXXX  U(6,N)   =  ARRAY OF TOTAL DISPLACEMENTS AT THE NODES      XX
C     XXXX              INVOLVED IN THE CONSTRAINT                     XX
C
C
C
C     XXXX  WHEN  JTYPE =2, THEN THERE WILL BE  5  NODE  NUMBERS,I.E. XX
C     XXXX                SHELL NODE TWICE (UZ,UX)  AND                XX
C     XXXX                BEAM NODE  THREE TIMES  (UZB,UXB, PHIZ)      XX
C
C     XXXX  WHEN  JTYPE =3, THEN THERE WILL BE  2  NODE NUMBERS,I.E.  XX
C     XXXX                THE SHELL NODE PHIY AND THE BEAM NODE PHIYB  XX
C
C     XXXX  WHEN  JTYPE =4, THEN THERE WILL BE  3  NODE NUMBERS,I.E.  XX
C     XXXX                THE SHELL NODE TWICE (PHIX,PHIZ) AND         XX
C     XXXX                THE BEAM NODE  ONCE  (PHIYB)                 XX
C
C     XXXX  WHEN  JTYPE =1, THEN THERE WILL BE ALL THE NODE NUMBERS   XX
C     XXXX                ASSOCIATED WITH THE BEAM NODE,INCLUDING THE  XX
C     XXXX                BEAM NODE                                    XX
C
C
C     XXXXXXXXXXXXXXXXXXXXXXXXXXXXXXXXXXXXXXXXXXXXXXXXXXXXXXXXXXXXXXXXXX
C     XXXXXXXXXXXXXXXXXXXXXXXXXXXXXXXXXXXXXXXXXXXXXXXXXXXXXXXXXXXXXXXXXX
C
C
```

```
C
      IF (JTYPE.NE.1) GOTO 200
C
C     XXXX  JTYPE = 1
C
      NODES = N- 1
      NN = (NODES-1)/2
      UE = 0.0
      DO 10 K1=1,NODES
      JDOF(K1) = 1
      T = 1.0
      IF (K1.EQ.1 .OR. K1.EQ.NODES) GOTO 5
      T = 4.000
      IF (( K1/2)*2.NE.K1) T=2.000
    5 CONTINUE
      A(K1) = T
      UE = UE + T* U(1,K1)
   10 CONTINUE
      A(N) = -6.0*FLOAT(NN)
      UE = -UE - A(N)*U(1,N) + U(1,1)
      JDOF(N) = 1
      GOTO  990
  200 CONTINUE
C
C     XXXX  JTYPE = 2
C     XXXX  SET UP DIRECTION COSINES
C
C     XXXX  INITIAL  DIRECTION COSINES, SINCE  PHIO = 0.0,
C     XXXX  ARE   1.0000,0.0000  RESPECTIVELY
C
      CBIGF = 1.0000
      SBIGF = 0.0000
C
C     XXXX  DIRECTION COSINES  OF ADDITIONAL ANGLE  PHIY
C
      CFIZ  = COS( U(5,N) )
      SFIZ  = SIN( U(5,N) )
C
      IF ( JTYPE.NE.2) GOTO 300
C
C     XXXX  JTYPE = 2
C
      A(1) = CBIGF * CFIZ - SBIGF*SFIZ
      A(2) = SBIGF * CFIZ + CBIGF*SFIZ
      A(3) = -A(1)
      A(4) = -A(2)
C
      A(5) = (U(1,1) + X(1,1) - U(1,N) - X(1,N)) * A(1) -
     X       (U(3,1) + X(3,1) - U(3,N) - X(3,N)) * A(2)
C
      UE   = U(3,N) + X(3,N) - X(3,1) + (U(1,N) + X(1,N) -
     X       U(1,1) - X(1,1))* A(2)/A(1)
C
      JDOF(1) = 3
      JDOF(2) = 1
      JDOF(3) = 3
      JDOF(4) = 1
      JDOF(5) = 5
      GOTO  990
  300 CONTINUE
```

```
      IF (JTYPE.NE.3)  GOTO 400
C
C     XXXX  JTYPE = 3
C
      A(1) = 1.000
      A(2) =-1.000
      JDOF(1) = 5
      JDOF(2) = 5
      UE = U(5,2)
      GOTO 990
  400 CONTINUE
C
C     XXXX  JTYPE = 4
C
      A(1) = CBIGF*CFIZ - SBIGF*SFIZ
      A(2) =-CBIGF*SFIZ - SBIGF*CFIZ
      A(3) = U(4,1) * A(2) - U(6,1) * A(1)
      JDOF(1) = 4
      JDOF(2) = 6
      JDOF(3) = 5
      UE = -U(6,1) * A(2)/A(1)
  990 CONTINUE
C
C
      RETURN
      END
```

DISTRIBUTION

	Copies
Chief of Naval Research	
Attn: ONT-023	2
Dr. A. J. Faulstich	2
Department of the Navy	
Arlington, VA 22217-5000	
Commander	
Naval Sea Systems Command	
Attn: SEA-05B	1
SEA-55B (J. B. O'Brian)	1
SEA-55Y1 (S. G. Arntson)	1
SEA-55Y1 (R. A. Sielski)	1
SEA-55Y2 (R. E. Provencher)	1
SEA-63R32 (D. Houser)	1
SEA-09B331	1
SEA-05R23 (C. Pohler)	1
PMS-402	1
PMS-406	1
PMS-407	1
Department of the Navy	
Washington, DC 20362-5101	
Commander	
David Taylor Naval Ship Research and Development Center	
Attn: Code 17 (M. Krenzke)	1
Code 175 (J. Sykes)	1
Code 175.2 (B. Whang)	1
Code 175.2	1
Code 175.2 (T. Gilbert)	1
Code 175.3 (W. Conley)	1
Code 175.3 (P. Manny)	1
Code 184.4 (M. Hurwitz)	1
Code 172	1
Code 1620.3 (R. Jones)	1
Code 1720.6 (A. E. Dadley)	1
Code 1730.5 (J. C. Adamchak)	1
Bethesda, MD 20084	

	Copies
David Taylor Naval Ship Research and Development Center	
Attn: Code 177 (R. Fuss)	1
Code 177.1 (V. Bloodgood)	1
Code 177.1 (M. Riley)	1
Code 177.1 (R. Higginbotham)	1
Underwater Explosion Research Division	
Portsmouth, VA 23709	
Naval Coastal Systems Center	
Attn: Code 4210 (J. Rumbough)	1
Panama City, FL 32407	
Commander	
Naval Weapons Center	
Attn: Code 533 (Technical Library)	1
China Lake, CA 93555	
Commander	
Naval Ocean Systems Center	
Attn: Technical Library	1
San Diego, CA 92152	
Commanding Officer	
Naval Underwater Systems Center	
Attn: D. J. Lepore	1
Newport, RI 02840	
Purdue University	
Attn: Prof. W. F. Chen	1
School of Civil Engineering	
West Lafayette, IN 47907	

DISTRIBUTION (Cont.)

	Copies
Massachusetts Institute of Technology	
Attn: Engineering Library	2
Prof. T. Wierzbicki, Department of Ocean Engineering	1
Prof. T.H. Pian	1
Prof. E. A. Witmer, Department of Aeronautics and Astronautics	1
Prof. K. J. Bathe, Department of Mechanical Engineering	1
Prof. J. J. Connor, Department of Civil Engineering	1
Cambridge, MA 02139	
Office of Naval Research	
Attn: Code 432 (Dr. A. Kushner)	1
800 North Quincy Street	
Arlington, VA 22217	
Director	
Defense Nuclear Agency	
Attn: SPSS (C. McFarland)	1
SPSS (P. T. Tsai)	1
SPSS (C. Carlin)	1
Washington, DC 20305-1000	
Defense Technical Information Center	
Cameron Station	
Alexandria, VA 22314	12
Weidlinger Associates	
Weidlinger Consultant	
Attn: Dr. M. Baron	1
Dr. M. Bowen	1
Dr. A. Misovich	1
333 7th Avenue	
New York, NY 10001	
Hibbitt, Karlson & Sorensen, Inc.	
Attn: Dr. B. Karlson	1
Dr. P. Sorensen	1
100 Medway Street	
Providence, RI 02906	

	Copies
American Bureau of Shipping	
Attn: Mr. Stanley G. Stiansen, Vice President	1
Dr. Y. K. Chen	1
Dr. D. Liu	1
45 Eisenhower Drive	
Paramus, NJ 07652	
Stevens Institute of Technology, Castle Point	
Attn: Prof. David Nicholson	1
Department of Mechanical Engineering	
Hoboken, NJ 07030	
Library of Congress	
Attn: Gift and Exchange Division	4
Washington, DC 20540	
Westinghouse Electric Corporation	
Attn; Dr. Aspi K. Dhalla	1
Advanced Energy Systems Division	
P.O. Box 158	
Madison, PA 15663	
Lockheed Palo Alto Research Laboratory	
Attn: Dr. David Bushnell	1
Dr. John DeRuntz	1
Dr. Charles Rankin	1
Dr. G. Stanley	1
Department 52-33, Building 205	
3251 Hanover Street	
Palo Alto, CA 94304	
Conoco, Inc.	
Attn: Dr. J. G. DeOliveira	1
Production Engineering	
Suite 2718, P.O. Box 2197	
Houston, TX 77252	
University of California	
Attn: Prof. A. E. D. Mansour	1
Department of Naval Architecture	
Berkeley, CA 94720	
Ballistic Research Laboratory	
Attn: Dr. K. Bannister	1
Dr. J. A. Zukas	1
Aberdeen Proving Ground, MD 21005	

DISTRIBUTION (Cont.)

	Copies
The George Washington University Attn: Prof. T. Toridis Department of Civil Engineering Washington, DC 20052	1
The George Washington University Center at NASA Attn: Prof. A. K. Noor Langley Research Center Hampton, VA 23665	1
Stanford University Attn: Prof. T. J. R. Hughes Division of Applied Mechanics Stanford, CA 94305	1
Northwestern University Attn: Prof. T. Belytschko Department of Civil and Mechanical/Nuclear Engineering Evanston, IL 60201	1
John J. McMullen Associates, Inc. Attn: Mr. Donald Wilson 3241 Jefferson Davis Highway Suite 715 Arlington, VA 22202	1
John J. McMullen Associates, Inc. Attn: Mr. Ivan Mertl 30th Floor 1 World Trade Center New York, NY 10048	1
Society of Naval Architects and Marine Engineers Attn: Library 1 World Trade Center Suite 1369 New York, NY 10048	1

	Copies
Martin Marietta Baltimore Aerospace Attn: Library	1
Structural and Mechanical Analysis (Arthur J. Rosenwach)	1
103 Chesapeake Park Plaza Baltimore, MD 21220	
Naval Research Laboratory Attn: Code 6382, Material Science and Technology Division	1
Dr. Mitchell Jolles	1
Library Washington, DC 20735	1
American Society of Civil Engineers Attn: Engineering Libraries 345 East 47th Street New York, NY 10017-2398	1
California Institute of Technology Attn: Aeronautics Library	1
Library	1
Jet Propulsion Laboratory Library Pasadena, CA 91109	1
University of California Attn: Library	1
Civil Engineering Library Berkeley, CA 94720	1
University of California Attn: Library Los Angeles, CA 90024	1
Harvard University Attn: Library Cambridge, MA 02138	1
National Bureau of Standards Attn: Library Washington, DC 20390	1
Columbia University Attn: Civil Engineering Library	1
Library New York, NY 10017	1

DISTRIBUTION (Cont.)

	Copies
Internal Distribution:	
R10	1
R10 (D. Phillips)	2
R10 (H. Huang)	1
R10A (W. K. Reed)	2
R102	2
R14	2
R14 (M. Moussouros)	35
R14 (K. Kiddy)	1
R14 (G. Harris)	1
R14 (S. Wilkerson)	1
R14 (F. Bandak)	1
R14 (D. Bendt)	1
R14 (J. Shaker)	1
R14 (J. Koenig)	1
R14 (T. Farley)	2
R14 (R. M. Barash)	1
R14 (N. Holland)	1
R14 (W. McDonald)	1
R16 (J. R. Renzi)	1
R32 (J. Matra)	1
E231	9
E232	3
E35	1
U01	1
G12 (M. Marshall)	2
E22	1

END

8-87

DTIC